University of São Paulo
"Luiz de Queiroz" College of Agriculture

Biochars in the mitigation of greenhouse gases and on phosphorus removal and reuse

Sarah Vieira Novais

Thesis presented to obtain the degree of Doctor in Science. Area: Soil and Plant Nutrition

Piracicaba
2018

Sarah Vieira Novais
Agronomist

Biochars in the mitigation of greenhouse gases and on phosphorus removal and reuse

versão revisada de acordo com a resolução CoPGr 6018 de 2011

Advisor:
Prof. Dr. **CARLOS EDUARDO PELLEGRINO CERRI**

Thesis presented to obtain the degree of Doctor in Science. Area: Soil and Plant Nutrition

Piracicaba
2018

Dados Internacionais de Catalogação na Publicação
DIVISÃO DE BIBLIOTECA – DIBD/ESALQ/USP

Novais, Sarah Vieira

Biochars in the mitigation of greenhouse gases and on phosphorus removal and reuse / Sarah Vieira Novais. - - versão revisada de acordo com a resolução CoPGr 6018 de 2011. - - Piracicaba, 2018.

111 p.

Tese (Doutorado) - - USP / Escola Superior de Agricultura “Luiz de Queiroz”.

1. Cana-de-açúcar 2. Dejeto de galinha 3. Estoques de C no solo 4. Adsorção de P 5. Dopagem I. Título

To those who direct their efforts in search of sustainable solutions for a better planet,
I DEDICATE

ACKNOWLEDGMENTS

I would like to express my greatest appreciation to:

- The University of São Paulo, specifically the Graduate Program in Soils and Plant Nutrition of the College of Agriculture "Luiz de Queiroz" (ESALQ);
- The Brazilian Federal Agency for the Support and Evaluation of Graduate Education (CAPES);
- The National Counsel of Technological and Scientific Development (CNPq);
- The National Laboratory of Synchrotron Light (LNLS);
- Nucleus of Research in Geochemistry and Geophysics of the Lithosphere (NUPEGEL);
- My adviser, Carlos Eduardo Pellegrino Cerri;
- My co-authors, mainly the researchers Mariana Delgado, Elizio Frade Junior and Renato Lima;
- All the professors and staff of the Department of Soil Science;
- The technicians of the Laboratory of Soil Organic Matter, Eleusa C. Bassi, Lilian A. C. Duarte and Taís Siqueira;
- The Federal Universty of Viçosa, Rio Paranaíba Campus;
- My father, Roberto Novais, for the inspiration and collaboration throughout my academic journey;
- My mother, Magda Novais, for all the candels and preys;
- My little princess, Isabel;
- My devoted and beautiful siblings, Manuela and Fernando;
- My beloved and supportive husband, Lucas;
- My second family, especially Fátima and Juliana Botelho;
- All my graduate colleagues, notably my dear friends and roomates, Mariana, Elizio and Junior;
- My friends in Viçosa, Piracicaba and those that are spread all over the world;

This triumph is ours! Many thanks!

“Experience is simply the name we give our mistakes.”

Oscar Wilde

“I hope to inspire people around the world to look up at the stars and not down at their feet.”

Stephen Hawking

“Adaptability is not imitation. It means power of resistance and assimilation.”

Mahatma Gandhi

CONTENT

RESUMO

Biocarvão na mitigação de gases de efeito estufa e na remoção e reuso de fósforo

Medidas que visam a mitigação de impactos ambientais, especialmente os antrópicos, estão sendo cada vez mais estudadas. A crescente emissão de gases de efeito estufa (GEE) está entre os maiores problemas mundiais, sendo a agricultura um dos grandes contribuintes para este impacto. A eutrofização de águas, ocasionada pelo mau uso do solo e dos sistemas agrícolas, também se encaixa em tal cenário de preocupação. O biocarvão, produto da pirólise de materiais orgânicos, aparece como recuperador de uma lista de problemas ambientais, dentre eles a mitigação de GEE e a recuperação de águas eutrofizadas ou residuárias. Neste sentido, biocarvões de palha de cana-de-açúcar (BPC) e de dejeto de galinha (BDG), foram utilizados em ensaios de emissão de GEE em solos com texturas contrastantes. Para tal, duas temperaturas de pirólise (350 e 650 °C), três doses (12,5; 25 e 50 Mg ha^{-1}), duas classes texturais (arenoso e argiloso) e dois pHs (pH original e pH 5.5), foram utilizados. Estes mesmos biocarvões foram submetidos a processos de dopagem pré-pirólise com Mg^{2+} e pós-pirólise com Al^{3+} para a adsorção de fósforo (P). Ensaios de dessorção e de adsorção em competição com outros ânions pelo sítio de troca foram feitos. O potencial mitigador de GEE de ambos os biocarvões foi comprovado nos ensaios de emissão de gases. O aumento da temperatura de pirólise (350 para 650 °C) eleva ainda mais a mitigação dos gases, sendo que a acidificação do pH original do biocarvão causa efeito semelhante. Os benefício de se pirolisar tais materiais orgânicos são melhores vistos no solo arenoso, sendo a produção de biocarvão a partir destes resíduos uma forma ambientalmente segura de deposição destes materiais, ao menos no que se diz respeito a emissão de GEE. Ambos os biocarvões não possuem capacidade de adsorção de P sem passar por modificação química, sendo que o processo de dopagem, seja ele com Mg ou Al, concedeu tal habilidade. O processo de pré-dopagem com Mg^{2+} gerou uma capacidade máxima de adsorção de P (CMAP) de 250,8; 163,6; 17,7; 17,6 mg g^{-1} para o BDG pirolisado a 350 e 650 °C e para o BPC também pirolisado a 350 e 650 °C, respectivamente. O processo de dopagem por pós-pirólise com Al^{3+} gerou uma CMAP de 701,6 e 758,9 mg g^{-1} para o BDG e BPC, ambos pirolisados a 350 °C, respectivamente. A superior CMAP dos biocarvões dopados com Al foi atribuída ao fato de o cátion que faz a ponte (Al^{3+}) ser trivalente, com elevada afinidade pelo P. A elevada adsorção de Al pelos biocarvões corrobora com tal afirmação. Ambos os biocarvões, produzidos pelos dois processos de dopagem, tiveram uma dessorção de P em torno de 80 % do valor adsorvido, permitindo a inferência de que estes produtos possuem a capacidade de serem utilizados no reuso de nutrientes, mitigando outro problema ambiental: o uso das reservas finitas de P. Com os resultados positivos advindos da pirolisação dos materiais nesta tese, constatamos o potencial do biocarvão como mitigador de GEE e recuperador de águas.

Palavras-chave: Cana-de-açúcar; Dejeto de galinha; Estoques de C no solo; Adsorção de P; Dopagem

ABSTRACT

Biochars in the mitigation of greenhouse gases and on phosphorus removal and reuse

Measures aimed at mitigating environmental impacts, especially the anthropic ones, are being progressively studied. Increasing greenhouse gases (GHG) emissions are among the biggest environmental problems in the world, with agriculture one of the major contributors to this impact. Water eutrophication from land misuse and agricultural systems also fits into such a scenario of concern. Biochar, the product of the pyrolysis of organic materials, appears as a recover of a list of environmental problems, among them the mitigation of GHG and the recovery of eutrophic or wastewater. In this sense, biochars of sugarcane straw (BCS) and poultry manure (BPM) were used in GHG emission tests in soils with contrasting textures. To do so, two pyrolysis temperatures (350 and 650 °C), three doses (12.5, 25 and 50 Mg ha^{-1}), two texture classes (sandy and clayey) and two pH values (original pH and pH 5.5) were used. These same biochars were submitted to doping processes pre-pyrolysis with Mg^{2+} and post-pyrolysis with Al^{3+} for the adsorption of phosphorus (P). Desorption and adsorption experiments in competition with other anions by the exchange sites were done. The potential GHG mitigation of both biochars has been proven in the gas emission tests. The increase of the pyrolysis temperature (350 to 650 °C) further increases the gas mitigation, and the acidification of the original pH of the biochar causes a similar effect. The benefits of pyrolyzing such organic materials are best seen in sandy soil, with the production of biochar from these residues being an environmentally safe way of depositing these materials, at least with regard to the emission of GHG. Both biochars do not have P adsorption capacity without passing through chemical modification, and the doping process, with Mg or Al, granted this ability. The pre-doping process with Mg^{2+} generated a P maximum adsorption capacity (PMAC) of 250.8; 163.6; 17.7; 17.57 mg g^{-1} for the pyrolyzed BPM at 350 and 650 °C and for the BCS also pyrolysed at 350 and 650 °C, respectively. The post-doping process with Al^{3+} generated a PMAC of 701.6 and 758.9 mg g^{-1} for BPM and BCS, both of which were pyrolysed at 350 °C, respectively. The superior PMAC of the Al doped biochars was attributed to the fact that the cation that makes the bridge (Al^{3+}) is trivalent, with high affinity for P. The high adsorption of Al by the biochars corroborates with such a statement. Both biochars, produced by the two doping processes, had a desorption of P around 80 % of the adsorbed value, allowing the inference that these products have the capacity to be used in nutrient reuse, mitigating another environmental problem: the use of the finite reserves of P. With the positive results coming from the pyrolysis of the materials in this thesis, we certify the biochar potential as a GHG mitigator, recovery for waters and a potential slow release fertilizer in P reuse.

Keywords: Sugarcane straw; Poultry manure; Soil C stocks; P adsorption; Doping

1. GENERAL INTRODUCTION

Problems caused by increase in the human population with the consequent growth in the demand for food and manufactured goods, the misuse of soils and water resources and finite reserves of most nutrients, make some environmental collapses predictable. The large waste production follows this scenario, with researches for environmentally safe depositions of these materials. Biochar, the product of pyrolysis of organic materials, may be the solution or at least mitigation of some of these problems.

The pyrolysis process confers increase in the stability of the material, guaranteeing greater stability of the C, with great generation of negative charges due to the high concentration of phenolic, fulvic and carboxylic acids in the final product. With such positive characteristics, the pyrolysis of organic materials has been applied to reduce the emission of greenhouse gases (GHG). Due to their high average residence time, studies on the use of the source materials and their respective forms of biochar in the soil point out not only to a reduction in GHG emissions compared to their raw material, but also to a mitigation of emissions even from the soil, showing the potential of this material as an environmentally safe disposal of tailings.

Due to its high cation exchange capacity (CEC), biochars have high adsorbent potential, being used in the recovery of eutrophic or wastewater and in soils contaminated with heavy metals. Anion exchange capacity (AEC), although not resulted from the pyrolysis process, can be chemically developed by a process called doping. This process consists in adding metallic cations such as Mg^{2+}, Ca^{2+}, Al^{3+} and $Fe^{2+/3+}$ in the biochar matrix, developing a cationic bridge that favors the adsorption of anions.

With the natural or developed ability of ions adsorption, biochars applied in eutrophic or wastewaters can be recovered for later reuse as a source of the adsorbed nutrients. As in the great majority of cases, the elements that cause water eutrophication are of agronomic interest, such as nitrogen (N), phosphorus (P) and sulfur (S). In their ionic forms, such nutrients when adsorbed and recovered may be reused or recycled. From this reuse or recycling, they can be returned to the soil, sparing finite reserves, such as P, or high energy consumption for the production of fertilizers, such as N.

The reuse or recycling of these nutrients does not only have the benefit of reducing the production of fertilizers. Tropical weathered soils, such as Oxisols in general, require slow release sources of P, characteristic of these materials, so that the plant-sink is favored in detriment of the soil-sink. In addition, the more stable matrix of the biochars guarantees a fertilizer with the organomineral focus, without the environmental problems that the great use of the mineral fertilizers can entail.

Biochar seems to be the solution to a number of environmental problems that were not thought to be connected. Its deposition on the soil not only guarantees a solution to environmental problems, but also brings physical, chemical and biological benefits to the soil. Its use in eutrophic or wastewater ensures its recovery with a possible reuse of the adsorbed ions. Nutrient reuse, like P, also provides a solution to another problem, with a special focus on very weathered tropical soils, in general so deficient in P and with a high demand for its finite reserves.

In this thesis, problems and solutions related to the production and use of biochars, their induced chemical changes, their chemical and physical characterization, their potential for GHG mitigation and some of their agronomic applications are addressed. In chapter I the potential use of biochars of sugarcane straw and poultry manure as a GHG mitigator in a sandy soil is addressed. In Chapter II, the GHG mitigation potential of these same biochars is tested in a clayey soil and compared to the data obtained in chapter I, in order to obtain a CO_2 emission model as a function of the applied biochar dose, the pyrolysis temperature, biochar pH and soil texture. In chapter III the adsorption capacity of P before and after the pre-doping process with Mg^{2+} is verified, as well as its desorption. In Chapter IV, the adsorption capacity of P and its desorption is also observed before and after the post-doping process with Al^{3+}. In this last chapter, we also tested the potential of biochars doped as a recover of eutrophic or wastewater and their possible reuse in agriculture.

2. MITIGATION OF GREENHOUSE GAS EMISSIONS FROM TROPICAL SOILS AMENDED WITH POULTRY MANURE AND SUGAR CANE STRAW BIOCHARS

ABSTRACT

Increases in greenhouse gases (GHG) emissions, upon changes in land use and agricultural management, lead to a search for techniques that enhance carbon residence time in soil. Pyrolysis increases the recalcitrance of organic materials and enhances their activities as physical, chemical and biological soil conditioners. Emissions of CO_2, CH_4 and N_2O quantified from a sandy soil that was treated with three rates (12.5, 25 e 50 Mg ha^{-1}) of either non-pyrolysed poultry manure and sugarcane straw or biochars, pyrolysed at two contrasting temperatures (350 e 650 °C). Subsequently, the flux of the three gases were converted and compared in a standard unit (CO_2eq). The added biochars, significantly reduced GHG emissions, especially CO_2, relative to the non-pyrolysed materials. The greatest differences between applied rates of poultry manure, relative sugarcane straw, both to biochar and raw material, and the positive response to the increase of pyrolysis temperture, confirms the importance of raw material choice for biochar production, with recalcitrance being an important initial characteristic. Greater emissions occurred with intermediate rate of biochars (25 Mg ha^{-1}) amendment to the soil. These intermediate rates had higher microbial biomass, provided by an intermediate C/N ratio derived from the original soil and the biochar, promoting combined levels of labile C and oxygen availability, leading to an optimal environment for microbiota.

Keywords: CO_2; CH_4; N_2O; Weathered soil

Published as: Novais, S. V., Zenero, M. D. O., Junior, E. F. F., de Lima, R. P., Cerri, C. E. P. (2017). Mitigation of Greenhouse Gas Emissions from Tropical Soils Amended with Poultry Manure and Sugar Cane Straw Biochars. Agricultural Sciences, 8(09), 887. DOI: 10.4236/as.2017.89065

2.1. INTRODUCTION

The predicted increase in greenhouse gas emissions (GHG) and the growing demand for manufactured goods [1] promotes the adoption of soil management techniques that mitigate these emissions [2] and [3]. Soils can sequester and accumulate larger quantities of carbon than plant biomass and the atmosphere [4]. For the global carbon cycle, any activity that favors the

decomposition and mineralization of organic material, with consequent carbon emission, should be avoided [1].

Numerous studies have investigated carbon residence time in soil, as in charcoal form ("biochar") [5] and [6]. Biochar is the product obtained from pyrolysis of various biomasses. This process occurs in the absence of oxygen (anoxic environment) or at a very low level (hypoxic environment), which produces condensable gases and vapor, as well as charcoal [7]. The pyrolysis temperature alters the proportion of fulvic and humic acids in biochar [5], concentration of nutrients, such as phosphorous and nitrogen [8], pH and porosity [9]. Aromatic and hydrophobic structures give stability, enhancing recalcitrance, and acidic groups give reactivity [4], making biochar useful to increase chemical, physical and biological qualities of soils. In regard of plant biomass, hemicellulose is the first to be lost in the pyrolysis process, since it degrades at 200 °C. From 240 °C to 350 °C, cellulose is degraded, followed by lignin at 280 °C a 500 °C [10].

There is a wide choice of raw materials that generate environmental problems upon their accumulation in the fields [11] and [12]. According to [13], agricultural soils, enteric fermentation and animal waste, are responsible for 70 % of GHG emissions in AFOLU areas (Agriculture, Forestry and Other Land Use), making necessary an appropriate management of these materials. For instance, sugar cane, planted on 8.8 million hectares in Brazil, which generates, approximately, 250 million tons of straw [14], had recent laws prohibiting straw burning, which limits the management options for this residue [15]. The straw left in the field retards sprouting and tillering, reduces productivity [16], and also affects the growth and development of sockets [16]. Since two thirds of biomass produced by sugarcane is considered bagasse and straw [17], biochar production is an alternative for the management of this waste [18]. Furthermore, animal residues also have a large contribution in GHG emissions [19], and are difficult in transport and store. Increased poultry production and concerns about the waste, poses the need for an environmentally secure deposit for this residue [20].

Since biochar has higher carbon stability than the original raw material, it is relevant to GHG mitigation [12]; [10]; [11] and [6]. [21] concluded that pyrolysis of wheat straw would avoid the emission of 0.9 to 1.06 t CO_2eq per ton of dry weight, if the non-pyrolysed straw was allowed to decompose in the field. [22] predicted that the use of biochar could sequester 3.7 to 6.6 Pg CO_2eq by 2050, contributing 7 to 13 % reduction in GHG emissions. [23] calculated a reduction of 0.7 to 1.3 t CO_2eq per ton of miscanthus, when the waste is used on biochar production. [24] compared biochar from corn and grass straw in the USA and demonstrated a reduction of 0.885 t CO_2eq per ton of dry weight in GHG emissions. [12] considered the energy used in pyrolysis and calculated that the incorporation of biochar into the soil would reduce emissions by 2.8 to 10.2 Mt

CO_2eq by 2030 and 2.9 to 10.6 Mt CO_2eq by 2050. The variation in emissions between these values is influence by the type of raw material used to produce the biochars. This author [12] observed that the highest potential for GHG emission reduction occurred with forestry residues, followed by straw from cereals and pastures; the lowest potential was biochars derived from cattle manure. [25] measured CO_2 and CH_4 emissions and did not obtain a significant difference between the untreated soil and soil amended with biochar from wheat straw; however, a significant difference in N_2O emission was observed. [26] observed an increase in CH_4 emissions of 200 mg m^{-2} when applying 20 Mg ha^{-1} of biochar from forestry residues on an unfertile tropical soil. However, [27] observed a reduction of 51.1 % in CH_4 emission from a waterlogged paddy soil when applied biochar from bamboo fragments and, a reduction of 91.2 %, when biochar from rice husks was applied, likely due to a reduction in methanogenic.

Under tropical soil conditions, there are a limited number of published results on biochar and its impacts on GHG emissions. Few investigations in Brazil compare different materials and rates of applied biochar. Therefore, the objective of this study was to quantify and compare GHG emissions from a tropical sandy soil, which received either different amounts of biochars from sugar cane straw and poultry manure, pyrolysed in two temperatures, or their respective non-pyrolysed materials.

2.2. MATERIAL AND METHODS

2.2.1. Soil characteristics

About 30 % of the Brazilian territory is occupied by sandy soils [28]. With proper management and fertilization, these soils are intensively cultivated and are highly productive [29]. Samples from the 0-20 cm layer of a Typic Quartzipsamment soil type (Table 1) were collected from the Anhembi region of São Paulo State (22° 43' 31.1"S e 48° 01' 20.2 W) under natural vegetation. The samples were dried, sieved to 2 mm size and 50 g of soil were incubated with the raw materials and the respective biochars, in different treatments.

Table 1 – Characteristics of the tropical sandy soil used in the experiment.

Soil	Sand/Silt/Clay	pH	C	N	C/N
	----- g kg^{-1} -----	-- $CaCl_2$ --	---------- % ----------		
Typic Quartzipsamment	900 / 22 / 78	4.1±0.1	0.9±0.1	0.1±0.0	14.3±0.1

Source: Abruzzini, 2015.

2.2.2. Raw materials selection

The raw materials were selected due to their abundant accumulation in the field, plus their contrasting attributes and characteristics of agronomic interests. Sugar cane straw was collected from a field of cane industry at Piracicaba-SP, and poultry manure was collected from a farm located at ESALQ-USP. The raw materials were dried at 45 °C, ground in a ball mill and sieved to 2 mm, forming a homogeneous material.

2.2.3. Biochar production

Pyrolysis process was carried out by SPPT Company, in metallic reactors, with an N_2-saturated atmosphere. The temperature was raised by 10 °C per minute during the first 30 min followed by 20 °C per min up to the desired temperatures [30].

Two pyrolysis temperatures, 350 and 650 °C, were chosen based on values cited in the literature. These temperatures cover the main phases of transformation of raw materials, that results in the final characteristics of the produced biochar. Temperatures below 350 °C are considered toast rather than pyrolysis, while above 650 °C results in weight loss of the material [31].

[30] previously characterized these biochars according to their pH, electrical conductivity (EC), cation exchange capacity (CEC), elemental analysis, humidity, relative proportions, yield and biochemical composition (Table 2), as well as spectrometric analysis.

Table 2 – Properties of the biochars from poultry manure (PM) and sugar cane straw (CS) pyrolyzed at 350 and 650 °C.

	Biochar			
Properties	PM 350 °C	PM 650 °C	CS 350 °C	CS 650 °C
pH ($CaCl_2$)	8.3	10.0	8.8	9.2
EC ($\mu S\ cm^{-1}$)	4256.3	4022.5	1788.7	1911.4
CEC ($mmol_c\ kg^{-1}$)	360.0	200.0	70.0	70.0
C (%)	36.3	32.6	60.8	68.2
N (%)	2.6	1.4	1.8	1.7
O (%)	37.5	26.8	53.4	62.3
H (%)	2.5	2.7	3.3	0.8
Moisture (%)	3.8	4.2	2.9	1.7
Volatile Material (%)	50.2	43.8	60.8	42.1
Ash (%)	24.2	13.9	32.2	48.8
C fixed (%)	21.9	36.7	0.0	7.5
Biochar yield (%)	41.5	32.8	59.6	40.2
Hemicellulose ($g\ kg^{-1}$)	53.2	78.8	211.5	291.0
Cellulose ($g\ kg^{-1}$)	56.9	72.3	82.3	75.3
Lignin ($g\ kg^{-1}$)	734.9	598.4	295.4	233.7

Source: Conz, 2015.

2.2.4. Treatments and experimental conditions

Each biochar and their respective raw material were homogenized with the soil at 60 % field water holding capacity. This soil moisture content approximated the filling of the micro-pores [32], guarantying microorganisms preservation. Each soil treatment mixture was placed in 650 mL glass pots, with a septum in the top, allowing gas collection with a syringe after sealing. A small vial containing deionized water was positioned in the glass pots to maintain humidity and the water was replenished upon observation of weight loss in the experimental unit.

The experiment consisted in a factorial treatment combination [3 x (2 + (2 x 2))] + 1, with three rates (12.5; 25 and 50 Mg ha^{-1}) of applied biochar or non-pyrolysed material, two raw materials (sugar cane straw and poultry manure), two biochars (from sugar cane straw and from poultry manure), and two pyrolysis temperatures (350 and 650 °C), totaling 18 treatments, with four replicates and a control with untreated soil.

The application rates, defined according to [22], correspond to the maximum viable amount of applied biochar, considered by these authors as 50 Mg ha^{-1}. The other two rates (12.5 and 25 Mg ha^{-1}) are fractions of this value.

The experimental units were maintained for 6 months in the Soil Organic Matter Laboratory, in Soil Science Department at ESALQ/USP, at a constant temperature of 25 °C. Starting time was when the biochar was incorporated into the soil and incubated in the glass pots.

2.2.5. Gas sampling

Gas emissions, collected daily during the first two weeks and less frequently during the rest of the experimental period, were sampled after sealing the vials for 30 min, using a 25 mL syringe and needle. Five empty flasks, used as control samples, were the background established levels used to calculate the effective concentration of the gasses emitted from each treatment (Equation 1). The gas samples were immediately transferred to vials under vacuum and analyzed by gas-chromatography (SRI 8610 – SRI Instruments) with a flame ionization detector (FID) and an electron capture detector ^{63}Ni (ECD), which permitted the detection of CO_2, CH_4 and N_2O in the same sample.

$$NET = AET - BEC \quad \text{(Equation 1)}$$

Where: NET is the net emission of GHG for the treatment; AET is the accumulated emission of GHG for the treatment; BEC is the background emissions in the control sample.

2.2.6. Post-experiment analysis

After the end of the experiment, carbon (C) and nitrogen (N) contents from each experimental unit were analyzed by dry combustion using a Leco TruSpec® CHN elemental analyzer, according to [33] Microbial biomass C and N (MBC and MBN) were determined by the fumigation-extraction method proposed by [34]. The extracts from each experimental unit were analyzed using a Shimadzu Total Organic Carbon Analyzer (TOC-L) and a Total Organic Nitrogen Analyzer (TON-L).

2.2.7. Data analysis and statistics

Mean gas concentrations were used to calculate flow and accumulation and were subjected to an adjustment by a second order polynomial equation (gas concentration versus time), as

proposed by [35]. The flows at zero time (empty vials) were calculated by the second order derivative equations and expressed per gram of C or N per unit area (m^2) or per unit time (h).

The conversion of the flux of the three gases into a standard unit (CO_2 equivalent), allowing a critical and ensemble view of GHG emissions, was obtained according to equation 2 and 3.

$$CO_{2eq=}\ C - CH_4 * \frac{16}{12} * 25 \text{ (Equation 2)}$$

$$CO_{2eq=}\ N - N_2O * \frac{44}{28} * 298 \text{ (Equation 3)}$$

Where: C-CH_4 and N-N_2O are gases fluxes ($mg.m^{-2}h^{-1}$); 16/12 is the ratio between the molecular mass of CH_4 and C; 44/28 is the rate between the molecular mass of N_2O and N; 25 is the Global Warming Potential (GWP) of CH_4 and 298 of N_2O [36].

The data from the raw materials, combined by application rate and feedstock, were subjected to a variance analysis, where a completely randomized design was adopted, in a factorial 2x3, with a control treatment and four replicates. To analyze the data from the biochars, the same experimental design was adopted, in a factorial 2x3x2. The factors were combined with the raw material used in pyrolysis process, application rates and temperatures, four replicates and the control. The means, treated as separate events, were compared between treatments at a confidence interval of 95 %. The treatments were considered not to be statistically different among themselves when there was an overlap of the mean intervals. Results on MBC, MBN, C and N contents and C/N ratio were statistically analyzed using a Tukey test at 5%. The statistical analyses and graphs were performed using the "plotrix" and "agricolae" packages available in the R software [37].

2.3. RESULTS

2.3.1. Raw materials

Poultry manure (PM) provided the largest CO_2 emissions and the largest amplitude between the applied rates (Figure 1a). The greater emissions of CO_2 by the raw materials, relative to their respective biochars (Figure 1a and 1b), can be observed by the magnitude of the y-axis, which are three times larger for the raw materials. Even though there was little or no statistical difference in CH_4 emissions among rates and raw materials, the pattern of higher emission occurred for the highest application rate (Figure 2a).

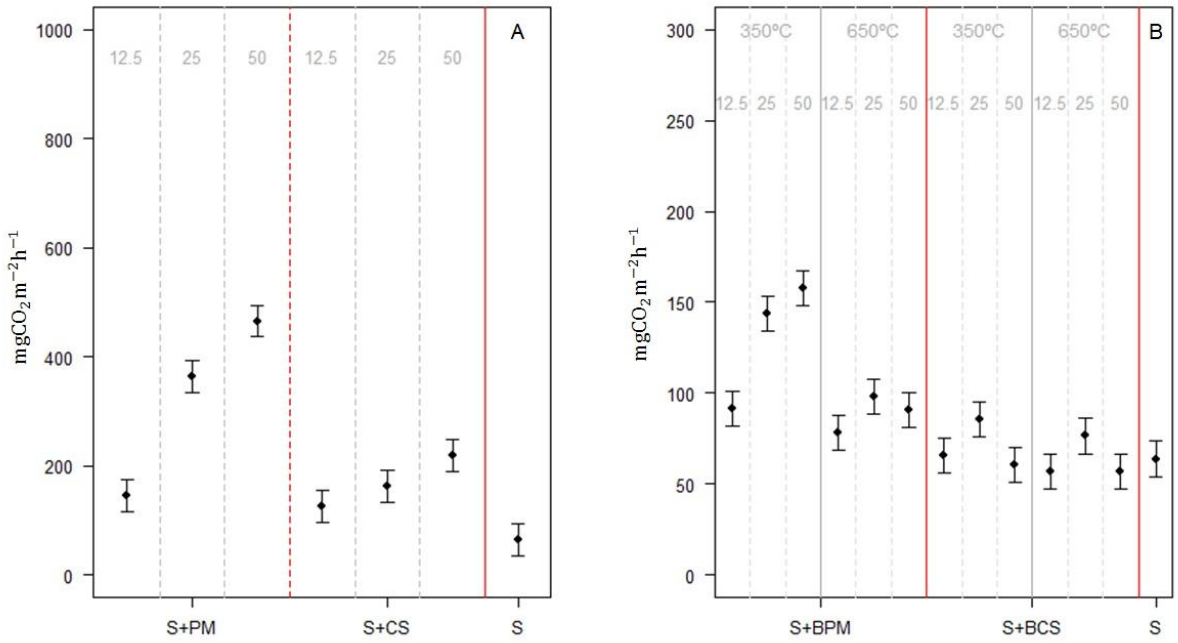

Figure 1 - Emission of CO_2 from a tropical sandy soil (S) amended with a) raw materials: poultry manure (S+PM) and sugar cane straw (S+CS); and b) biochars: biochar poultry manure (S+BPM) and biochar of sugar cane straw (S+BCS).

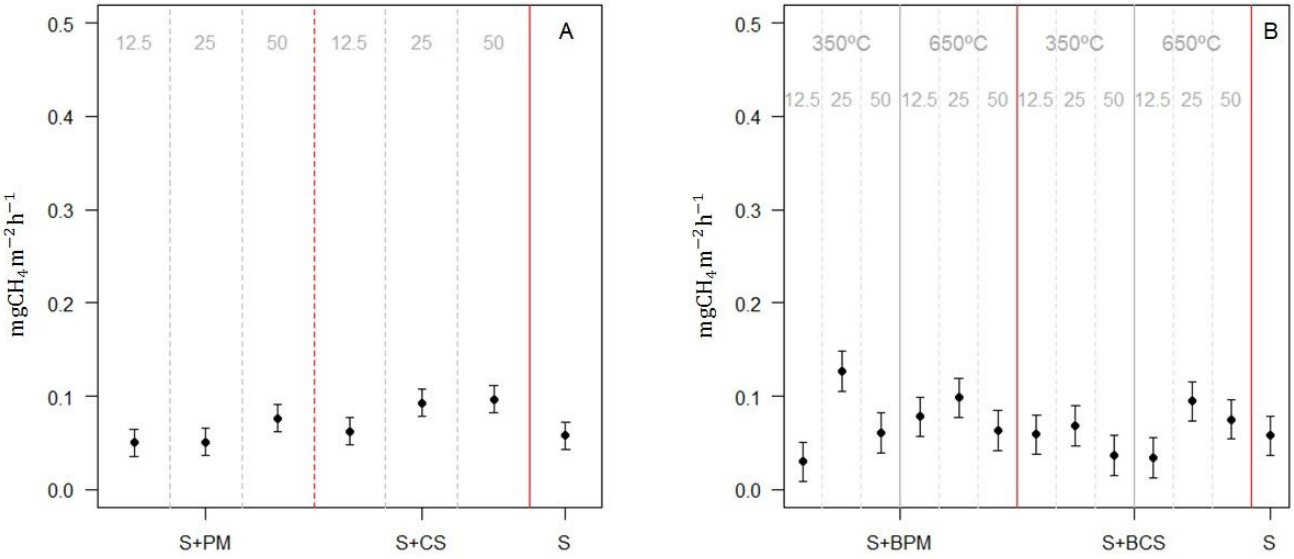

Figure 2 - Emission of CH_4 from a tropical sandy soil (S) amended with a) raw materials: poultry manure (S+PM) and sugar cane straw (S+CS); and b) biochars: biochar poultry manure (S+BPM) and biochar of sugar cane straw (S+BCS).

2.3.2. Biochars

When the emissions of CO_2 from the biochars were compared (Figure 1b), the same trends between raw materials were observed. Even after pyrolysis, PM emitted higher levels of CO_2, and

showed a greater variation among rates, despite no statistical difference between the poultry manure biochar (BPM) rates of 25 and 50 Mg ha^{-1}, regardless pyrolysis temperature. The BPM also presented a statistical difference between the two pyrolysis temperatures. The sugar cane straw biochar (BCS) had a small amplitude of gas emissions between treatments, with little or no significative response.

2.3.3. Application Rate

The lowest rate (12.5 Mg ha^{-1}) of both raw materials showed higher emissions of CO_2 than the control (Figure 1a). As expected, there was an increase in CO_2 and CH_4 emissions (Figure 1a and 2a) with increased application rate, such that the highest rate of both raw materials (50 Mg ha^{-1}) provided the greatest emission of these gases. For CH_4 emissions (Figure 2a), only the application of 25 and 50 Mg ha^{-1} of SC resulted in higher emissions than the control. For N_2O (Figure 3a), only the application of 25 Mg ha^{-1} of PM resulted in a superior emission compared to the control.

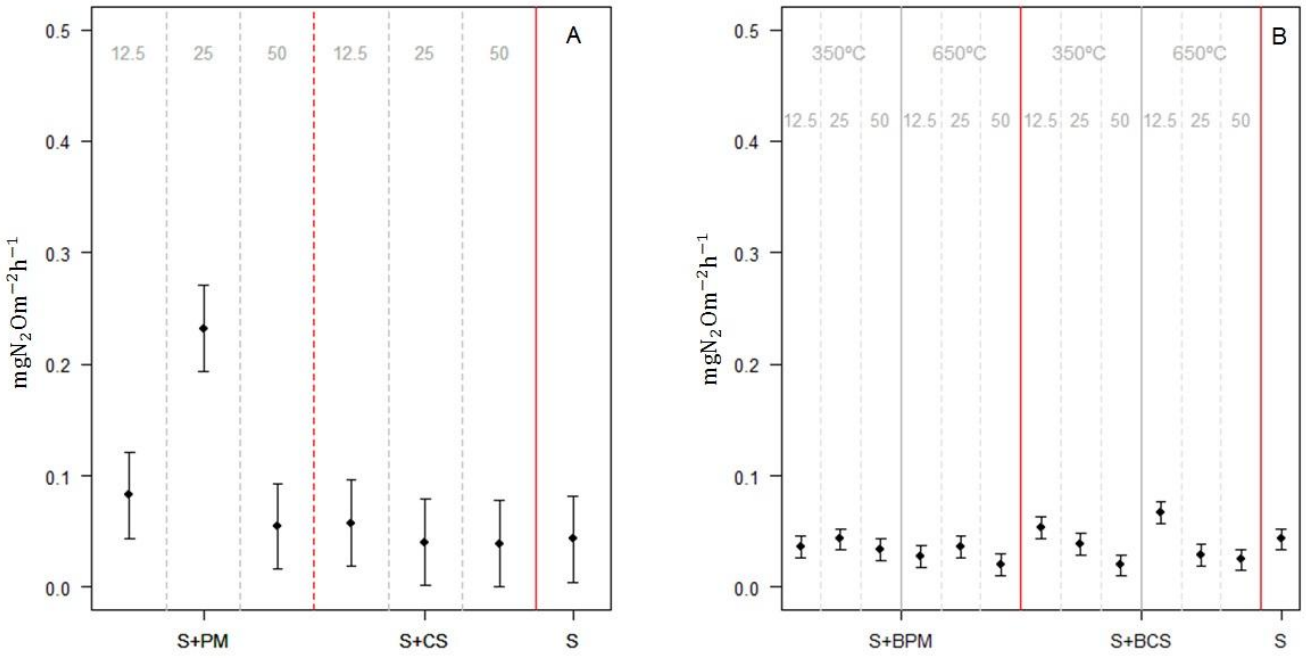

Figure 3 - Emission of N_2O from a tropical sandy soil (S) amended with a) raw materials: poultry manure (S+PM) and sugar cane straw (S+CS); and b) biochars: biochar poultry manure (S+BPM) and biochar of sugar cane straw (S+BCS).

The intermediate rate of applied BCS had higher CO_2 emissions than the other rates, at both pyrolysis temperatures (Figure 1b). This pattern, also observed for CH_4 emissions (Figure 2b), had

the largest emission values observed with the 25 Mg ha^{-1} rate, regardless biochar raw material source or pyrolysis temperature. Both observations are in agreement with the higher MBN values found for this rate (Table 3).

Table 3 – Effects of raw materials, biochar application rates and pyrolisis temperature on C and N in a tropical sandy soil.

Treatment	Dose	MBC[(1)]		MBN[(2)]		C[(3)]		N[(3)]		C/N		Cmic:Ctot[(4)]	
	Mg.ha^{-1}	---------- mg L^{-1} ----------										%	
Raw Materials													
S+PM	12.50	38.78	Cb	6.73	Ab	0.75	Bb	0.06	Ba	12	Aa	0.19	Ca
	25.00	72.69	Ba	20.30	Ab	0.90	Abb	0.08	Aba	11	Ab	0.80	Ba
	50.00	170.25	Aa	25.67	Aa	1.12	Ab	0.11	Aa	10	Ab	1.53	Aa
S+CS	12.50	73.71	Aa	29.84	Ba	0.95	Ca	0.06	Aa	17	Ba	0.82	Aa
	25.00	36.32	Cb	41.49	Aa	1.19	Ba	0.05	Ab	26	Aa	0.31	Aa
	50.00	54.98	Bb	15.62	Ba	1.91	Aa	0.07	Ab	28	Aa	0.29	Ab
Biochar													
S+BPM 350 °C	12.50	170.49	Ca	93.19	Ba	0.93	Ba	0.06	Aa	15	Aa	1.85	Aa
	25.00	204.04	Ba	124.95	Aa	1.22	Ba	0.08	Aa	17	Aa	1.68	Aa
	50.00	223.96	Aa	39.95	Cb	1.79	Aa	0.12	Aa	16	Aa	1.29	Aa
S+BPM 650 °C	12.50	190.16	Ba	101.16	Bb	0.95	Ca	0.06	Aa	16	Ba	2.00	Aa
	25.00	116.51	Ca	112.13	Aa	1.16	Ba	0.07	Aa	17	Ba	1.03	Ba
	50.00	213.99	Aa	94.46	Ba	1.70	Aa	0.09	Aa	21	Aa	1.27	Aba
S+BCS 350 °C	12.50	127.93	Aa	72.24	Aa	1.25	Ca	0.08	Aa	16	Ba	1.04	Aa
	25.00	106.28	Ba	76.91	Aa	1.92	Ba	0.12	Aa	17	Ba	0.58	Ba
	50.00	126.04	Aa	63.09	Aa	2.80	Aa	0.11	Aa	26	Aa	0.41	Ba
S+BCS 650 °C	12.50	103.41	Ab	49.87	Ba	1.34	Ba	0.07	Aa	22	Ba	0.77	Aa
	25.00	85.58	Ba	63.24	Aa	1.78	Ba	0.07	Aa	29	Ba	0.50	ABa
	50.00	111.84	Aa	59.65	Aba	3.18	Aa	0.09	Aa	37	Aa	0.36	Ba

S+PM: Soil + Poltry Manure; S+CS: Soil + Case Straw; S+BPM 350 °c: Soil + Biochar of Poultry Manure pyrolysed at 350 °C; S+BPM 650 °C: Soil+ Biochar of Poultry Manure pyrolysed at 650 °C; S+BCS 350 °C: Soil + Biochar of Case Straw pyrolysed at 350 °C; S+BCS 650 °C: Soil + Biochar of Case Straw pyrolysed at 650 °C; [(1)]Microbial Biomass Carbon; [(2)]Microbial Biomass Nitrogen; [(3)]Total C and N of the treatments; [(4)]Ratio of Microbial Biomass C/Total C. Averages followed by the same capital letter refer to the comparison among doses of the same treatment; Averages followed by the same lowercase letters refer to the comparison of the same dose among treatments.

The application of BCS at the lowest rate resulted in a higher emission than the control treatment, regardless of the pyrolysis temperature (Figure 3b). Emission values for N_2O decreased with the increasing application rates above 12.5 Mg ha^{-1}. No statistical differences were detected for N_2O emissions by BPM, regardless the applied rate or pyrolysis temperature (Figure 3b).

2.3.4. Pyrolysis temperatures

When the pyrolysis temperatures were compared for BPM (Figure 1b), the higher GHG emission levels at 350 °C were to be expected. For BCS the pyrolysis temperature did not affect CO_2 emission (Figure 1b), since no significant differences were observed between temperatures, comparing the same rate.

The CO_2 emissions for the soil without the addition of residue (control) did not significantly differ from the emissions obtained from the soil after the BCS addition, regardless of the applied rate or pyrolysis temperature (Figure 1b). When the addition of CS (Figure 1a) is compared to its respective biochar, produced at 350 °C (Figure 1b), the emissions were 1.89, 1.90 and 3.60 times higher for non-pyrolyzed material at the rates 12.5, 25 and 50 Mg ha^{-1}, respectively. When compared to the biochar produced at 650 °C the non-pyrolyzed material produced emissions 2.19, 2.13 and 3.82 times higher, at the same rates. For BPM the same pattern was observed. Although the emissions were slightly higher than the control, when compared to the raw material, the non-pyrolyzed form showed emissions 1.36, 2.58 and 3.03 times higher than the biochar produced at 350 °C, for the rates 12.5, 25 and 50 Mg ha^{-1}, respectively. Using a pyrolysis temperature of 650 °C, the emissions from the raw materials were 1.67, 3.95 and 5.78 times higher, at the same rates.

2.3.5. CO_2 equivalent

The same pattern obtained in CO_2 emissions (Figure 1) was observed for CS and biochars (BPM and BCS) at the standard unit (Figure 4), regardless the different treatments. For poultry manure as a raw material, the highest rates (25 and 50 Mg ha^{-1}) were not statistically different, which does not occur for CO_2 emission (Figure 1a).

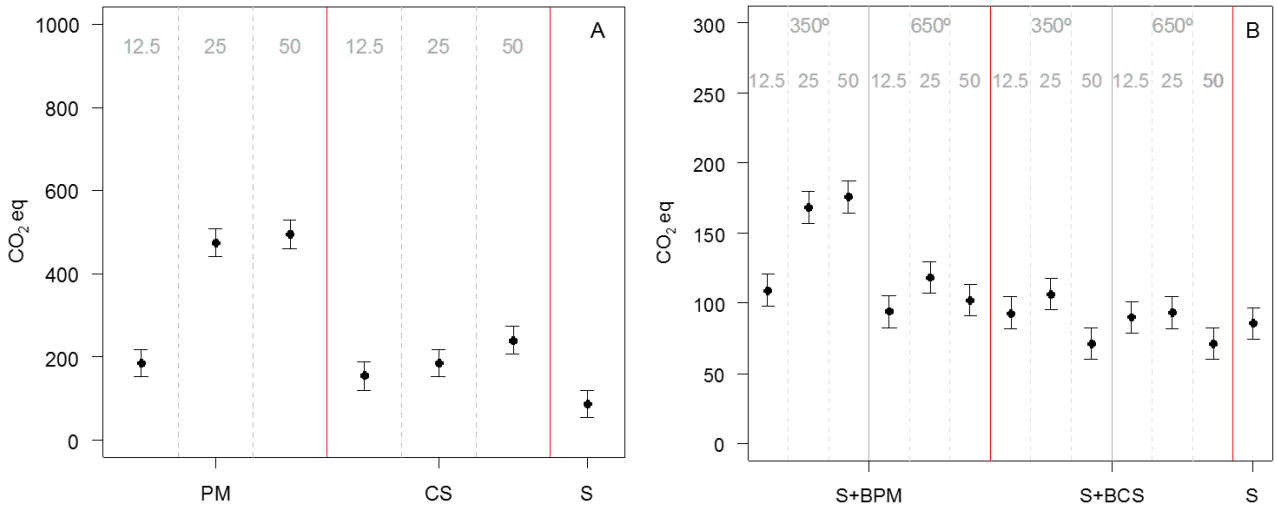

Figure 4- Emissions in CO_2equivalent from a tropical sandy soil (S) amended with a) raw materials: poultry manure (S+PM) and sugar cane straw (S+CS); and b) biochars: biochar poultry manure (S+BPM) and biochar of sugar cane straw (S+BCS).

2.4. DISCUSSION

The largest emission of GHG, observed during the first 15 days, was slowly reduced. From day 36, treatments were no longer statistically different from the control, confirming that the gas emissions had already stabilized and no longer needed to be collected (Figure 5). The gas sampling continued for more 103 days, in order to confirm that the microbiota had already stabilized and would not have a new peak of emission, as sometimes reported by few authors [38]; [39] and [40].

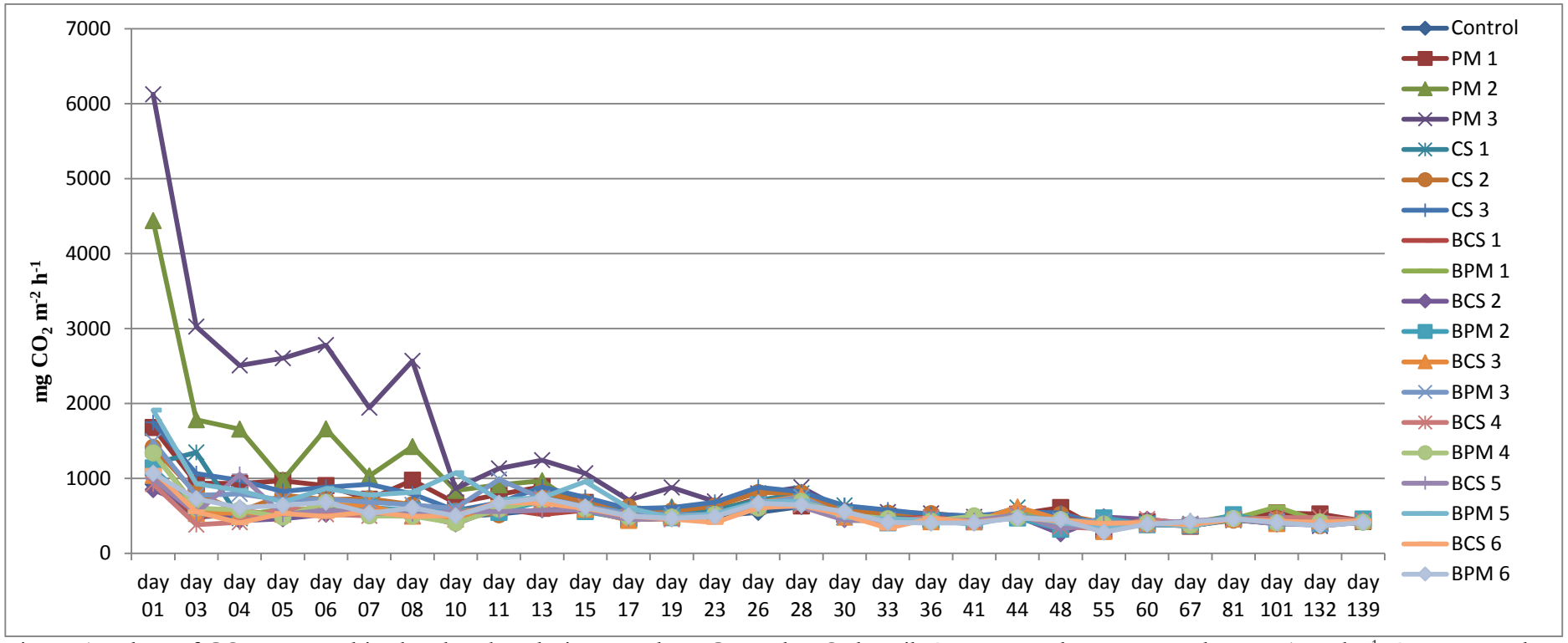

Figure 5 - Flow of CO_2 measured in the chamber during 139 days. Control = Only soil; PM 1 = poultry manure dose 12.5 $Mg.ha^{-1}$; PM 2 = poultry manure dose 25 $Mg.ha^{-1}$; PM 3 = poultry manure dose 50 $Mg.ha^{-1}$; CS 1 = Cane Straw dose 12.5 $Mg.ha^{-1}$; CS 2 = Cane Straw dose 25 $Mg.ha^{-1}$; CS 3 = Cane Straw dose 50 $Mg.ha^{-1}$; BCS 1 = Biochar Cane Straw dose 12.5 $Mg.ha^{-1}$ Temperature of pyrolysis 350 °C; BPM 1 = Biochar poultry manure dose 12.5 $Mg.ha^{-1}$ Temperature of pyrolysis 350 °C; BCS 2 = Biochar Cane Straw dose 12.5 $Mg.ha^{-1}$ Temperature of pyrolysis 650 °C; BPM 2 = Biochar poultry manure dose 12.5 $Mg.ha^{-1}$ Temperature of pyrolysis 650 °C; BCS 3 = Biochar Cane Straw dose 25 $Mg.ha^{-1}$ Temperature of pyrolysis 350 °C; BPM 3 = Biochar poultry manure dose 25 $Mg.ha^{-1}$ Temperature of pyrolysis 350 °C; BCS 4 = Biochar Cane Straw dose 25 $Mg.ha^{-1}$ Temperature of pyrolysis 650 °C; BPM 4 = Biochar poultry manure dose 25 $Mg.ha^{-1}$ Temperature of pyrolysis 650 °C; BCS 5 = Biochar Cane Straw dose 50 $Mg.ha^{-1}$ Temperature of pyrolysis 350 °C; BPM 5 = Biochar poultry manure dose 50 $Mg.ha^{-1}$ Temperature of pyrolysis 350 °C; BCS 6 = Biochar Cane Straw dose 50 $Mg.ha^{-1}$ Temperature of pyrolysis 650 °C; BPM 6 = Biochar poultry manure dose 50 $Mg.ha^{-1}$ Temperature of pyrolysis 650 °C.

The higher emissions by both raw materials, relative to the control, demonstrates that even small quantities of applied feedstocks increase CO_2 emissions (Figure 1a). The higher values of CO_2 emissions by the addition of PM, non-pyrolysed or pyrolysed, than with applied CS (Figure 1a and 1b), suggests greater stability of cane straw and a less drastic effect on the environment, from GHG emissions point of view.

For the raw materials, the CO_2 and CH_4 emissions (Figure 1a and 2a) increased with increasing application rates. According to [41], the waste management is one of the principle causes of GHG emissions in the agricultural environment, which corroborates the loss of C and N after the application of these residues to soil. The higher emission of N_2O (Figure 3a) for the 25 Mg ha^{-1} rate of applied PM (the only one that differs statistically from the control) was attributed to a combination of oxygen and C availability. The hypothesis, based on a perfect environment, which combines oxygen availability and labile C for the microbiota, was found on the intermediate rate. However, this assumption was not confirmed by the values found in the microbial biomass (Table 3), perhaps because these data were obtained only at the end of the experiment, when the GHG emissions were already stable.

We could imply that the absence of statistical difference between the BPM rates of 25 and 50 Mg ha^{-1}, for both pyrolysis temperatures, is due to a "maximum point", above which there is no effect on CO_2 emission. According to [27], the flow of CO_2 presents higher relative reductions with application of raters lower than 20 Mg ha^{-1} of biochar, while the total organic carbon increases at applied rates from 20 to 40 Mg ha^{-1}. This is due to an increase in microbial biomass of 50% in rates lower than 20 Mg ha^{-1}, in contrast to an increase of only 8 % in 20 to 40 Mg ha^{-1} rates. The negative effect of applying high rates of biochar to the soil microbiota is justified by the high C/N ratio of the applied material, inducing N immobilization and reducing microbial activity (Table 3).

The higher emissions of CO_2 and CH_4 (Figure 2b and 3b) from the intermediate rate (25 Mg ha^{-1}) of the BCS, are in agreement with the higher MBN values for these treatments (Table 3) and was attributed to a more beneficial environment at this application rate. [42] and [43] also found a similar pattern in their studies, with application of three different rates of biochar. These authors assumed that the higher gas emission values for the intermediate rate could be due to a combined C/N ratio, coming from the original soil and the biochar. Considering that the soil´s C/N ratio will prevail in the lowest applied rate whereas the biochar´s C/N ratio will prevail at the highest rate, it is plausible to assume that on the intermediate rate there will be an intermediate C/N ratio providing an optimal environment for microbiological growth. Although we did not find a statistical difference for all treatments, we can observe this pattern occurring among

treatments, where the C/N ratio of the intermediate application rate approaches the average of the extreme rates (Table 3).

The higher emissions of GHG for BPM pyrolysed at 350 °C was due to the maintenance of the original characteristics of the material. With pyrolysis temperature at 650 °C, aliphatic chains, aromatic rings and elemental composition of C, N and O are reduced, making the biochar more recalcitrant [44]. Many characteristics, such as ash content, CEC and C/N ratio, vary according to the raw material [45] and [46], which justifies similar CO_2 emission values for the BCS, whether pyrolyzed at 350 or 650 °C. The BCS material is already highly recalcitrant, producing a biochar with lower ash content, lower nutrient diversity and greater surface area [47]. We can also infer that BPM pyrolysed at 650 °C is more efficient in GHGs mitigation, since this procedure will increase surface area, ash content and stability of the biochar [48] and [49], reducing, CO_2 emissions, mostly at higher applied rates. In a study with biochar from sugar cane straw, [50] observed an 80 % loss of N from the material, using a pyrolysis temperature of 750 °C. These authors reached a C/N ratio of 47 after using pyrolysis at 450 °C, whereas the C/N ratio was 280 when pyrolyzed at 750 °C. They also observed a reduction in the H/C and O/C ratios and an increase in the ash content with the increase in the pyrolysis temperature. This suggests an increase in aromatic structures and degree of carbonization, when compared to the raw material. The similarity in CO_2 emissions between the pyrolysis temperatures of BCS (Figure 1b) can be attributed to the nature of the raw material, allowing the inference that there is no advantage in GHG mitigation when pyrolyzing material such as straws at temperatures above 350 °C.

The lower CO_2 emission values of biochars relative to the raw materials, in the same applied rate and pyrolysis temperature (for the biochars), allowed the conclusion that the production of biochars from these raw materials is a viable solution for adding these residues to soil, without an increase in GHG emissions. [51] observed a decomposition of 56 % of the C added as wheat straw after 84 days, while over the same period, only 2.8 % of the C from its respective biochar had decomposed.

However, regardless the higher N_2O emission for the lower rate of BCS application at either pyrolysis temperature (Figure 3b), relative to the control, is probably due to the formation of aerobiotic sites in the extremely porous biochar. This observation leads us to think that increases in this biochar application would increase the availability of oxygen, reducing the anaerobic environment and N_2O emissions. No statistical difference was observed for N_2O emissions from BPM, regardless the applied rate or pyrolysis temperature (Figure 3b). We assume that this material reduces the chance of anaerobiosis through a higher amount of micropores than the BCS, and its lower C/N ratio (Table 3) limits the amount of soluble C available for microbiota performance.

The CO_2 equivalent graph (Figure 4) indicates there are few differences between the combined emission of the three gases and CO_2 emissions alone. In soils that are not flooded or for any reason have hypoxic/anoxic condition, there are no expressive emissions of CH_4 and N_2O. Even though we found statistical differences among some treatments of these two gases, the emission were small. The lack of differences between the highest rates of PM (Figure 4a), differently from CO_2 emissions alone (Figure 1a), is due to the high emission of N_2O in the intermediate rate (25 Mg ha^{-1}) that raised the value close to the rate of 50 Mg ha^{-1} when added into the standard unit. Even though the initial value of N_2O emission in 25 Mg ha^{-1} rate is low (0.23 mg N_2O m^{-2} h^{-1}), its GWP is high (298); when calculated for CO_{2eq} (Equation 3) this contribution is amplified.

Agricultural production, since 1970, has grown 118% and livestock production 102 %, with an increase in emissions of 65 and 119%, per harvest and per head, respectively [19]. This implies that a secure environmental destination has to be found, for plant and animal residues.

2.5. CONCLUSIONS

The biochar from poultry manure causes higher GHG emissions than the biochar produced from sugar cane straw, but both cause a significant reduction in the CO_{2eq} emission and represent an environmentally secure way of depositing residual material in the field. For the poultry manure biochar, higher pyrolysis temperatures have a significant effect in reducing GHG emissions, however this was not observed for the biochar produced from sugar cane straw thus it is much more recalcitrant and is not affected by different managements. There is a greater emission of the three gases when applying the intermediate rate, demonstrated by a greater microbial biomass in this treatment, nevertheless, the cause is still not well known and deserves to be furthered studied.

REFERENCES

[1] Lamb, A., Green, R., Bateman, I., Broadmeadow, M., Bruce, T., Burney, J., Goulding, K. (2016) The potential for land sparing to offset greenhouse gas emissions from agriculture. Nat. Clim. Change. 6, 488-492. doi:10.1038/nclimate2910

[2] Cotrufo, M.F., Soong, J.L., Horton, A.J., Campbell, E.E., Haddix, M.L., Wall, D.H., Parton, W.J. (2015) Formation of soil organic matter via biochemical and physical pathways of litter mass loss. Nat. Geosci. 8, 776–779. doi:10.1038/ngeo2520

[3] Cardozo, N.P., Bordonal, R.D.O., La Scala, N. (2016) Greenhouse gas emission estimate in sugarcane irrigation in Brazil: is it possible to reduce it, and still increase crop yield? J. Clean. Prod. 112, 3988–3997. doi:10.1016/j.jclepro.2015.09.040

[4] Madari, B.E., de Freitas Maia, C.M.B., Novotny, E.H. (2012) Preface: Context and importance of biochar research. Pesqui. Agropecu. Bras. 47, 1–2. doi:10.1590/S0100-204X2012000500001

[5] Agegnehu, G., Bass, A.M., Nelson, P.N., Bird, M.I. (2016) Benefits of biochar, compost and biochar-compost for soil quality, maize yield and greenhouse gas emissions in a tropical agricultural soil. Sci. Total Environ. 543, 295–306. doi:10.1016/j.scitotenv.2015.11.054

[6] Smith, P. (2016) Soil carbon sequestration and biochar as negative emission technologies. Glob. Chang. Biol. 22, 1315–1324. doi:10.1111/gcb.13178

[7] Verheijen, F., Jeffery, S., Bastos, A.C., Van Der Velde, M., Diafas, I. (2010) Biochar application to soils: a critical review of effects on soil properties, processes and functions, JRC Scientific and technical Report. doi:10.2788/472

[8] Sánchez-García, M., Sánchez-Monedero, M.A., Roig, A., López-Cano, I., Moreno, B., Benitez, E., Cayuela, M.L. (2016) Compost vs biochar amendment: a two-year field study evaluating soil C build-up and N dynamics in an organically managed olive crop. Plant Soil 408, 1–14. doi:10.1007/s11104-016-2794-4

[9] Atkinson, C.J., Fitzgerald, J.D., Hipps, N.A. (2010) Potential mechanisms for achieving agricultural benefits from biochar application to temperate soils: A review. Plant Soil, 337, 1–18. doi:10.1007/s11104-010-0464-5

[10] Lehmann, J., Joseph, S. (2015) Biochar for environmental management: science, technology and implementation, Routledge.

[11] Puga, A.P., Abreu, C.A., Melo, L.C.A., Paz-Ferreiro, J., Beesley, L. (2015) Cadmium, lead, and zinc mobility and plant uptake in a mine soil amended with sugarcane straw biochar. Environ. Sci. Pollut. Res. 22, 17606–17614. doi:10.1007/s11356-015-4977-6

[12] Teichmann, I. (2014) Technical greenhouse-gas mitigation potentials of biochar soil incorporation in Germany, Berlim, DIW Discussion Paper, 1406, pp. 92.

[13] IPCC; Intergovernmental Panel on Climate Change, 2015 Climate Change 2014: Mitigation of Climate Change (Vol. 3), Cambridge University Press.

[14] CONAB - Companhia Nacional de Abastecimento Acompanhamento da safra Brasileira: Cana de açúcar; agosto/2013. Conab, Brasília, p 19.

[15] Castro, L.T., Fava Neves, M., Fava Scare, R. (2015). Eficiência de representação das associações de produtores de cana-de-açúcar no Brasil. Organizações Rurais & Agroindustriais, 17(3).

[16] Orlando, F.J., Carmello, Q.A.C., Pexe, C.A., Glória, A.M. (1994) Adubação de soqueira de cana-de-açúcar sob dois tipos de despalha: cana crua x cana queimada. STAB- Açúcar, Álcool e Subprodutos, Piracicaba, 12(4), 7-11.

[17] Goldemberg, J., Nigro, F.E.B., Coelho, S.T. (2008) Bioenergia no estado de São Paulo: situação atual, perspectivas e propostas. São Paulo: Imprensa Oficial do Estado de São Paulo, pp. 152.

[18] Melo, L.C.A., Puga, A.P., Coscione, A.R., Beesley, L., Abreu, C.A., Camargo, O.A. (2016) Sorption and desorption of cadmium and zinc in two tropical soils amended with sugarcane-straw-derived biochar. J. Soils Sediments 16, 226–234. doi:10.1007/s11368-015-1199-y

[19] Bennetzen, E.H., Smith, P., Porter, J.R. (2016) Agricultural production and greenhouse gas emissions from world regions - The major trends over 40 years. Glob. Environ. Chang. 37, 43–55. doi:10.1016/j.gloenvcha.2015.12.004

[20] Vieira, A.S. (2015) Gestão Ambiental: Uma Visão Multidisciplinar. Clube de Autores, São Paulo, pp. 285.

[21] Gaunt, J., Cowie, A. (2009) Biochar, greenhouse gas accounting and emissions trading, in: Lehmann, J., Joseph, S. (Eds.), Biochar for environmental management: Science and technology, Earthscan, London, pp. 317-340.

[22] Woolf, D., Amonette, J.E., Street-Perrott, F.A., Lehmann, J., Joseph, S. (2010) Sustainable biochar to mitigate global climate change. Nature Commun. 1, 56. doi: 10.1038/ncomms1053

[23] Hammond, J., Shackley, S., Sohi, S., Brownsort, P. (2011) Prospective life cycle carbon abatement for pyrolysis biochar systems in the UK. Energy Policy 39, 2646–2655. doi:10.1016/j.enpol.2011.02.033

[24] Roberts, K.G., Gloy, B.A., Joseph, S., Scott, N.R., Lehmann, J. (2010) Life cycle assessment of biochar systems: Estimating the energetic, economic, and climate change potential. Environ. Sci. Technol. 44, 827–833. doi:10.1021/es902266r

[25] Wu, F., Jia, Z., Wang, S., Chang, S.X., Startsev, A. (2013) Contrasting effects of wheat straw and its biochar on greenhouse gas emissions and enzyme activities in a Chernozemic soil. Biol. Fertil. Soils 49, 555–565. doi:10.1007/s00374-012-0745-7

[26] Rondon, M.A., Molina, D., Hurtado, M., Ramirez, J., Lehmann, J., Major, J., Amezquita, E. (2006) Enhancing the productivity of crops and grasses while reducing greenhouse gas emissions through bio-char amendments to unfertile tropical soils. In 18th World Congress of Soil Science, pp. 9-15.

[27] Liu, Y., Yang, M., Wu, Y., Wang, H., Chen, Y., Wu, W. (2011) Reducing CH4 and CO2 emissions from waterlogged paddy soil with biochar. J. Soils Sediments 11, 930–939. doi:10.1007/s11368-011-0376-x

[28] EMBRAPA (2006). Sistema brasileiro de classificação de solos. Centro Nacional de Pesquisa de Solos: Rio de Janeiro.

[29] Novais, R.F., Smith, T.J. Fósforo em solo e planta em condições tropicais. Viçosa: UFV-DPS, 1999. p.62-64.

[30] Conz, R.F. (2015) Caracterização de matérias-primas e biochars para aplicação na agricultura. Master's Thesis– University of São Paulo/ESALQ, São Paulo, pp. 135.

[31] Crombie, K., Mašek, O., Cross, A., Sohi, S. (2015) Biochar - synergies and trade-offs between soil enhancing properties and C sequestration potential. GCB Bioenergy, 7, 1161–1175. doi:10.1111/gcbb.12213

[32] Reichardt, K. (1988) Capacidade de campo. Rev. Bras. Ciência do Solo. 12: 211-216.

[33] ASTM D 5373/2008; Standard test methods for instrumental determination of carbon, hydrogen, and nitrogen in laboratory samples of coal and coke, American Society for Testing and Materials (ASTM), Pennsylvania.

[34] Tedesco, M.J., Gianello, C., Bissani, C.A., Bohnen, H., Volkweiss, S.J. Análise de solo, plantas e outros materiais. Porto Alegre, Universidade Federal do Rio Grande do Sul, 1995. 174p. Boletim técnico, 5.

[35] Sánchez-Monedero, M.A., Serramiá, N., Civantos, C.G.O., Fernández-Hernández, A., Roig, A. (2010) Greenhouse gas emissions during composting of two-phase olive mill wastes with different agroindustrial by-products. Chemosphere. 81(1), 18-25. doi:10.1016/j.chemosphere.2010.07.022

[36] Wang, W., Wu, X., Chen, A., Xie, X., Wang, Y., & Yin, C. (2016) Mitigating effects of ex situ application of rice straw on CH4 and N2O emissions from paddy-upland coexisting system. Scientific Reports, 6. doi:10.1038/srep37402

[37] Team, R.C. (2015) R: a language and environment for statistical computing, Vienna, Austria.

[38] Gomez, J. D., Denef, K., Stewart, C. E., Zheng, J., & Cotrufo, M. F. (2014) Biochar addition rate influences soil microbial abundance and activity in temperate soils. European Journal of Soil Science, 65(1), 28-39. doi:10.1111/ejss.12097

[39] Budai, A., Rasse, D. P., Lagomarsino, A., Lerch, T. Z., & Paruch, L. (2016) Biochar persistence, priming and microbial responses to pyrolysis temperature series. Biology and Fertility of Soils, 52(6), 749-761.

[40] Jiang, X., Denef, K., Stewart, C. E., Cotrufo, M. F. (2016) Controls and dynamics of biochar decomposition and soil microbial abundance, composition, and carbon use efficiency during long-term biochar-amended soil incubations. Biology and Fertility of Soils 52(1), 1-14. doi:10.1007/s00374-015-1047-7

[41] Pratt, C., Redding, M., Hill, J., Shilton, A., Chung, M., Guieysse, B. (2015) Good science for improving policy: Greenhouse gas emissions from agricultural manures. Anim. Prod. Sci. 55, 691–701. doi:10.1071/AN13504

[42] Asai, H., Samson, B.K., Stephan, H.M., Songyikhangsuthor, K., Homma, K., Kiyono, Y., Inoue, Y., Shiraiwa, T., Horie, T. (2009) Biochar amendment techniques for upland rice production in Northern Laos. 1. Soil physical properties, leaf SPAD and grain yield. F. Crop. Res. 111, 81–84. doi:10.1016/j.fcr.2008.10.008

[43] Gaskin, J.W., Speir, R.A., Harris, K., Das, K.C., Lee, R.D., Morris, L.A., Fisher, D.S. (2010) Effect of peanut hull and pine chip biochar on soil nutrients, corn nutrient status, and yield. Agron. J. 102, 623–633. doi:10.2134/agronj2009.0083

[44] Cimo, G., Kucerik, J., Berns, A.E., Schaumann, G.E., Alonzo, G., Conte, P. (2014) Effect of heating time and temperature on the chemical characteristics of biochar from poultry manure. J. Agric. Food Chem. 62, 1912–1918. doi:10.1021/jf405549z

[45] Kloss, S., Zehetner, F., Dellantonio, A., Hamid, R., Ottner, F., Liedtke, V., Schwanninger, M., Gerzabek, M.H., Soja, G. (2011) Characterization of slow pyrolysis biochars: effects of feedstocks and pyrolysis temperature on biochar properties. J. Environ. Qual. 41, 990–1000. doi:10.2134/jeq2011.0070

[46] Novotny, E.H., Maia, C.M.B. de F., Carvalho, M.T. de M., Madari, B.E. (2015) Biochar: Pyrogenic Carbon for Agricultural Use - a Critical Review. Rev. Bras. Ciência do Solo 39, 321–344. doi:10.1590/01000683rbcs20140818

[47] Deng, W., van Zwieten, L., Lin, Z., Liu, X., Sarmah, A.K., Wang, H. (2016) Sugarcane bagasse biochars impact respiration and greenhouse gas emissions from a latosol. J. Soils Sediments 1–9. doi:10.1007/s11368-015-1347-4

[48] Heitkötter, J., Marschner, B. (2015) Interactive effects of biochar ageing in soils related to feedstock, pyrolysis temperature, and historic charcoal production. Geoderma 245–246, 56–64. doi:10.1016/j.geoderma.2015.01.012

[49] Ronsse, F., van Hecke, S., Dickinson, D., Prins, W. (2013) Production and characterization of slow pyrolysis biochar: Influence of feedstock type and pyrolysis conditions. GCB Bioenergy 5, 104–115. doi:10.1111/gcbb.12018

[50] Jeong, C.Y., Dodla, S.K., Wang, J.J. (2016) Fundamental and molecular composition characteristics of biochars produced from sugarcane and rice crop residues and by-products. Chemosphere 142, 4–13. doi:10.1016/j.chemosphere.2015.05.084

[51] Zavalloni, C., Alberti, G., Biasiol, S., Vedove, G.D., Fornasier, F., Liu, J., Peressotti, A. (2011) Microbial mineralization of biochar and wheat straw mixture in soil: A short-term study. Appl. Soil Ecol. 50, 45–51. doi:10.1016/j.apsoil.2011.07.012

[52] Abruzzini, T.F. (2015) The role of biochar on greenhouse offsets, improvement of soil attributes and nutrient use efficiency in tropical soils. PhD Thesis – University of São Paulo/ESALQ, São Paulo, pp. 104.

3. MITIGATION OF GREENHOUSE GASES BASED ON THE APPLICATION OF BIOCHARS WITH DIFFERENTE PH VALUES IN SOILS WITH DIFFERENT TEXTURES

ABSTRACT

The need to reduce greenhouse gas (GHG) emissions means that environmentally safe waste disposal techniques are sought. Biochar, a product of pyrolysis under controlled atmosphere, appears in several studies as a mitigator of the emissions of waste used for its production and of the soil that receives it. In this work, biochars of poultry manure and sugarcane straw, pirolysed at 350 and 650 °C were applied in three doses (12.2, 25 and 50 Mg ha^{-1}), with their original pH and modified to 5.5, in a sandy soil and a clayey soil. The quantification of the three GHGs (CO_2, CH_4 and N_2O) was done by gas chromatography and a model for the CO_2 emission of poultry manure biochar was proposed at the end of the experiment. The pyrolysis of these materials significantly reduces the emission of gases, and the increase in the pyrolysis temperature increases the mitigation potential of the biochars. The reduction of the original pH to 5.5 causes an effect similar to elevation of pyrolysis temperature. The mitigating effect of biochars is better seen in the sandy soil, since the clayey soil has high buffering power and needs higher doses for the same response. The CO_2 emission is explained by the variables dose, pyrolysis temperature, pH and soil texture, with high R^2 for the proposed model.

Keywords: CO_2; CH_4; N_2O; Pyrolysis; Sandy soil; Clayey soil; Model

3.1. INTRODUCTION

It is increasingly necessary to reduce greenhouse gas (GHG) emissions, based on improved land use and soil management techniques, as well as environmentally secure forms of waste disposal (Lamb et al., 2016). The various types of organic waste may undergo a pyrolysis process, becoming more stable, thereby increasing their residence time in the soil and their ability to sequester carbon. This pyrolyzed waste is referred to as "biochar" (Brunn et al., 2017; Deng et al., 2017). The pyrolysis process occurs in an environment with little or no oxygen (hypoxic or anoxic) and leads to the thermal degradation of the biomass constituents, producing, in addition to charcoal, condensable gases, and vapors. This process increases the number of aromatic components, which are more resistant to microbial degradation, making the pyrolyzed material more recalcitrant compared to its original biomass (Lehmann & Joseph, 2015).

The wide choice of raw materials for biochar production and the pyrolysis temperature define many of its characteristics and determine its capacity as a GHG mitigator (Lehmann & Joseph, 2015, Shackley et al., 2016). Higher-recalcitrance raw materials (higher lignin content, lower nutrient content, higher C content, and higher C/N ratio, among other characteristics) and higher pyrolysis temperatures produce biochars with greater potential for mitigation (Agegnehu et al. 2016; Conz et al., 2017). Soil characteristics such as water retention capacity and texture also exert an influence on biochar's GHG mitigation potential (Lehmann & Joseph, 2015), but little is known about these effects.

Ameloot et al. (2016) reported the biochar mechanisms involved in reducing N_2O emission. The application of biochar resulted in an increase in soil porosity, leading to greater aeration and the subsequent inhibition of denitrification while suppressing the emissions of this gas. These authors found support in works such as Abel et al. (2013), who report that the application of biochar reduces soil density.

Soil texture plays a role in favoring C and N mineralization, while clayey soils have greater protection against decomposition and less biochar exposure to microbial activity (Stewart et al., 2013). Butnan et al. (2015) conclude that biochar is more beneficial to sandy than clayey soils. These authors found an ideal dose of 1 % m/m for sandy soil and 2 % m/m for clayey soil, considering the same biochar. The reason for this effect lies in the finer texture and higher buffering power of the clayey soils, requiring a higher dose to observe the positive effects of the biochar application.

Some biochars produce high ash content, which is usually accompanied by high nutrient content, an attribute that controls soil pH and CEC (Butnan et al., 2015). These characteristics depend on the material used in the production of the biochar and its pyrolysis temperature. Lower temperatures during the process produces a biochar with characteristics closer to its source material (Agegnehu et al., 2016). Beneficial biochar characteristics such as increased CEC and pH are more significant in clayey soils (Abujabhah et al., 2016). These authors have found, after application of eucalyptus biochar, a greater increase of CEC and pH in soils with higher clay content, leading to higher ammonium leaching in these soils.

In Brazil, a large portion of the territory is covered by very weathered soils, typical of regions of tropical climate, where acidity provides aluminum toxicity (Ferraz et al., 2015). Yuan et al (2012) reported the reduction of aluminum toxicity in acidic soils in China after the application of biochar. This fact was corroborated by the decrease in the exchangeable acidity of the soil and the increase in CEC due to the basic cations from the source material. According to Yuan et al (2011), during the incubation, exchanges occur between the exchangeable acidity of the soil and

the basic cations of the biochars, leading to its decrease. The concentration of basic cations depends on the raw material used to produce biochar, and these authors found the highest levels in the biochars produced from legumes and corn straw. Dai et al. (2014) have demonstrated the importance of the alkalinity of biochar on its ability to reduce soil acidity. In the comparison between biochar produced from pig manure and sugarcane straw, these authors found a six-fold higher pH soil conditioning power for the swine manure biochar. This fact being corroborated by the higher concentration of alkaline substances inherited from the raw material. These authors also reported an increase in the pH buffering power of soils, the highest values being found on biochar from swine manure.

The purpose of this paper was to quantify GHG emissions based on the application of biochar from poultry manure and sugarcane straw, in two pH values, in a sandy soil and a clayey soil, compared to their respective raw materials.

3.2. MATERIAL AND METHODS

3.2.1. Raw material and biochar production

Sugarcane straw and poultry manure were used as raw materials for this study. The sugarcane straw was collected in a planting area of a power plant in Piracicaba, state of São Paulo, while the poultry manure originated in a farm located at the Luiz de Queiroz College of Agriculture (ESALQ-USP). Such materials were chosen due to their large production, which raises concern regarding their accumulation in the field. With recent laws prohibiting the burning of sugarcane straw and the high GHG emissions from the poultry manure, along with its difficult storage and transportation, biochar becomes an interesting option for this waste (Conz et al., 2017).

The raw materials were dried at 45 °C, ground in a ball mill and sieved to 2 mm, forming a homogeneous material, to be mixed later in the soil. For the production of their respective biochars, the raw materials were submitted to pyrolysis at two temperatures – 350 and 650 °C. The pyrolysis process was carried out by the company SPPT in a metal reactor, saturating the sample with N_2 and raising the temperature by 10 °C every minute during the first 30 min and after the initial 30 min at 20 °C at each minute, until reaching the desired temperature (Conz et al., 2017). The biochars were passed through a 2-mm sieve until they formed a homogeneous material that could be mixed with the soil.

3.2.2. Soil characteristics and sampling

Two soils with distinct textures, under native forest, were used in this study (Table 1): (1) Typic Quartzipsamment, collected in the region of Anhembi, state of São Paulo (22°43'31.1" S and 48°01'20.2" W); (2) Oxisol collected at ESALQ, (22°42'05.1" S and 47°37'45.2" W). The soils were sampled in the 0-20 cm layer, air-dried and passed through a 2-mm sieve. Samples with 50 g of soil were incubated with their raw materials and respective biochars.

Table 1. Properties of soil samples used to evaluate the effects of biochars from sugarcane straw and poultry manure and their raw materials.

Soil	Sand/Silt/Clay	pH*	C	N	C/N
	($g\ kg^{-1}$)		%		
(1) Quartzipsamment	900 / 22 / 78	4.1±0.1	0.9±0.1	0.1±0.0	14.3±0.1
(2) Oxisol	406 / 277 / 317	6.2±0.0	1.9±0.1	0.2±0.0	11.3±0.2

Source: Abruzzini, T. F. The role of biochar on greenhouse makes offsets, soil improvement and nutrient use efficiency in tropical soils. 2015. 104 p. Thesis (Doctorate in Sciences) - Luiz de Queiroz College of Agriculture, University of São Paulo, São Paulo. 2015.
Mean ± standard deviation (n = 3). *pH in $CaCl_2$.

3.2.3. Experimental units

The raw materials and their respective biochars were placed in glass vials with a capacity of 650 mL and homogenized with soils with humidity corresponding to 60 % of the field capacity. This value was necessary to maintain the activity of the microorganisms (Reichardt, 1988). A small vial of deionized water was placed in each experimental unit to maintain moisture during the experiment. The experiment consisted of three levels of the dose factor (12.5, 25, and 50 Mg ha^{-1}), two levels of the biochar factor (sugarcane straw biochar and poultry manure biochar), two pyrolysis temperatures (350 and 650 °C) two pH values (original pH of the biochars – 7.5 for the BPM and 8.8 for the BCS; and pH 5.5), two soils (sandy and clayey) – only the treatment with modified pH being carried out in the sandy soil, and two controls (sandy soil only and clayey soil only), with four replications. For the clayey soil, an additional treatment was carried out, with the addition of the raw materials, in the same three doses. The values emitted by the raw material incubated with the sandy soil and by the sandy soil in its original pH for the different treatments were obtained in a previous experiment (Novais et al., 2017) and used in the analysis and comparison of the results.

The highest dose of biochar applied (50 Mg ha^{-1}) was suggested by Woolf et al. (2010), which assume that this is the maximum application rate of biochar in agricultural soils, which still causes positive response of the biochar/soil interaction. The other doses were defined based on its division.

The alteration of the original biochar pH of 7.5 in the poultry manure and 8.8 in the sugarcane straw to a final pH of 5.5 for both occurred daily with the biochars suspended in distilled water and addition of HCl 0.1 mol L^{-1}, until the desired pH was reached, guaranteeing its maintenance for three days. After the pH adjustment, the biochars were oven-dried and mixed with soils, following the same procedures as the other treatments.

The experimental units were maintained at the Soil Organic Matter Laboratory of the Department of Soil Science of ESALQ/USP at a constant temperature of 25 °C. The experiment was conducted for six months, guaranteeing that, at the end of the experiment, the treatments did not differ statistically from the control, with the gases emissions stabilized from day 36.

3.2.4. Gas collection

Gas collection was carried out daily during the first 15 days of incubation and spaced as the experiment was extended. The vials were closed for 30 minutes for the collection of gases with 25 mL syringes. Six empty vials, considered time zero, were added to the experiment to subtract the gases emitted by the environment at the time of collection (Equation 1). The gas volumes collected at each time were immediately transferred to vials under vacuum and then analyzed in a chromatograph (SRI 8610 – SRI Instruments) using a Flame Ionization Detector (FID) and a 63Ni Electron Capture Detector (ECD), which allowed the quantification of CO_2, CH_4 and N_2O, all in the same sample.

$$ELT = EAT - EAA \quad \text{(Equation 1)}$$

Where: ELT is the net GHG emission from the treatment; EAT is the cumulative emission of GHG in the treatment, disregarding the emission of the environment; EAA is the accumulated emission of GHG in the empty vials and regarding the emission of the environment at that time.

3.2.5. Post-incubation analyzes

At the end of the experiment, the mixtures with soil, biochars and source materials were recovered and used for analysis of carbon (C), nitrogen (N), and microbial biomass carbon and nitrogen (MBC and MBN). To obtain the C and N contents, the samples were analyzed by combustion using Leco TruSpec® CHN the elemental analyzer, according to ASTMD 5373/2008. The MBC and MBN were determined by the fumigation-extraction process proposed by Tedesco et al. (1995) and the extracts were analyzed in the Shimadzu Total Organic Carbon Analyzer (TOC-L) and Total Organic Nitrogen Analyzer (TON-L).

3.2.6. Data analysis

The data obtained from the raw materials were submitted to variance analysis. The experimental design was completely randomized in a 2x2x3 factorial scheme, with additional treatment [(2x2x3) +1] and four replications. The factors were combined for raw material, texture, doses, and treatment control, respectively. The data from the biochars were treated with the same experimental design, in a 2x2x2x2x3 factorial scheme, and factors combined with biochars, temperature, texture, pH, and doses, with four replications, respectively, as well as additional treatment.

The gas concentration averages were used in the flow and accumulation calculation and were submitted to the adjustment of a second-order polynomial equation (gas concentration versus time), according to Sánchez-Monedero et al. (2010). The flows at time zero were calculated by the derivative of the second-order equations and expressed per gram of C or N per unit area (m^2) and time (d). The means were discriminated and compared in the treatments using a 95 % confidence interval. The treatments were considered statistically non-different when the mean intervals overlapped. Statistical and graphical assessment were performed using the *plotrix* and *agricolae* packages, available in the R software program (R Core Team, 2017).

3.2.7. Model

The effects of clay content (C_{clay}), pH, pyrolysis temperature ($T_{pyolysis}$) and biochar doses applied ($D_{biochar}$) on CO_2 emission were evaluated quantitatively by multiple linear regression for the biochars of poultry manure and sugarcane straw (that is, a model generated and tested for each raw material), in which the model was statistically adjusted according to the expression:

$$y_i = \beta_0 + \beta_1 C_{clay} + \beta_2 pH + \beta_3 T_{pyrolysis} + \beta_4 D_{biochar} + \varepsilon \quad (1)$$

in which y_i is the i-th observation of CO_2 ($i = 1, 2, \ldots, n$), β_j are the model parameters ($j = 0, 1, \ldots, 7$), ε_i is the random error associated with observation y_i.

The least square estimates of the βj parameters were obtained using the Gauss-Newton algorithm. Student's t-test was applied to these estimations for selection of variables with significant effects at 95 % probability.

The quality of the equation adjustment was evaluated by means of the adjusted multiple coefficient (R^2_{Aj}) for the number of parameters (p), considering *n* observations, given by:

$$R^2_{Aj.} = \frac{R^2(n-1)-p}{n-p-1} \quad (2)$$

Confidence bands at 95 % probability were adjusted to the prediction of the significant models using the *"predict"* function in the R software program (R Core Team, 2017), in order to compare predicted and measured values. All modeling, adjustment and significance testing procedures were performed through the R software (R Core Team, 2017).

3.2.8. Model validation

To validate the model, two procedures, described here as internal (IV) and external (EV) validation, were used. The IV was performed with experimental data from the adjustment stage of the equation, while the EV was performed with independent experimental data (Conz et al., 2017). For this purpose, the procedure described by Smith et al. (1997), which compares the sensitivity of predictions with respect to measurements via statistical parameters, was used.

3.2.9. Simulations

Simulations with the adjusted model were made to investigate the behavior of CO_2 as a function of each explanatory variable (i.e., C_{clay}, pH, $T_{pyolysis}$, and $D_{biochar}$). The simulations were performed by numerically changing the explanatory variable under analysis, within the scope of this study, and setting the other explanatory variables, according to the scenarios in Table 2.

Table 2. Scenarios for simulation of CO_2 emission as a function of the variation of clay content (C_{clay}), pH, pyrolysis temperature ($T_{pyolysis}$) and doses of biochar applied ($D_{biochar}$).

Explanatory variable evaluated	C_{clay}	pH	$T_{pyrolysis}$	$D_{biochar}$
	g k^{-1}	-	°C	Mg ha^{-1}
C_{clay}	78 - 17	7.5	350 and 650	50
pH	78	5.5 - 7.5	350 and 650	50
$T_{pyrolysis}$	78	7.5	350 - 50	50
$D_{biochar}$	78	7.5	350 and 650	12.5 - 50

In order to observe the effects of the variations of the attributes on the emission of CO_2, the variable dose was set at 50 Mg ha^{-1}, as this value is considered as the maximum viable biochar amount to be applied to the soil (Woolf et al., 2010). The pH variable was set at 7.5 – the average pH value of the biochars – and the pyrolysis temperature variable was fixed at 350 °C (a) and at 650 °C (b), as they covered the main transformation phases of the raw material. Temperatures below 350 °C are considered to be roasting, as opposed to pyrolysis, whereas pyrolysis above 650 °C results in insufficient yields (Crombie et al., 2015). The clay content was fixed at 78 % – the value corresponding to the sandy soil used in the experiment and responsible for the greater responses to the treatment variations.

3.3. RESULTS AND DISCUSSION

The emission values for the raw materials and the respective biochars, in their original pH, and after being applied to the sandy soil, were obtained in a previous experiment (Novais et al., 2017) and will be used throughout the discussion of this article.

3.3.1. Source material

The application of the source material – Poultry manure (PM) or cane straw (CS) – leads to gas emissions (Figure 1) equal to or greater than the control (soil only), with both residues being higher than the emissions of their respective biochars (Figure 2, 3, and 4). Despite the non-statistical difference for the lower dose (12.5 Mg ha^{-1}) of both raw materials compared to the control (Figure 1a), the pattern is not maintained for the higher doses, with CO_2 emissions exceeding soil

as a control, which encourages us to find a way to dispose of this waste in an environmentally safe manner.

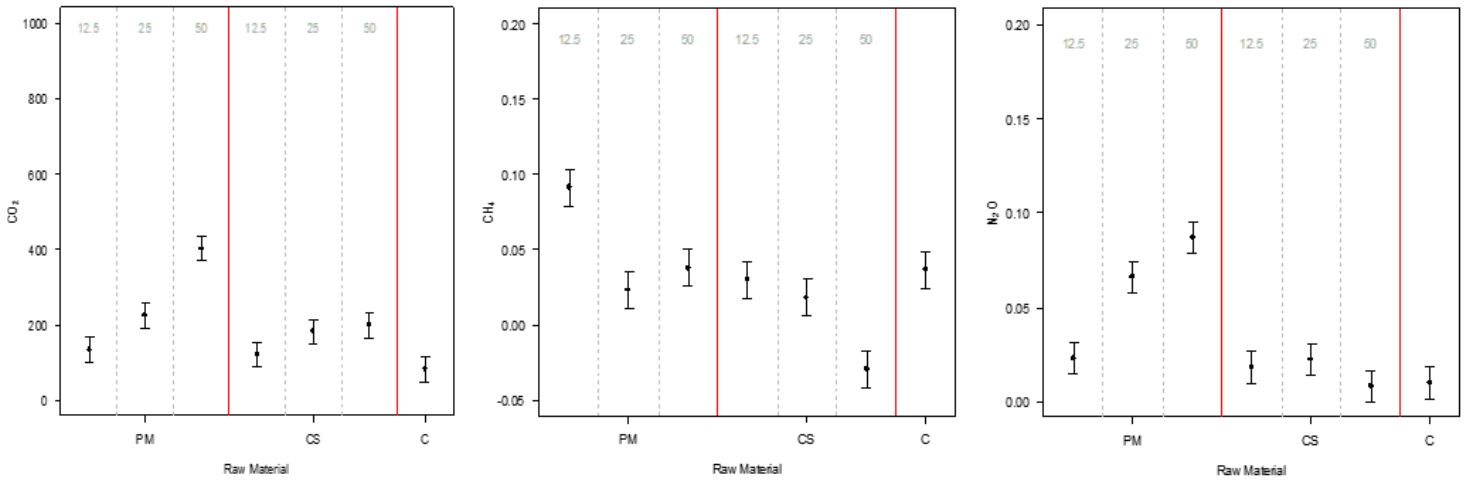

Figure 1. Emissions of CO_2, CH_4 and N_2O of the poultry manure (PM) and cane straw (CS) as raw materials and the control (C).

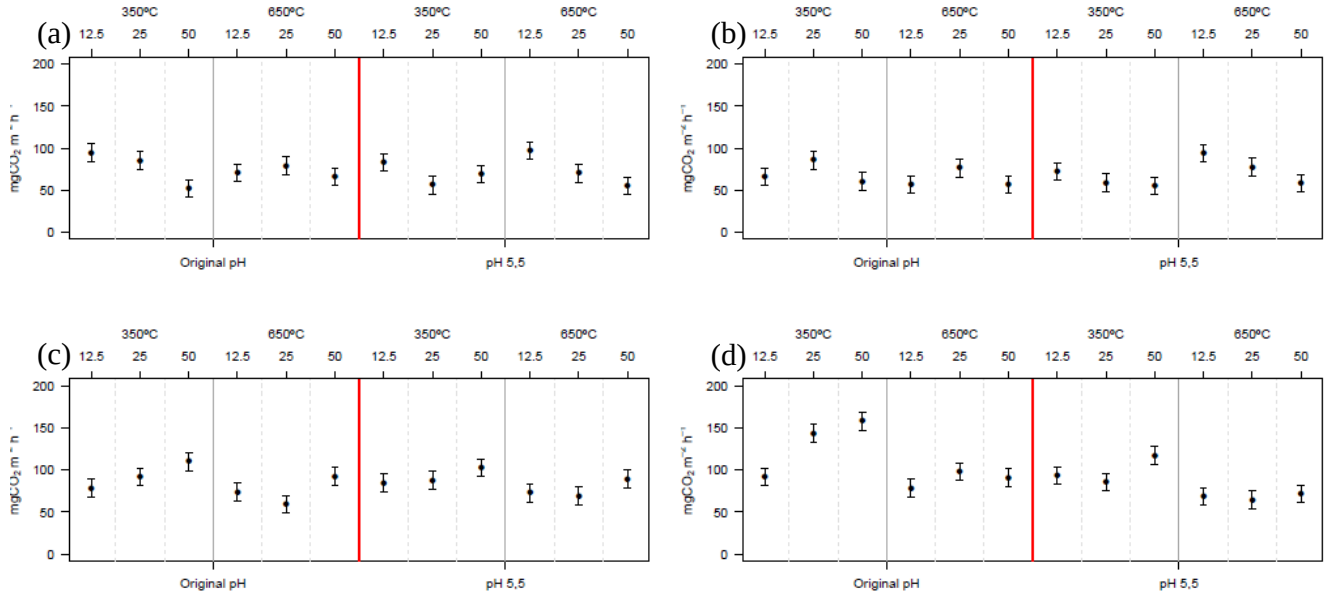

Figure 2. CO_2 emissions from the clayey soil with sugarcane straw biochar applied (a), from the sandy soil with sugarcane straw biochar applied (b), from the clayey soil with poultry manure biochar applied (c) and from the sandy soil with poultry manure biochar applied (d).

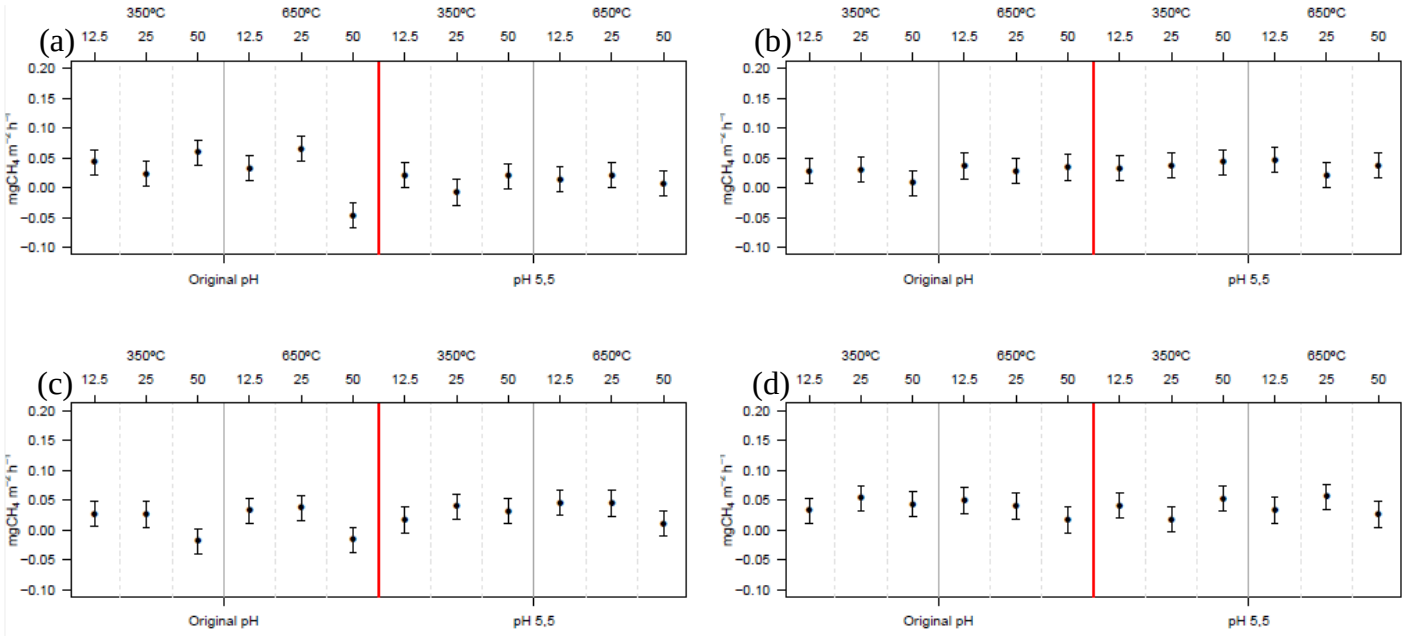

Figure 3. CH_4 emissions from the clayey soil with sugarcane straw biochar applied (a), from the sandy soil with sugarcane straw biochar applied (b), from the clayey soil with poultry manure biochar applied (c) and from the sandy soil with poultry manure biochar applied (d).

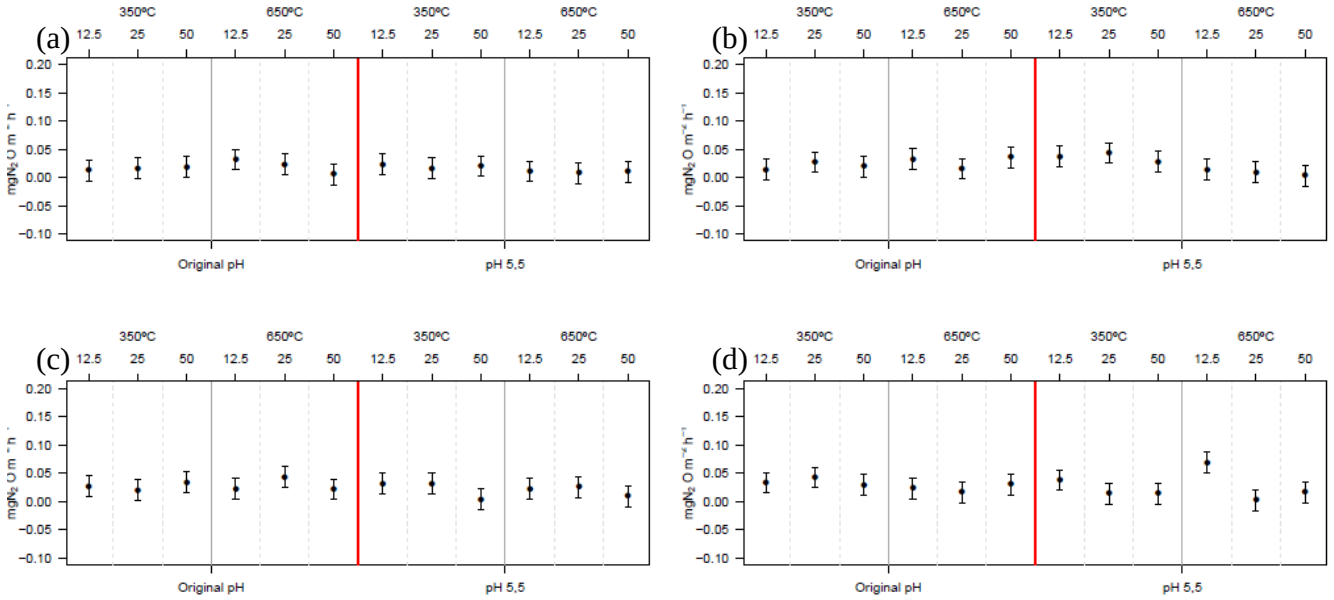

Figure 4. N_2O emissions from the clayey soil with sugarcane straw biochar applied (a), from the sandy soil with sugarcane straw biochar applied (b), from the clayey soil with poultry manure biochar applied (c) and from the sandy soil with poultry manure biochar applied (d).

For the CH_4 emissions (Figure 1b), only the lowest dose of PM applied as raw material results in an emission superior to the control, finding support in its higher MBC value (Table 3), compared to the MBC of the control and the intermediate dose (25 Mg ha^{-1}). The higher doses (25 and 50 Mg ha^{-1}) of PM applied generated higher N_2O emissions than the control (Figure 1c), which

are also in agreement with the higher MBN values (Table 3), compared to the lower dose and the control.

Table 3. Crbon (C), nitrogen (N), and microbial biomass carbon and nitrogen (MBC and MBN) in the clayey soil and in the sandy soil.

Raw material											
Treatment	**Dose**	**MBC**		**MBN**		**C**		**N**		**C/N**	
	–Mg ha^{-1}–	——————————mg L^{-1}——————————									
Clayey soil[(1)]											
Control	0	71.29		26.33922		0.27		2.763		10	
PM	12.50	95.15	a§	41.85	bc	0.35	a	3.19	a	9	a
	25.00	76.84	b	68.44	b	0.36	a	3.19	a	8	a
	50.00	108.63	a	311.8	a	0.42	a	3.35	a	7	a
CS	12.50	83.38	b	18.29	b	0.29	a	3.03	ab	10	ab
	25.00	60.19	b	29.25	b	0.30	a	3.49	ab	11	ab
	50.00	166.01	a	41.53	a	0.31	a	4.37	a	13	a
Biochar											
Sandy soil (pH 5.5)[(2)]											
PMB 350 °C	12.50	202.41	a	122.54	b	0.06	a	0.95	a	15	a
	25.00	178.97	b	119.25	b	0.16	a	1.29	a	9	b
	50.00	185.46	a	145.46	a	0.10	a	1.45	a	16	a
PMB 650 °C	12.50	117.80	b	76.86	b	0.07	a	0.96	ab	16	b
	25.00	129.84	b	95.64	a	0.07	a	1.18	ab	17	b
	50.00	153.65	a	67.53	b	0.09	a	1.74	a	20	a
CSB 350 °C	12.50	126.85	a	75.33	a	0.07	a	1.23	bc	17	bc
	25.00	81.63	b	60.40	a	0.08	a	1.67	b	20	b
	50.00	90.19	b	76.76	a	0.11	a	2.96	a	27	a
CSB 650 °C	12.50	88.76	a	75.67	b	0.07	a	1.24	c	21	b
	25.00	39.37	c	93.59	a	0.08	a	2.03	b	29	ab
	50.00	67.71	b	67.00	b	0.09	a	3.03	a	34	a
Clayey soil (original pH)											
PMB 350 °C	12.50	119.14	b	39.34	a	0.29	a	3.17	a	10	a
	25.00	69.00	c	21.07	b	0.30	a	3.45	a	11	a
	50.00	160.67	a	19.51	b	0.33	a	3.89	a	11	a
PMB 650 °C	12.50	11.04	b	12.05	ab	0.31	a	3.32	a	10	a
	25.00	10.41	b	16.41	a	0.29	a	3.34	a	11	a
	50.00	70.94	a	17.29	a	0.31	a	3.69	a	11	a
CSB 350 °C	12.50	37.32	b	23.51	a	0.26	a	3.63	ab	14	ab
	25.00	23.15	bc	27.81	a	0.26	a	3.96	ab	15	ab
	50.00	60.63	a	15.30	b	0.28	a	5.03	a	18	a
CSB 650 °C	12.50	46.49	a	17.61	a	0.28	a	3.36	ab	11	ab
	25.00	47.56	a	12.87	ab	0.28	a	3.97	ab	13	ab
	50.00	45.97	a	12.26	ab	0.31	a	5.09	a	16	a

Clayey soil (pH 5.5)											
PMB 350 °C	12.50	112.96	a	41.96	a	0.31	a	3.26	a	10	a
	25.00	82.17	ab	28.08	b	0.34	a	3.56	a	10	a
	50.00	89.64	ab	22.27	b	0.36	a	4.00	a	10	a
PMB 650 °C	12.50	74.76	a	10.18	b	0.29	a	3.06	a	10	a
	25.00	48.05	b	21.77	a	0.31	a	3.38	a	10	a
	50.00	57.54	b	21.14	a	0.32	a	3.88	a	11	a
CSB 350 °C	12.50	45.32	a	17.81	a	0.30	a	3.40	a	11	ab
	25.00	47.71	a	16.75	a	0.32	a	4.15	a	12	ab
	50.00	33.91	b	5.67	b	0.33	a	4.87	a	14	a
CSB 650 °C	12.50	101.70	a	15.45	a	0.30	a	3.34	ab	10	b
	25.00	17.00	c	8.65	ab	0.31	a	3.97	ab	12	b
	50.00	31.60	b	12.15	a	0.32	a	5.52	a	16	a

(1) Raw material values applied to the sandy soil are found ih Novais et al., 2017 as well as the sandy soil values for the original pH (2).
Numbers followed by the same letter within the column do not differ statistically from each other.

The comparison between these raw material emission values obtained in the clayey soil with the values previously obtained in the sandy soil (Novais et al., 2017) shows that, although the pattern is maintained, the proportion is not preserved, with the highest values observed in the sandy soil. Stewart et al. (2013) justified the higher CO_2 emission in sandy soils due to the lower protection against decomposition offered by these soils, in addition to exposing biochar to microbial activity. Harrison-Kirk et al. (2013) reported the importance of soil organic matter texture and content in carbon and nitrogen mineralization and production of CO_2 and N_2O. These authors noted an increase in C mineralization in soils with higher organic matter content and a lower CO_2 emission (2.13 times lower) in soil with higher clay content. In two riverside areas in North Carolina, greater CO_2 flows were observed in the restored area, while higher CH_4 flows were noted in the unrestored area (Vidon et al., 2015). The authors justified the difference found in soil texture, as the soil of the restored area, with higher clay content and slightly higher humidity, implying areas of aerobic respiration depletion, which leads to low CO_2 flows and high methanogenesis.

3.3.2. Pyrolysis temperature effect

The application of the poultry manure biochar (PMB) to the clayey soil shows a reduction in CO_2 emissions (Figure 2c) based on the increase of the pyrolysis temperature of the material (350 to 650 °C). The same is observed for the sandy soil, but with a larger amplitude between the emission values and no statistical difference between the applied doses for the temperature of 650 °C (Figure 2d). A number of authors related this fact to the greater maintenance of the

characteristics of the source material when pyrolyzed at lower temperatures, while the reduction of aliphatic and aromatic chains of the material occurs at high pyrolysis temperatures, leaving it more recalcitrant (Cimo et al., 2014; Heitkötter et al., 2015).

The effect of the pyrolysis temperature is observed for the PMB at its original pH when applied at the highest dose (50 Mg ha^{-1}) to the clayey soil (Figure 3a). The statistically significant reduction of this dose after pyrolysis at the highest temperature is in agreement with the reduction of the microbial biomass (MBC and MBN) and the increase in the C/N ratio (Table 3). Pyrolyzing the material at high temperatures, it becomes more recalcitrant and, subsequently, more difficult to break down (Cimo et al., 2014). Additionally, the biochar pyrolyzed at higher temperatures has a higher pore density, which reduces the chance of metanogenesis, as such metabolism requires anaerobiosis to occur (Jeffery et al, 2016).

3.3.3. Texture effect

In the observation of the lowest CO_2 emission values in the clayey soil (Figure 1a), it was concluded that the benefits of PMB as a GHG mitigator are higher when applied to this soil, mainly when pyrolyzed at higher temperatures (Figure 2). Jein et al. (2005) found higher values of CO_2 emissions in a soil with a higher sand content (594 mg Kg^{-1} C-CO_2) compared to a soil with a higher silt content (213 mg Kg^{-1} C-CO_2) this fact was related to the high content of readily oxidizable carbon of the silty soil compared to the others.

In the clayey soil (Figure 2c), the emissions of the highest doses (25 and 50 Mg ha^{-1}) of PMB at their original pH do not differ statistically from the lowest dose (12.5 Mg ha^{-1}) applied to the sandy soil (Figure 2d), with 25 and 50 Mg ha^{-1} being deposited in the soil with higher sand content than all other treatments. This fact was related to the greater buffering of the clayey soils, which are more resistant to changes (Maluf et al., 2015). Borges et al. (2015) observed an important contribution of soil texture and its total organic carbon content (TOC) to CO_2 emissions. The highest values of CO_2 emitted were found in the forest area, due to its clayey texture, which corresponds to the higher humidity values and higher content of organic matter, providing greater microbial activity compared to the sandy soil area. These authors observed a close relationship between soil TOC and its texture. In turn, in clayey soil, with its higher reactivity and greater specific surface area, contributed to the stabilization of the aggregates and higher TOC content.

Due to the high recalcitrance of the sugarcane straw, which causes this material to be indifferent to variations, the same is not observed for its biochar (Figure 2a and 2b), while all comparisons between doses, pyrolysis temperature, and texture are statistically the same. In a meta-

analysis of 46 surveys that applied biochar to the soil, Sagrilo et al. (2015) reported increased CO_2 emissions in clayey soils only when applying a biochar with a C/N ratio of less than two, the raw material being responsible for this ratio. Variations between CO_2 emissions due to the raw material used for biochar production are also observed by Sigua et al. (2015). These authors observed a higher evolution of C-CO_2 for poultry manure biochar, followed by swine manure biochar, and lower values for grass and pinus bark biochars. Due to the high C/N ratio of the pinus bark biochar (213/1), its mineralization was slower, leading to a lower CO_2 emission compared to swine manure biochar (C/N ratio of 8/1) which resulted in the highest emission values and a higher rate of mineralization. In this paper, the authors observed the highest emissions in the soil with higher sand content, regardless the biochar applied.

3.3.4. pH effect

The reduction in the CO_2 emission in the sandy soil becomes clear after reducing the pH of the PMB, originally at 7.5 (Figure 2d). When observing the non-statistical difference between the biochar pyrolyzed at 350 °C (pH 5.5) and the biochar pyrolyzed at 650 °C (original pH of 7.5), it can be concluded that the reduction of the original pH in the biochar pyrolyzed at 350 °C is the same as pyrolyzing this biochar at 650 °C for the lowest doses (12.5 and 25 Mg ha^{-1}), also causing a reduction by 1.15 in CO_2 emissions (Figure 2d). This fact allows us to conclude that, when there is interest in reducing GHG emissions, one can simply reduce the pH of the biochar, as opposed to pyrolyzing it at high temperatures, causing loss of many characteristics of interest. The same pattern is not observed when applying the biochar of poultry manure in the clay soil (Figure 2c), with no statistical difference between the biochars and their respective pyrolysis temperatures when reducing their original pH. This fact was related to the greater buffering power of clayey soils and the subsequent lower response to changes.

Luo et al. (2011) used biochar pyrolyzed at two temperatures (350 and 700 °C) and at two pH values and observed a higher mineralization of the biochar C in the soil with the highest pH value, justifying the fact by the lower Al and Mn content in this soil, both toxic to the microbiota. In this work (Luo et al., 2011), a higher CO_2 emission was reported for the biochar pyrolyzed at 350 °C in the soil with lower pH value and a similar emission was reported for the biochar pyrolyzed at 700 °C at both pH values. This fact may be due to non-neutralization of the inorganic C (carbonate) in the soil with high pH and the low contribution of carbonate C in the biochar pyrolyzed at 700 °C. In a similar paper, Blagodatskaya & Kuzyakov (2008) reported a higher

priming effect in soils with lower pH values, as the biochar neutralization capacity is higher, reducing microbial activity as nutrient and soil organic matter (SOM) adsorption by the biochar surface increased.

For the sugarcane straw biochar - CSB (Figure 2a, 2b), as mentioned previously, the increase in the pyrolysis temperature did not cause a reduction in the CO_2 emission, nor does the increase of the applied dose leads to an increase in emissions. For this biochar, regardless the soil texture, the pH reduction did not lead to a reduction in CO_2 emissions between the pyrolysis temperatures. This fact was again related to the greater recalcitrance of its source material, not being influenced by changes in the environment.

For CH_4 emissions (Figure 3a), the pH effect is subtler, although still observed. The emission values of this gas are slightly higher for the original pH, compared to pH 5.5, when applying the PMB to the clayey soil, again showing that reducing in the original pH value of this biochar may be an interesting technique to increase the mitigating potential of this material. N_2O emissions (Figure 4) do not vary with the changes, all emissions being statistically equal across treatments.

3.3.5. Biochars mitigating potential

When comparing the application of cane straw biochar (Figure 2a, 2b) with its raw material (Figure 1a), an emission 1.72, 2.30, and 3.01 times higher is observed for doses of 12.5, 25 and 50 Mg ha^{-1}, respectively, in the non-pyrolyzed material compared to biochar at its original pH incorporated into the clayey soil. In the sandy soil, Novais et al. (2017) obtained an emission 1.89, 1.90 and 3.60 times higher for the doses of 12.5, 25 and 50 Mg ha^{-1}, respectively, in the non-pyrolyzed material compared to biochar at its original pH. This fact allows us to conclude that the production of biochar from cane straw is an environmentally viable solution to deposit this material in the soil, at least in regards of GHG mitigation.

The same pattern can be observed for the poultry manure biochar (Figure 2c, 2d) compared to its respective raw material (Figure 1a). Higher emission values were obtained at 1.71, 2.43 and 3.64 for the doses of 12.5, 25 and 50 Mg ha^{-1}, respectively, in the material pyrolyzed at 350 °C, while values 1.75, 3.02 and 4.36 times higher were obtained for the doses of 12.5, 25, and 50 Mg ha^{-1}, respectively, in the material pyrolyzed at 650 °C, when applying these materials in the clayey soil. Emissions found in sandy soil by Novais et al. (2017) were 1.36, 2.58 and 3.03 times higher for the doses of 12.5, 25 and 50 Mg ha^{-1}, respectively, in the material pyrolyzed at 350 °C, while

values 1.67, 3.95 and 5.78 times higher were found for the doses of 12.5, 25 and 50 Mg ha^{-1}, respectively, in the material pyrolyzed at 650 °C. This fact confirms that the production of biochar from this raw material is a solution for the deposition of this residue to the soil without propitiating an increase in GHG emissions.

3.3.6. Model

3.3.6.1. Significance of models and adjustment quality

The analysis of variances for PMB and CSB showed a significant effect of the explanatory variables (C_{clay}, pH, $T_{pyrolysis}$, and $D_{biochar}$) on CO_2 emission. For CSB, there was a significant effect only of C_{clay} and $D_{biochar}$, but these effects explained only 28 % (R^2) of the CO_2 variation. For PMB, a significant effect of the combination of C_{clay}, pH, $T_{pyrolysis}$ and $D_{biochar}$ was observed, which explains the 65 % CO_2 emission. The result of the analysis of variance for the PMB, a significant effect of the explanatory variables by the t-test and the adjusted model are presented in Table 4.

Table 4. Result of the analysis of variance for the multiple regression model according to the expression $CO_2 = \beta_0 + \beta_1 C_{clay} + \beta_2 pH + \beta_3 T_{pyrolysis} + \beta_4 D_{biochar}$ for the biochar produced with poultry manure.

Parameter	Variable	Estimate	*p*-value
β_0	Intercept	82.2835	<0.001
β_1	T_{clay}	-0.0528	<0.001
β_2	pH	6.9836	<0.001
β_3	$T_{pyrolysis}$	-0.0866	<0.001
β_4	$D_{biochar}$	0.6414	<0.001
	Fitted model		R^2
$CO_2 = 82.2835 - 0.0528C_{argila} + 6.9836pH - 0.0866T_{pirolise} + 0.6414D_{biochar}$			0.65

The model for the PMB, presented in Table 4, is represented in Figure 5 as a function of the variation of C_{clay}, pH, $T_{pyrolysis}$ and $D_{biochar}$ in a comparison of the predicted and measured values. The black color line represents the CO_2 variation measured over the course of the treatments, while the red color line denotes the adjusted model and its respective confidence band at 95 % probability. In the projection, we noted a slight underestimation of the CO_2 emission for the

highest emissions (greater than 120 mg m^{-2} h^{-1}). Along the variation, the model closely follows the measurements with overlapping bands (shaded area) of confidence to the measured values.

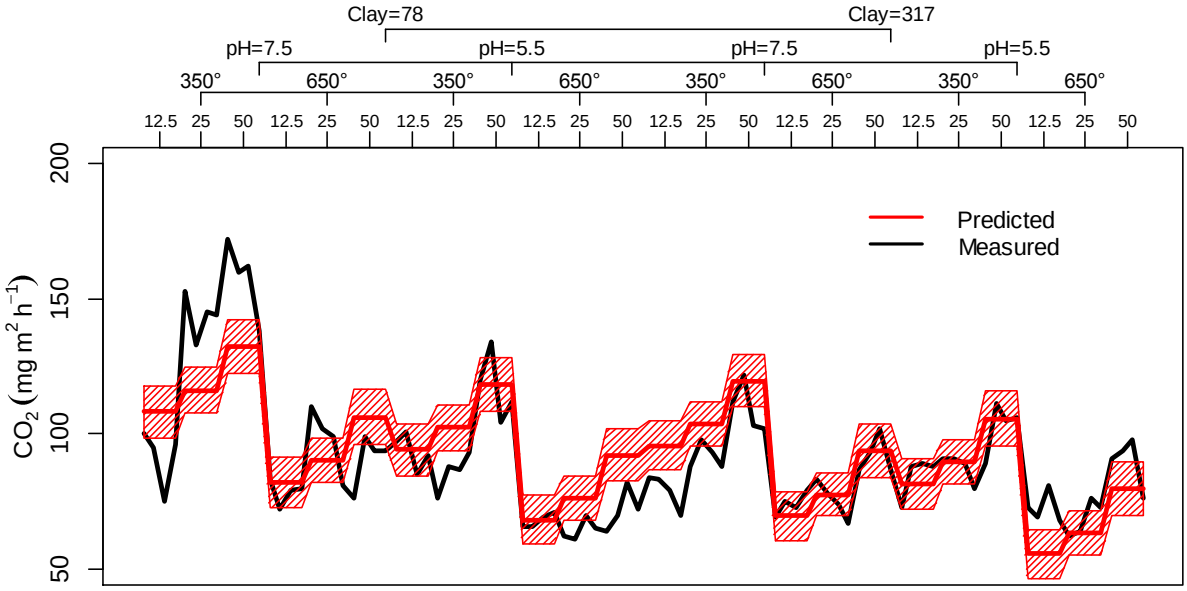

Figure 5. CO_2 variation in response to changes in clay content, pH, pyrolysis temperature and doses of chicken manure biochar. Trusted bands at 95 % probability built for the model and prediction.

The quality of the model adjustment can also be verified in a 1:1 projection, given in Figure 6. Figure 6 shows a low dispersion of the measured values in relation to the projection of a perfect ratio of measurements and predictions (1: 1 line). A good adjustment can be verified mainly in values up to 120 mg CO_2 $m^{-2}h^{-1}$ (where most of the observations are concentrated), in agreement with the results of the variation of the predictions given in Figure 5. The correlation between measured and predicted data, estimated by the Pearson correlation coefficient was 0.79, being statistically significant with a p-value < 0.001.

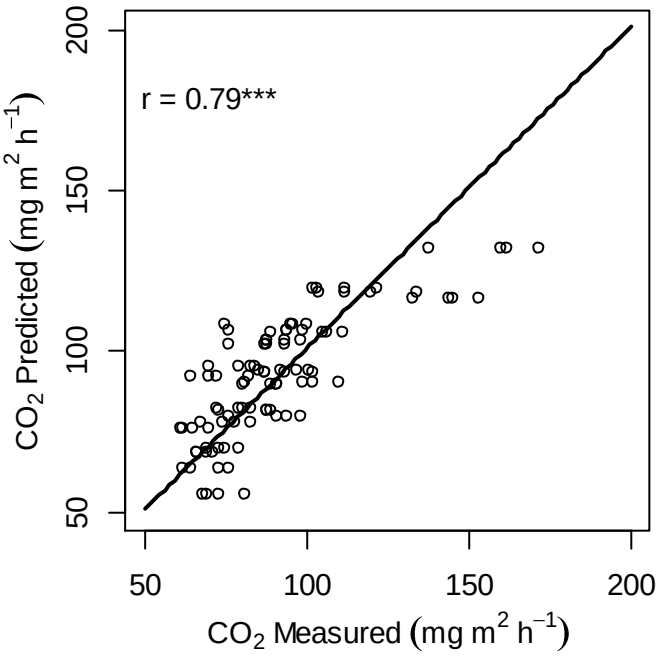

Figure 6. Comparison of predicted CO_2 values (estimated by the adjusted model) and measured experimentally based on a 1:1 line. r: Pearson correlation coefficient. ***p-value <0.001.

3.3.6.2. Internal and external model validation

The internal validation gave us a good perspective of the model (Figure 5), with emission values of up to 100 mg CO_2 $m^{-2}h^{-1}$ (Figure 6) showing excellent prediction ($p < 0.001$). The parameters obtained through the model proposed by Smith et al. (1997) prove this statement.

Both correlation coefficients (r) are greater than zero (0.83 and 0.98 in Table 5), showing a positive correlation between simulated and measured values. The estimated values close to zero (-1.29 for internal validation) for the mean difference between observation and simulation (M) indicate that bias (or consistent error) was small for the internal validation. As M does not include a square term, simulated values above and below the measurements are canceled out, and thus, inconsistent errors are ignored (Smith et al., 1997).

Table 5. Parameters of the internal and external validation.

	Parameter						
	r	RMSE	EF	CD	M	E	CRM
Internal validation	0.83	13.79	0.68	1.37	-1.29	-2.63	-0.01
External validation	0.98	44.56	0.42	4.40	28.44	-1.07	0.20

r: Correlation Coefficient; RMSE: Root mean square error of model; EF: Modelling Efficiency; CD: Coefficient of Determination; M: Mean difference; E: Relative error; CRM: Coefficient of Residual Mass; ME: Maximum Error.

Therefore, the coincidence between measured and simulated values was assessed by calculating an absolute value for total difference, expressed as the root mean square error (RMSE). Our results showed good fit for internal validation (RMSE = 13.79) but, as expected, with a reduction in quality in external validation (44.56).

The efficiency of the model (EF) provides a comparison between the efficiency of the chosen model and that of describing the data as the mean of the observations (Smith et al., 1997). Positive values of 0.68 (internal validation) and 0.42 (external validation) indicate that the simulated data describe the trend of the measurements better than the mean of the observations (Table 5). In addition to the results reported for EF, the coefficients of determination (CD) with values 1.37 and 4.40 (Table 5) represent a measure of the proportion of the total variance. Considering that both values are greater than 1, it is verified that the deviation from the mean of the measured values is lower than that observed in the measurements, i.e., the model again describes the measured data better than its mean.

The CRM close to zero (a perfect fit would be equal to zero) for both internal and external validations indicates the low tendency of the model to overestimate or underestimate the measurements. Positive values for CRM, such as 0.2 for the external validation indicate that the model underestimates the measurements and negative values for CRM (-0.01 for internal validation) indicates a tendency to overestimate (Table 5).

3.3.6.3. Influence of explanatory variables on CO_2 variation

3.3.6.3.1. Effect of clay content for different pyrolysis temperatures

C_{clay} had a negative influence on CO_2 emissions. The simulated scenarios using the model adjusted for the PMB, with a variation in C_{clay} to a pH of 7.5, $T_{pyrolysis}$ of 350 and 650 °C and $D_{biochar}$ of 50 Mg ha^{-1}, show a decrease in CO_2 emission with the increase of C_{clay} (Figure 3), and this

decrease was lower for $T_{pyrolysis}$ at 650 °C. The emission of CO_2 with the largest C_{clay} was approximately 120 mg $m^{-2} h^{-1}$ in the $T_{pyrolysis}$ of 350 °C, whereas, for the 650 °C $T_{pyrolysis}$, this emission fell to approximately 92 mg $m^{-2}h^{-1}$ (Figure 7).

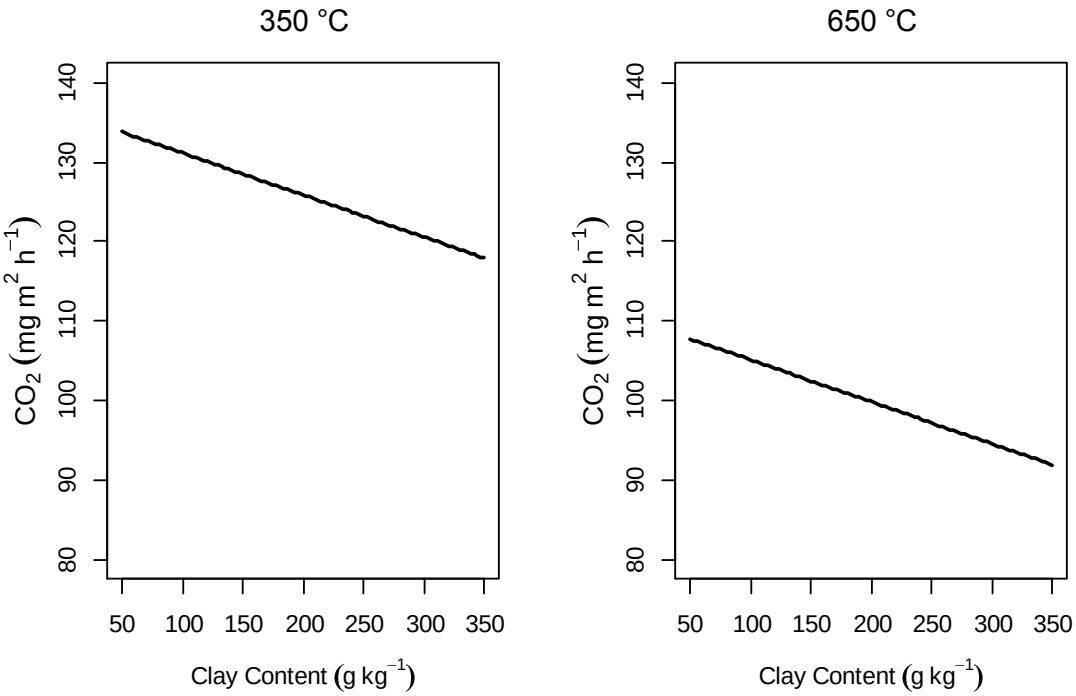

Figure 7. Simulation with the adjusted model (Table 2) for CO_2 emission in response to the clay content variation for the pyrolysis temperatures of 350 and 650 °C, pH 7.5 and dose of biochar of poultry manure of 50 Mg ha^{-1}, according to the scenarios established in Table 4.

3.3.6.3.2. Effect of pH for different pyrolysis temperatures

The simulations presented in Figure 8 show that pH, in the range from 5.5 to 7.5, had a positive influence on CO_2 emission for a C_{clay} of 78 g kg^{-1}, $T_{pyrolysis}$ at 350 and 650 °C and $D_{biochar}$ of 50 Mg ha^{-1}. The CO_2 emission increased linearly from approximately 120 mg $m^{-2} h^{-1}$ to 135 mg m^{-2} h^{-1} for $T_{pyrolysis}$ at 350 °C, and from approximately 90 mg $m^{-2} h^{-1}$ to 105 mg $m^{-2} h^{-1}$ for $T_{pyrolysis}$ at 650 °C.

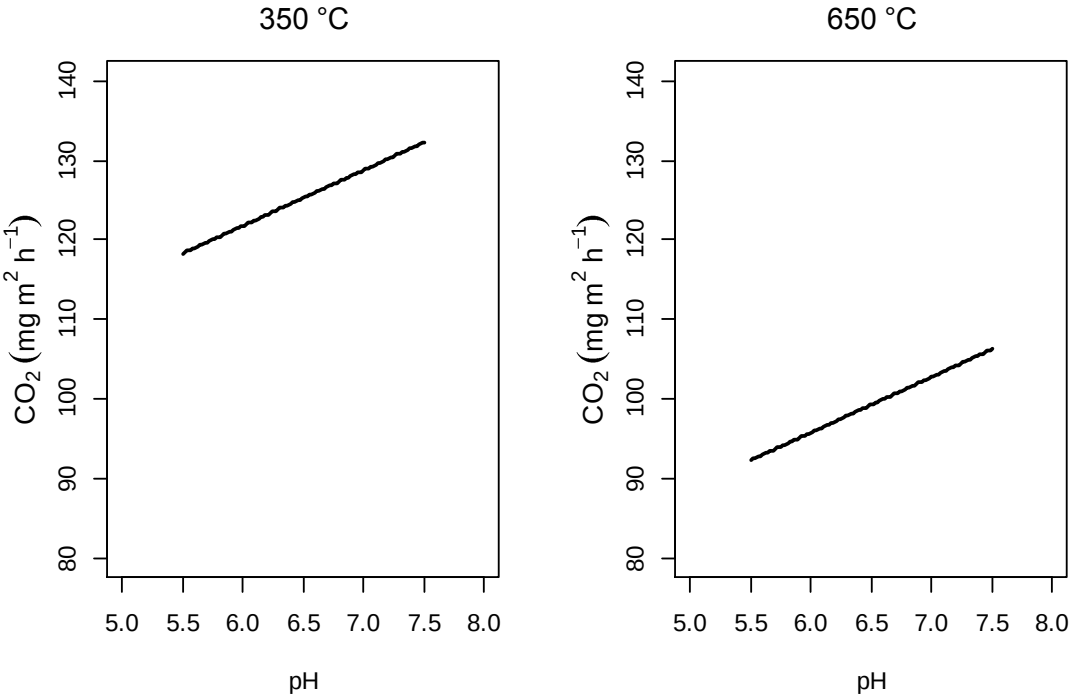

Figure 8. Simulation with adjusted model (Table 2) for CO_2 emission in response to pH variation for pyrolysis temperatures of 350 and 650 °C, clay content of 78 g kg^{-1} and biochar dose of chicken manure of 50 Mg ha^{-1}, according to the scenarios established in Table 4.

3.3.6.3.3. Effect of the biochar dose applied at different pyrolysis temperatures

CO_2 emission simulations varying with $D_{biochar}$ in a range of 12.5 to 50 Mg ha^{-1}, with a C_{clay} of 78 g kg^{-1}, $T_{pyrolysis}$ at 350 and 650 °C and a pH of 7.5, are given in Figure 9 The $D_{biochar}$ positively influenced CO_2 emission, where increases were observed in the increase of $D_{biochar}$. For $T_{pyrolysis}$ of 350 °C, the CO_2 concentration went from about 110 to 132 mg m^{-2} h^{-1}, whereas for $T_{pyrolysis}$ at 650 °C, the concentrations increased from 80 to 105 mg $m^{-2}h^{-1}$, showing a drop in CO_2 emissions influenced by the $T_{pyrolysis}$ in the higher $D_{biochar}$.

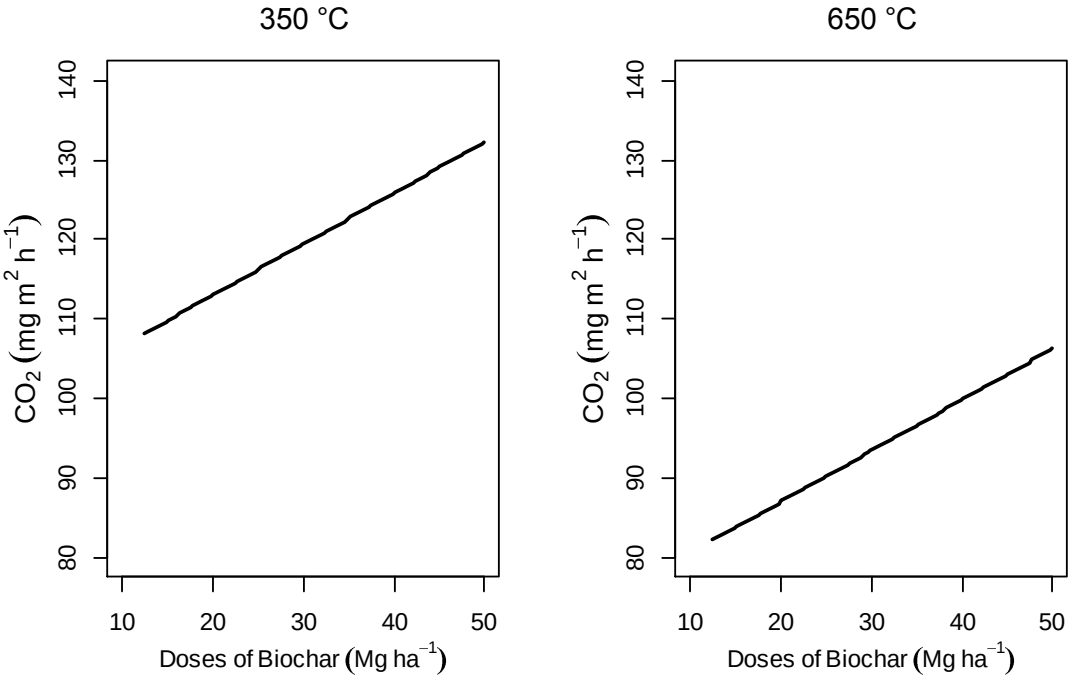

Figure 9. Simulation with adjusted model (Table 2) for CO_2 emission in response to the variation of doses of poultry manure biochar for pyrolysis temperatures of 350 and 650 °C, pH of 7.5 and 78 g kg^{-1} clay content, according to the scenarios established in Table 4.

3.3.6.3.4. CO_2 variation trend

As the clay content increases, the same trend is observed for both pyrolysis temperatures (Figure 7), with a reduction in CO_2 emission. Nevertheless, the higher pyrolysis temperature (Figure 7b) presents CO_2 significantly lower emissions than the lower pyrolysis temperature (Figure 7a), and this observation was confirmed in the experimental data. Similarly, as the pH value is increased, the same pattern observed for the increased clay content occurs (Figure 8). This arrangement is in agreement with the measured data, where the reduction of the original pH values of the biochar (alkaline pH) to 5.5 resulted in a significant reduction of the CO_2 emission. Again, the higher pyrolysis temperature (Figure 8b) presents reduced emissions compared to the lower temperature (Figure 8a). As noted in this work and in several others (Subedi et al., 2016; Deng et al., 2017; Novais et al., 2017), the increase in the pyrolysis temperature leads to a reduction in the CO_2 emission. That is because, at high pyrolysis temperatures, a reduction in aliphatic and aromatic chains in the material occurs, leaving it more stabilized (Cimo et al., 2014; Heitkötter et al., 2015).

Although a number of articles note that biochar's GHG mitigating ability has its potential expanded, not always proportionally, by increasing the applied dose (Abbruzzini et al., 2017; Deng

et al., 2017), others, as was the case in this experiment (Novais et al., 2017; Awasthi et al., 2017) report an increase in the applied dose, resulting in an increase in CO_2 emissions.

3.4. CONCLUSIONS

The application of the pyrolyzed raw material (biochar) causes a significant reduction in CO_2 emissions compared to the non-pyrolyzed material, with biochar as an environmentally safe way of depositing these materials in the soil. Poultry manure and the respective biochar have higher CO_2 emissions compared to sugarcane straw and its biochar. Additionally, this biochar has lower CO_2 emissions when pyrolyzed at 650 °C, and with its original pH reduced to 5.5, presenting lower CO_2 emissions. Changing the original pH of the poultry manure biochar to 5.5 causes reductions in emissions similar to reductions caused by increased pyrolysis temperature. The sugarcane straw biochar, made of a more recalcitrant material, does not have emission values altered according to pyrolysis temperature or when the pH value is altered. Nevertheless, when transformed into biochar, its emission is less than that of its raw material – or equivalent to the emission of the soil. The beneficial effects of biochar as a GHG mitigator are better observed in sandy soil, compared to clayey soil. The CO_2 emission can be explained by the variables of soil texture, pH, applied dose, and pyrolysis temperature.

REFERENCES

Abbruzzini, T. F., M. D. O. Zenero, P. A. M. de Andrade, F. D. Andreote, J. Campo, and C.E.P. Cerri. 2017. Effects of Biochar on the Emissions of Greenhouse Gases from Sugarcane Residues Applied to Soils. Agric. Sci. 8(09):869.

Abujabhah I.S., R. Doyle, S.A. Bound, and J.P. Bowman. 2016. The effect of biochar loading rates on soil fertility, soil biomass, potential nitrification, and soil community metabolic profiles in three different soils. J.Soil Sed. 1-12:2016.

Agegnehu G., A.M. Bass, P.N. Nelson, and M.I. Bird. 2016. Benefits of biochar, compost and biochar–compost for soil quality, maize yield and greenhouse gas emissions in a tropical agricultural soil. Sci. Tot. Environm. 543: 295-306.

Ameloot, N., P. Maenhout, S. De Neve, and S. Sleutel. 2016. Biochar-induced N2O emission reductions after field incorporation in a loam soil. Geoderma. 267:10-16.

ASTMD 5373/2008; Standard test methods for instrumental determination of carbon, hydrogen, and nitrogen in laboratory samples of coal and coke, American Society for Testing and Materials (ASTM), Pennsylvania.

Awasthi, M.K., M. Wang, H. Chen, Q. Wang, J. Zhao, X. Ren, and Z. Zhang. 2017. Heterogeneity of biochar amendment to improve the carbon and nitrogen sequestration through reduce the greenhouse gases emissions during sewage sludge composting. Bio. Technol. 224:428-438.

Blagodatskaya E., and Y. Kuzyakov. 2008. Mechanisms of real and apparent priming effects and their dependence on soil microbial biomass and community structure: critical review. Biol. Fert. Soil. 45:115–131.

Borges C.S., B.T. Ribeiro, B. Wendling, and D.A. Cabral. 2015. Agregação do solo, carbono orgânico e emissão de CO2 em áreas sob diferentes usos no Cerrado, região do Triângulo Mineiro/Soil aggregation, organic carbon and CO2 emission in different land uses in Brazilian Savanna, Triangulo Mineiro region. Ver. Amb. Água 10(3): 660.

Butnan S., J.L. Deenik, B. Toomsan, M.J. Antal, and P. 2015. Vityakon. Biochar characteristics and application rates affecting corn growth and properties of soils contrasting in texture and mineralogy. Geoderma 237:105-116.

Cimo G., J. Kucerik, A.E. Berns, G.E. Schaumann, G. Alonzo, and P. Conte. 2014. Effect of heating time and temperature on the chemical characteristics of biochar from poultry manure. Environ. Sci. Technol. 62: 1912–1918.

Conz, R.F., T.F. Abbruzzini, C.A. Andrade, D.M.B.P. Milori, and C.E.P. Cerri. 2017. Effect of Pyrolysis Temperature and Feedstock Type on Agricultural Properties and Stability of Biochars. Agric. Sciences. 8(09):914-933.

Crombie K, O. Mašek, A. Cross, and S. Sohi. 2015 Biochar–synergies and trade-offs between soil enhancing properties and C sequestration potential. GCb bioenergy. 7(5):1161-1175.

Dai, Z., Y. Wang, N. Muhammad, X. Yu, K. Xiao, J. Meng, and P.C. Brookes. 2014. The effects and mechanisms of soil acidity changes, following incorporation of biochars in three soils differing in initial pH. Soil Sci. Soc. America J. 78(5):1606-1614.

Deng, W., L. Van Zwieten, Z. Lin, X. Liu, A.K. Sarmah, and H. Wang. 2017. Sugarcane bagasse biochars impact respiration and greenhouse gas emissions from a latosol. J. Soils Sed. 17(3):632-640.

Ferraz S.R.L., A.M. Barbosa, J.L. Batista, I.D. Magalhães, F.G. Dantas, and F. Oliveira. 2015. Calagem em cana-de-açúcar: efeitos no solo, planta e reflexos na produção. InterfacEHS, 10(1).

Harrison-Kirk T., M.H. Beare, E.D. Meenken, and L.M. Condron. 2013. Soil organic matter and texture affect responses to dry/wet cycles: effects on carbon dioxide and nitrous oxide emissions. Soil Bio. Biochem. 57: 43–55.

Heitkötter J., and B. Marschner. 2015. Interactive effects of biochar ageing in soils related to feedstock, pyrolysis temperature, and historic charcoal production. Geoderma. 245: 56-64.

Jeffery, S., F.G. Verheijen, C. Kammann, and D. Abalos. 2016. Biochar effects on methane emissions from soils: A meta-analysis. Soil Biol. Biochem. 101:251-258.

Lamb, A., R. Green, I. Bateman, M. Broadmeadow, T. Bruce, J. Burney, and K. Goulding. 2016. The potential for land sparing to offset greenhouse gas emissions from agriculture. Nat. Clim. Change. 6:488-492.

Lehmann J, and S. Joseph (Eds.) 2015. Biochar for environmental management: science, technology and implementation. Routledge.

Luo Y., M. Durenkamp, M. De Nobili, Q. Lin, and P.C. 2011. Brookes. Short term soil priming effects and the mineralisation of biochar following its incorporation to soils of different pH. Soil Biol. Biochem. 43(11):2304-2314.

Maluf H.J.G.M., E.M.B. Soares, I.R.D. Silva, J.C.L. Neves, and M.F.D.O. Silva. 2015. Nutrient availability and recovery from crop residues in soil with different textures. Rev. Bras. Ci. Solo 39(6):1690-1702.

Novais, S.V., M.D.O. Zenero, E.F.F. Junior, R.P. de Lima, and C.E.P. Cerri. 2017. Mitigation of Greenhouse Gas Emissions from Tropical Soils Amended with Poultry Manure and Sugar Cane Straw Biochars. Agric. Sci. 8(09):887.

R Core Team. 2017. R: A language and environment for statistical computing. R Foundation for Statistical Computing, Vienna, AT.

Reichardt, K. 1988. Capacidade de campo. Rev. Bras. Ci. Solo. 12: 211-216.

Abel S., A. Peters, S. Trinks, H. Schonsky, M. Facklam, and G. 2013. Wessolek Impact of biochar and hydrochar addition on water retention and water repellency of sandy soil Geoderma. 202:183-191.

Sagrilo E., S. Jeffery, E. Hoffland, and T.W. Kuyper. 2015. Emission of CO2 from biochar-amended soils and implications for soil organic carbon. GCB Bioenergy. 7(6): 1294-1304.

Sánchez-Monedero, M.A., N. Serramiá, C.G.O. Civantos, A. Fernández-Hernández, and A. Roig. 2010. Greenhouse gas emissions during composting of two-phase olive mill wastes with different agroindustrial by-products. Chemosphere. 81(1):18-25.

Shackley S., G. Ruysschaert, K. Zwart, and B. Glaser. (Eds.) 2016. Biochar in European Soils and Agriculture: Science and Practice. Routledge.

Sigua G.C., J.M. Novak, D.W. Watts, K.B. Cantrell, P.D. Shumaker, A.A. Szögi, and M.G. Johnson. 2014. Carbon mineralization in two ultisols amended with different sources and particle sizes of pyrolyzed biochar. Chemosphere. 103: 313-321.

Smith, P., J.U. Smith, D.S. Powlson, W.B. McGill, J.R.M. Arah, O.G. Chertov, and L.S. Jensen. 1997. A comparison of the performance of nine soil organic matter models using datasets from seven long-term experiments. Geoderma. 81(1-2):153-225.

Stewart C.E., J. Zheng, J. Botte, and M.F. Cotrufo. 2013. Co-generated fast pyrolysis biochar mitigates greenhouse gas emissions and increases carbon sequestration in temperate soils. Global Change Biol. Bio. 5:153–164.

Subedi, R., N. Taupe, S. Pelissetti, L. Petruzzelli, C. Bertora, J.J. Leahy, and C. Grignani. 2016. Greenhouse gas emissions and soil properties following amendment with manure-derived biochars: influence of pyrolysis temperature and feedstock type. J. Environm. Manag. 166:73-83.

Tedesco, M.J., H. Bohnem, C. Gianello, C.A. Bissani, and S.J. Volkweiss. 1995. Análise de solo, plantas e outros materiais. 2.ed. Porto Alegre, Universidade Federal do Rio Grande do Sul, 174p. (Boletin Técnico, 5)

Vidon P., S. Marchese, M. Welsh, and S. McMillan. 2015. Short-term spatial and temporal variability in greenhouse gas fluxes in riparian zones. Environ. Monitoring Assessment. 187(8):1-9.

Woolf, D., J.E. Amonette, F.A. Street-Perrott, J. Lehmann, and S. Joseph. 2010. Sustainable biochar to mitigate global climate change. Nature communications. 1:56.

Yuan, J. H., and R.F. Xu. 2012. Effects of biochars generated from crop residues on chemical properties of acid soils from tropical and subtropical China. Soil Research, 50(7): 570-578.

Yuan, J. H., R.K. Xu, and H. Zhang. 2011. The forms of alkalis in the biochar produced from crop residues at different temperatures. Bio. Technol.102(3):3488-3497.

4. BIOCHAR MODIFIED WITH $MgCl_2$ FOR PHOSPHORUS ADSORPTION

ABSTRACT

Increases in agricultural productivity associated to the crescent use of the finite reserves of phosphorus improved the demand for ways to recycle and reuse this nutrient. Biochars, after doping processes, seems to be an alternative to mitigate such impasse. Sugarcane straw and poultry manure were submerged in an $MgCl_2$ solution in a 1:10 solid/liquid ratio and subsequently pyrolyzed at 350 and 650 °C producing biochar. The P adsorbed in its maximum adsorption capacity (MPAC) was extracted, successively, with H_2SO_4 (0.5 mol L^{-1}), $NaHCO_3$ (0.5 mol L^{-1} a pH 8.5) and H_2O, until no P was detected in the solution. Biochars without the addition of Mg did not have the ability to adsorb P but had this property developed after the doping process. The poultry manure biochar presented higher MPAC (250.8 and 163.6 mg g^{-1} of P at 350 and 650 °C, respectively) than that of sugarcane straw (17.7 and 17.6 mg g^{-1} of P at 350 and 650 °C, respectively). The pyrolysis temperature changed, significantly, the MPAC values for the poultry manure biochar, with an increase in the adsorbed P binding energy for both biochars. The H_2SO_4 showed the best extraction power, desorbing, with a lower number of extractions the greater amount of the adsorbed P. These materials doped with Mg and subjected to pyrolysis have characteristics that allow their use in P adsorption from eutrophic and wastewaters.

Keywords: Sugar cane straw; Poultry manure; Mg doping; P desorption; Potencial reuse; Langmuir isotherm

4.1. INTRODUCTION

Increases in population associated with the consequent increase in the demand for food and reduction of the finite reserves of phosphorus (P), have generated great concern in agriculture, mainly about the increasing use of phosphate fertilizers. Particularly in tropical soils, where reduced levels of available P are associated with elevated levels of Fe and Al oxyhydroxides, large doses of phosphate fertilizers are necessary for high yields, directing the main focus of this concern to agriculture based countries such as Brazil (Roy et al., 2016).

P recycling and reusing strategies have thus become recently studied (Drenkova-Tuhtan et al., 2016; Fink et al., 2016). The reuse of P can be achieved by immobilization, from the locations where it previously caused an environmental problem, such as in eutrophic or wastewater, for latter use as a phosphate fertilizer in agriculture. Eutrophic waters, according to CONAMA (2005), have values equal to or greater than 0.025 mg L^{-1} of P, but in some countries this value is not permitted to exceed 0.020 mg L^{-1} (Klein and Agne, 2013).

Among several approaches aiming P reuse, biochar can be used as a P adsorbent. Biochar is the product formed by pyrolysing vegetable or animal residues at high temperatures and under hypoxic conditions (Lehmann and Joseph, 2015). Previous studies, however, have proven that biochars without any additional treatment have very low or none P adsorption capacity (Jung et al., 2015; Cui et al., 2016), due to its behavior as a "great anion", with a high proportion of carboxylic and phenolic groups, which prevents the adsorption of anions such as phosphates (Agegnehu et al., 2016). Enhanced biochar P adsorption capacity can be achieved through the "doping" treatment. This procedure consists in adding metallic cations, such as Mg^{2+} and Ca^{2+}, to the raw material. These cations are precipitated onto the surface of the biochar during the pyrolysis reaction, creating cationic bridges that can adsorb anions such as phosphate (Jing et al., 2015).

Doped biochars have high capacity for P adsorption and can be used efficiently in P recovery from eutrophic or wastewater. Cui et al. (2016) observed that although untreated biochar did not adsorb P, even at high P concentrations (50 mg L^{-1} of P), the doping process with $MgCl_2$ reached 98.3% removal of the P from a eutrophic water, which contained 1.82 mg L^{-1} of P. Jung et al. (2016a) observed an increase of almost six times in the P adsorption by a biochar doped with $MgCl_2$ and Yu et al. (2016) reported a maximum P adsorption capacity (MPAC) of 129.9 mg g^{-1} with a biochar from cotton pyrolyzed at 600 °C and doped with $MgCl_2$.

Variations in the MPAC depends on the pyrolysis process and the raw material characteristics. The increase in temperature leads to an increase in surface area, in C content and reduces the H content, leading to an increase in the P adsorption, besides increasing the KL and KF values (Langmuir and Freudelich isothermic constants respectively), proportionally associated with adsorption energy (Fang et al., 2015). Fang et al. (2014) reported an increase in adsorption of 2.5, 5.0 and 6.2-fold after doping with Mg at pyrolysis temperatures of 300, 450 and 600 °C, respectively. Fang et al. (2015) reported a MPAC of 293.2, 315.3 and 326.6 mg g^{-1}, respectively, for a biochar doped with Ca and Mg and pyrolyzed at 300, 450 and 600 °C. A 1.1-fold increase in the KL constant and a 1.3-fold increase in the KF constant, with the temperature increase from 300 to 600 ° C were observed.

Additionally, raw material characterisitics and the properties of its respective biochar after pyrolysis reaction influence the MPAC. Biochar produced at lower pyrolysis temperature will have similar properties that of their respective raw material, while higher pyrolysis temperaure cause greater changes biochar's properties, with little resemblance to its original material, but to grafite.(Lehmann and Joseph 2015). The doping treatment is affected by the stability of the original material. In this sense, unreactive materials produce biochars with lower MPAC when compared to biochars derived from reactive materials. Zhang et al. (2012), observed a high variation in MPAC

when studying biochars of five raw materials doped with Mg under an electric field. The highest adsorption was obtained for the biochar from sugarcane beet tailings (835 mg g^{-1}), followed by those from cotton, sugarcane bagasse and pinus bark. The lowest MPAC was obtained with the biochar from pinus bark (3.17 mg g^{-1}). This variation was consistent with the surface area of the biochars produced, with the lowest specific surface area observed for pinus bark (2.8 mg g^{-1}) and the highest (122.5 mg g^{-1}) for sugarcane bagasse

There are some works that modifie biochar with Mg for P adsorption with positive response (Sizmur et al., 2017), but few look after its possible reuse in agriculture or what to do with the material after de recovery of P in waste waters. Thus, the present work aimed at the production and characterization of biochars from sugarcane straw and poultry manure, doped with $MgCl_2$ and pyrolyzed at 350 and 650 °C, as well as the determination of their MPAC values and their abilities to release adsorbed P.

4.2. MATERIAL AND METHODS

4.2.1. Raw material Selection

The raw materials used were sugarcane straw, collected from a plantation in Piracicaba-SP and poultry manure collected from the University of Sao Paulo farm (ESALQ-USP). The raw materials were selected because of their contrasting physical and chemical attributes, permitting the investigation of the effects of contrasting materials on the P adsorption capacity. In addition, the high production of these residues and their accumulation in the field have created a management problem for many companies.

4.2.2. Biochar production

The raw materials (sugarcane straw and poultry manure) were immersed in a solution of $MgCl_2$ (60 g $MgCl_2$ $6H_2O$ in 90 mL of deionized water) in a proportion solid: liquid of 1:10 and incubated for 2 h, as suggested by Jung et al. (2016a). The material was dried in an oven at 80 °C for 3 h and pyrolysis was carried out by SPPT Research Technologies, in a metallic reactor, under a N_2 atmosphere, heating rate of 10 °C/min for the first 30 min and 20 °C/min until the final temperature. The raw untreated materials were pyrolyzed under the same conditions.

Two pyrolysis temperatures were used, 350 and 650 °C. The main physical and chemical changes of raw biomass are carried within this temperature range and largely affect the final characteristics of biochars, generating products with contrasting attributes (Novotny et al., 2015).

After processing, eight biochars were produced: sugarcane straw pyrolyzed at 350 °C (BCS 350 °C); sugarcane straw pyrolyzed at 650 °C (BCS 650 °C); sugarcane straw pyrolyzed at 350 °C and doped with $MgCl_2$ (BCS-Mg 350 °C); sugarcane straw pyrolyzed at 650 °C and doped with $MgCl_2$ (BCS-Mg 650°C); poultry manure pyrolyzed at 350 °C (BPM 350 °C); poultry manure pyrolyzed at 650 °C (BPM 650 °C); poultry manure pyrolyzed at 350 °C and doped with $MgCl_2$ (BPM-Mg 350 °C) and poultry manure pyrolyzed at 650 °C and doped with $MgCl_2$ (BPM-Mg 650 °C).

4.2.3. Biochars characterization

Chemical and Physical analysis followed the methodology recommended by the International Biochar Initiative Guideline (IBI, 2015) and are thoroughly described in Conz et al. (2017) and were previously done in Novais et al. (2017). The crystallography of the biochars was carried out using X-ray diffraction (LabX, XRD-6000, Shimadzu X-ray Diffractometer) with a scanning angle between 4 and 70 º 2θ (λ 0.02 °s-1). The biochars were investigated in infrared spectroscopy (ATR/FTIR-4100, Jasco, Fourier Transform Infrared Spectrometer). Finally, the biochars were coated with gold (SCD 050 Sputter Coater, Bal-Tec) and photographed using a scanning electron microscope-SEM (EVO 50, Carl Zeiss). Qualitative analysis of the chemical composition was performed using X-ray dispersive energy and EDS-Energy Dispersive Spectroscopy (500 Digital Processing, IXRF Systems).

4.2.4. Adsorption isotherms

Each point of the adsorption isotherm consisted of 0.15 g of the doped or undoped biochar and 75 mL of the KH_2PO_4 solution as the raw of P. Increasing concentrations of P, ranging from 0 to 1500 mg L^{-1} (0; 10; 25; 50; 75; 100; 150; 200; 250; 375; 500; 560; 620; 750; 850; 1000; 1250; 1500 mg L^{-1}) for the biochar from poultry manure and 0 to 1000 mg L^{-1} (0; 10; 25; 50; 75; 100; 150; 250; 500; 750; 1000 mg L^{-1}) for the biochar from sugarcane straw. Biochar and the respective P solution was shaken in horizontal stirrer, for 24 h, at 120 rpm, and the solution was filtered through a Whatman filter paper (white band). The P in the filtrate was read in a UV/VIS spectrophotometer, λ 720 nm (600 Plus, FEMTO), allowing the adjustment of the adsorption

curves, plotted from Langmuir (Equation 1) and Freundlich (Equation 2) isotherms, with the aid of the Origin-Pro 8 program.

$$q_e = K_L C_e / (1 + K_L C_e) \quad \text{(Equation 1)}$$

$$q_e = K_F C^n_e \quad \text{(Equation 2)}$$

Where K_L represents the interaction energy (L mg^{-1}) and K_F represents Freudlich´s coefficient of affinity (mg (1-n) Ln g^{-1}), q_e is the maximum adsorption capacity (mg g^{-1}), C_e is the concentration of P in the equilibrium solution (mg L^{-1}) and n is Freudlich´s linearity constant.

4.2.5. Desorption

Biochar samples previously doped with the P content at their MPAC, were submitted to successive extractions with H_2SO_4 (0.5 mol L^{-1}), $NaHCO_3$ 0.5 mol L^{-1} at pH 8.5 (Olsen´s extractor) and H_2O, individualy, in order to recover the largest amount of the adsorbed P. These extractors cover different pH ranges and have different extraction powers, all of which are representative of P-available to the plant (Zhang et al., 2016).

A 1.0 g of each biochar, doped with Mg and at their MPAC, was shaken at a ratio solid: liquid of 1:300 for 48 h on a horizontal stirrer at 120 rpm (Zhang et al., 2016). After that the samples were filtered through a Whatman filter paper (white band) and the P in the filtrates analyzed in a UV/VIS spectrophotometer to determine the level of P desorption. This process was repeated until the concentration of P was below the detection limits of the spectrophotometer using a 10mm wide cuvette.

4.3. RESULTS

4.3.1. Characterization of the biochars

4.3.1.1. X-Ray Difraction

The X-ray diffractograms confirm the efectiveness of the Mg doping process, showing several peaks which identify Mg precipitated within the crystal structure of the biochars (Figure 1). Biochars obtained from sugarcane straw - BCS (Figure 1a and 1b) possess “shoulders” on the diffractogram, characteristic of amorphous material. In addition, BCS have low background noise

and almost no peaks beyond those related to the added Mg and silicon, the principal component. Poultry manure biochar - BPM (Figure 1c and 1d) had high background noise, with several other peaks besides those of the Mg added caused by the predominant component, Ca in its various forms. From the diffractograms it is possible to observe the predominant formation of pyroxene (MgSiO) in the biochar pyrolyzed at 350 ° C (Figure 1a and 1c), but at the highest temperature (650 ° C) the formation of periclase (MgO) is predominant (Figure 1b and 1d).

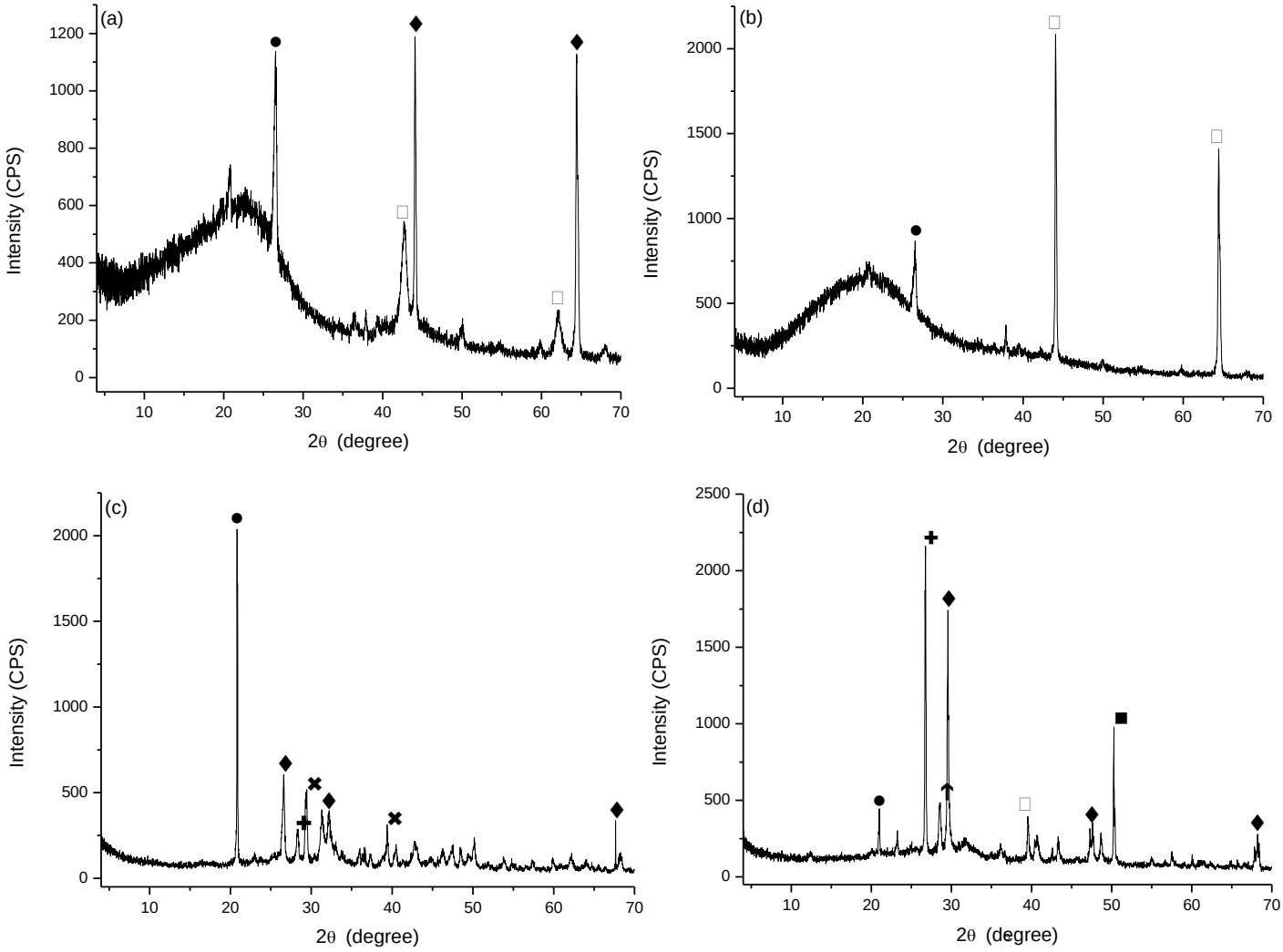

Figure 1. X-ray diffractograms of sugarcane straw biochar pyrolyzed at 350 °C (a) and at 650 °C (b) and biochar of poultry manure, pyrolyzed at 350 °C (c) and 650 °C (d). The simbols are for: ●SiO2 (Quartz); ♦MgSiO (Pyroxene); ◀MgO (Periclase); ■CaMgO (Dolomite); ↑KCl (Silvite); ✕CaO (Calcite); ✚AlSiO (Kyanite).

4.3.1.2. Infrared spectroscopy (FTIR)

Bands values for the carboxylic acids (1500 cm^{-1} region), with higher intensity for the material without doping (Figure 2), especially for BPM pyrolyzed at 350 ° C (Figure 2a), as well as for the bands at 850 and 1400 cm^{-1} region, related to aromatic C-H and aromatic C-O, respectively, indicates that in such regions the added Mg is adsorbed. The higher intensity of the band at the 400 cm^{-1} region for the doped biochars, compared to the non-doped ones, also confirms the effectiveness of doping, since it is in this region that the metals bounded to oxygen are found, as periclase (MgO) and pyroxene (MgSiO). The few bands with low intensity for BCS (Figure 2a and 2c) is in agreement with the high stability of its raw material and agrees with the low MPAC values for these biochars, for both pyrolysis temperatures.

The band in 1100 cm^{-1} relative to P-O stretching vibration and in 540 relative to O-P-O have growth in the dopped material with added P, as aspected. The region at 2927 and 2853 are CH_3/CH_2 vibration. The bands at 3230 and 2300 are responsible for O-H vibrations and CO_2 of the surroundings, respectively.

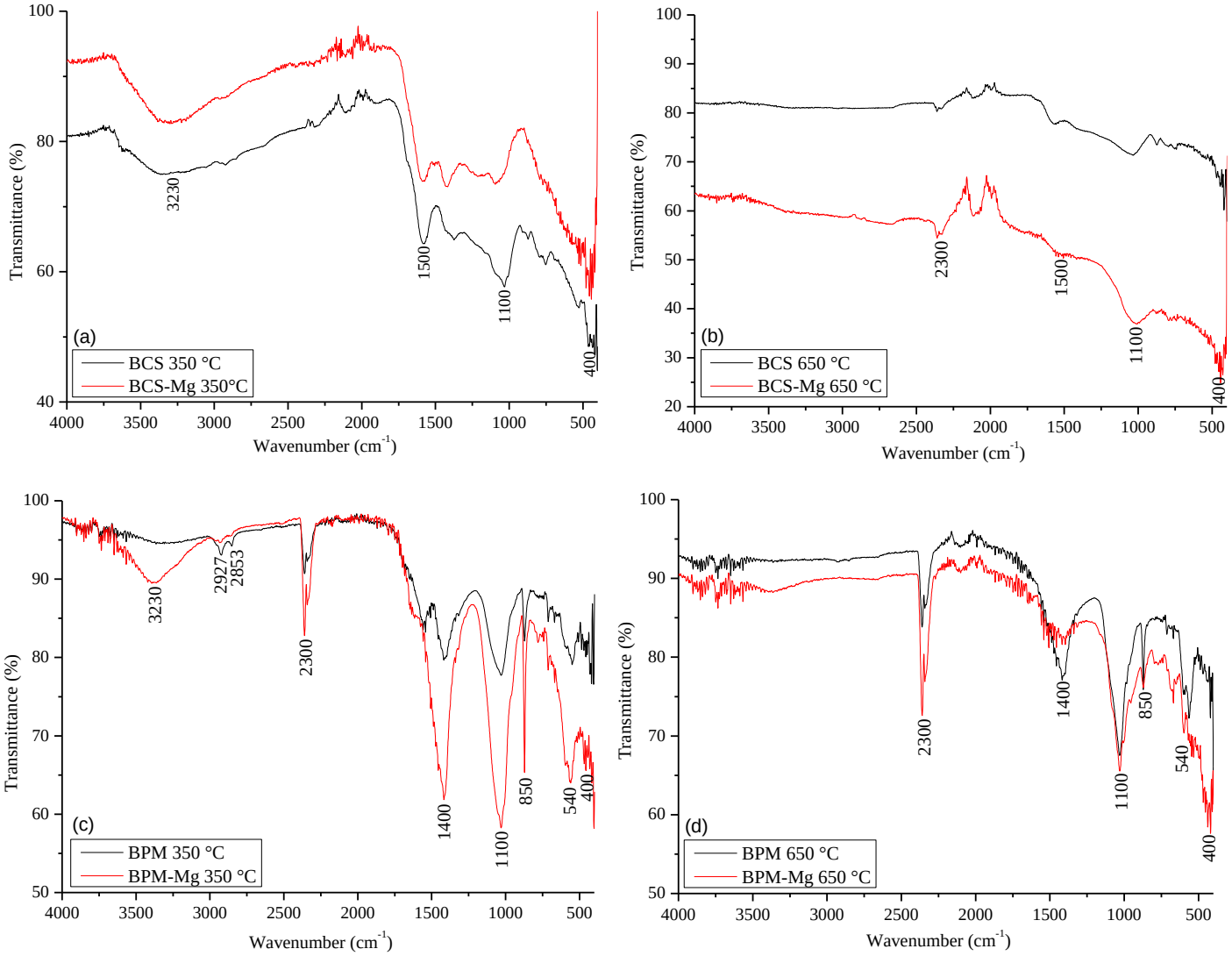

Figure 2. Infrared spectra (FTIR) for (a) biochar of sugarcane straw pyrolyzed at 350 °C (BCS 350 °C) and biochar of Mg-doped sugarcane straw pyrolyzed at 350 °C (BCS-Mg 350 °C); (b) biochar of sugarcane straw pyrolyzed at 650 °C (BCS 650 °C) and biochar of Mg-doped sugarcane straw pyrolyzed at 650 °C (BCS-Mg 650 °C) (c) biochar of poultry manure pyrolyzed at 350 °C (BPM 350 °C) and biochar of Mg-doped poultry manure pyrolyzed at 350 °C (BPM-Mg 350 ° C); (d) biochar of poultry manure pyrolyzed at 650 °C (BPM 650 °C) and biochar of Mg-doped poultry manure pyrolyzed at 650 °C (BPM-Mg 650 °C).

4.3.1.3. Scanning Electron Microscopy (SEM) and Energy Dispersive X-ray (EDS)

The elemental analysis (Table 1) showed an increase in C content and a reduction in O content with increasing pyrolysis temperature (350 to 650 °C). Other elements, such as Mg, K and P were released during pyrolysis of poultry manure, however, the same trend was not observed for

sugarcane straw (Table 1). After the doping process, the increase in pyrolysis temperature caused a higher accumulation of Mg in both biochars, also indicating the success of the treatment.

Table 1. Elemental analysis of the raw materials, the pre-treated biochars and the biochars doped with Mg and in their maximum P adsorption capacity (MPAC).

Treatments	C	O	Mg	P	Si	Ca	K	Cl	S
					%				
Raw materials*									
CS	43.3	51.1	1.53	0.98	-	7.67	9.52	-	0.43
PM	32.2	65.3	5.87	20.22	-	129.93	23.21	-	3.20
Biochar*									
BCS 350 °C	62.3	38.4	2.28	0.94	-	2.91	6.75	-	0.59
BCS 650 °C	68.6	29.3	2.36	0.92	-	6.10	13.65	-	1.08
BPM 350 °C	43.8	37.5	1.16	1.73	-	52.51	3.13	-	0.75
BPM 650 °C	39.2	26.8	1.28	1.54	-	52.57	3.05	-	0.65
Mg-doped biochar in their MPAC									
BCS 350 °C	39.02	22.86	5.29	0.32	20.64	1.29	2.72	1.59	0.07
BCS 650 °C	31.08	44.59	7.25	0.05	12.24	0.00	0.24	2.63	0.04
BPM 350 °C	1.34	43.17	8.31	10.54	0.59	17.90	5.90	12.46	0.89
BPM 650 °C	11.43	37.29	14.44	7.35	1.73	15.65	2.30	5.77	0.33

***** Values obtained previously by Conz et al., 2015.

The success of the doping process is also confirmed by SEM and EDS (Figure 3), where Mg peaks have a high intensity for all doped biochars. Again, the distinct composition of the biochars is evident. On one hand BCS exhibited few peaks besides those of the added Mg and P, with high Si peak, proper of the sugarcane straw tissue (Figure 3a, 3b). While on the other hand, BPM possessed a greater variety of peaks with intensity equal to or greater than those of the added elements, particularly for Ca in this biochar (Figure 3c, 3d). The total P levels were in accordance with the MPAC of the materials: high MPAC for BPM (Figure 3c and 3d) and lower values for BCS (Figure 3a and 3b).

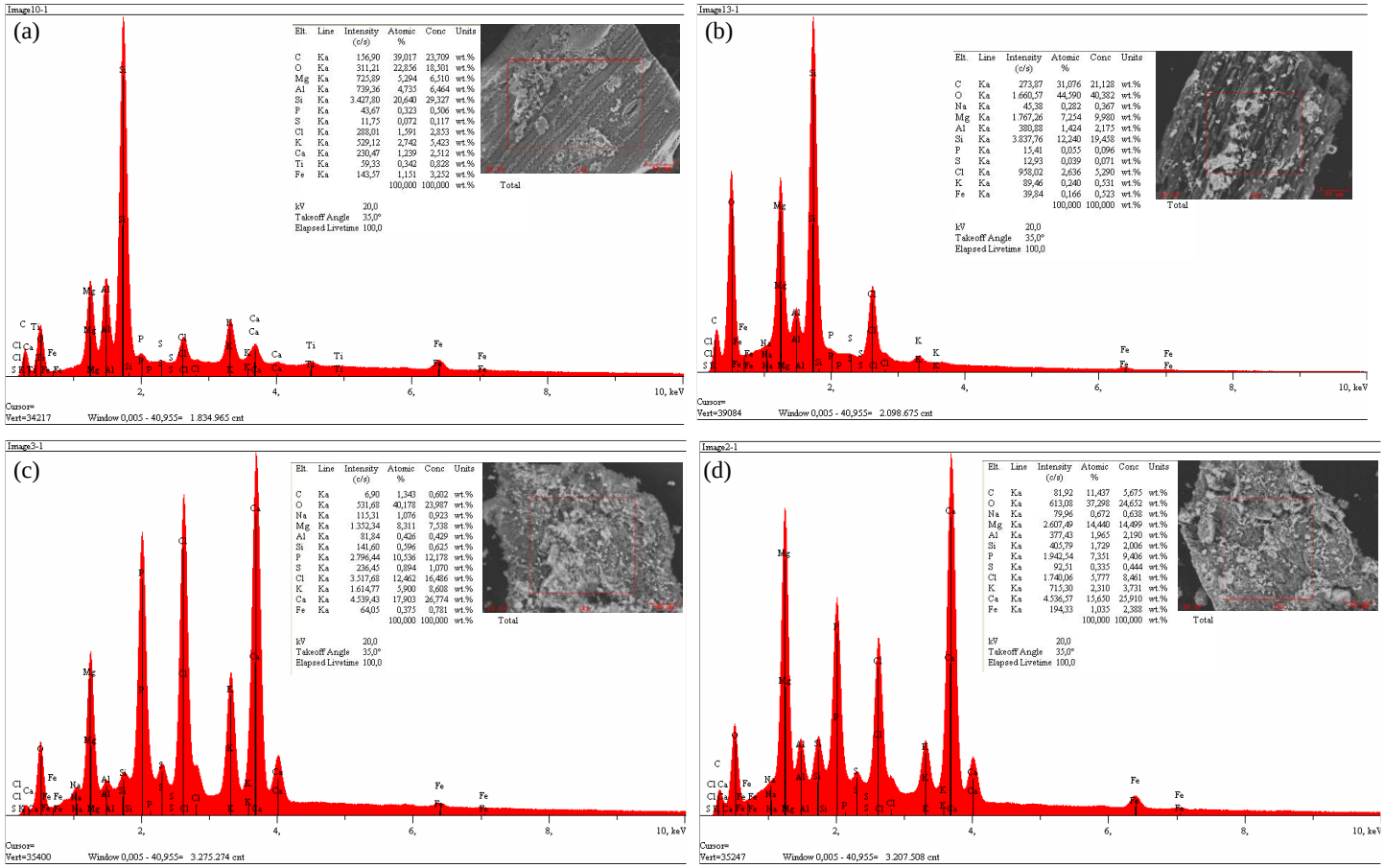

Figure 3. SEM and EDS of sugarcane straw biochar pyrolyzed at 350 °C (a) and at 650 °C (b) and poultry manure biochar, also pyrolyzed at 350 °C (c) and 650 °C (d) after doping process and in their maximum P adsorption capacity (MPAC).

4.3.2. Phosphorus adsorption

The Langmuir isotherm presented a better fit, with a higher R^2 than Freundelich's isotherm (Table 2). All of the biochars, before doping, did not have the capacity to adsorb P. Poultry manure, having a higher natural content of this element, desorbed only a small amount (2.03 mg L^{-1}) after agitation with deionized water, as can be observed from the other points of the curve. On the other hand, doping with Mg made them efficient P adsorbents.

The biochar from poultry manure (BPM), regardless of pyrolysis temperature, had a much greater MPAC than the biochar from sugarcane straw (BCS) (Table 2). When comparing the different pyrolysis temperatures within the same biochar for both materials, there was no effect of the temperature on P adsorption. However, the constants that represent the binding energy (K_F and K_L) increased for the higher pyrolysis temperature (650 ° C) for both biochars (Table 2).

Table 2. Values of K_L, qe, K_F, n and R^2 for the Langmuir and Freudelich isotherms for the biochars of poultry manure pyrolyzed at 350 °C (BPM 350°C) and at 650 °C (BPM 650°C) and of sugarcane straw pyrolyzed at 350 °C (BCS 350 °C) and at 650 °C (BCS 650 °C)

	Langmuir		
	K_L	q_e	R^2
	L mg^{-1}	mg g^{-1}	
BPM 350 °C	0.00155	250.7	0.96
BPM 650 °C	0.00396	163.5	0.97
BCS 350 °C	0.00869	17.7	0.93
BCS 650 °C	0.00992	17.5	0.99
	Freudelich		
	K_F	n	R^2
	mg (1-n) Ln g^{-1}		
BPM 350 °C	2.19	1.6	0.92
BPM 650 °C	6.40	2.2	0.92
BCS 350 °C	1.25	2.7	0.92
BCS 650 °C	1.54	2.8	0.94

4.3.3. Phosphorus desorption

The desorption process adopted did not allow the removal of 100% of the adsorbed P from any of the biochars (Table 3). In agreement with the higher values of K_L and K_F, the biochars pyrolyzed at 650 °C (Table 2) released a lower quantity of P when treated with any of the three extraction solutions (Table 3). In addition to extracting a larger amount of the total P adsorbed, sulfuric acid required a lower number of extractions to complete extraction. The sulfuric acid extraction corresponds to the exchange of ligands between the phosphate adsorbed and the sulfate of the extractor. The sodium bicarbonate (pH 8.5), was less aggressive and extracted a smaller quantity, needing a larger number of extractions, since the extraction corresponds to the exchange of ligands between the adsorbed phosphate and hydroxyls of the extractor. With very low extraction power, water did not desorb the P adsorbed with high binding energy (Table 3).

Table 3. Concentrations of desorbed P after successive extractions with H_2SO_4, $NaHCO_3$ e H_2O.

	Successive extractions								
Biochar	1th	2nd	3rd	4th	5th	6th	7th	Total	Dessorbed
	P mg L^{-1}								%
	H_2SO_4								
BPM 350 °C	145.5	75.4	2.8	-	-	-	-	223.7	89.2
BPM 650 °C	86.7	33.5	8.5	3.2	2.8	-	-	134.7	82.3
BCS 350 °C	5.5	3.3	0.0	-	-	-	-	8.8	49.7
BCS 650 °C	3.8	2.8	1.9	-	-	-	-	8.5	48.3
	$NaHCO_3$								
BPM 350 °C	121.6	72.4	15.2	5.3	3.8	-	-	218.3	87.0
BPM 650 °C	56.3	24.5	17.4	12.7	10.9	7.1	4.2	133.1	81.4
BCS 350 °C	4.5	2.4	-	-	-	-	-	6.9	38.9
BCS 650 °C	3.7	1.9	-	-	-	-	-	5.6	31.9
	H_2O								
BPM 350 °C	24.0	5.4	-	-	-	-	-	29.4	11.7
BPM 650 °C	17.1	4.2	-	-	-	-	-	21.3	13.0
BCS 350 °C	-	-	-	-	-	-	-	0.0	0.0
BCS 650 °C	-	-	-	-	-	-	-	0.0	0.0

4.4. DISCUSSION

The effectiveness of the doping process in both biochars and the pyrolysis temperatures, confirmed by X-rays, FTIR, SEM and EDS, is supported by several other studies (Cui et al., 2016; Wang et al., 2016; Moazzam et al., 2017). Mg added in the doping process appears as pyroxene (MgSiO) at lower pyrolysis temperature (Figure 1a and 1c), and is associated with a higher concentration of this element in lower pyrolysis temperatures. For BPM, even forms of dolomite (CaMgO) were found, since at low temperatures the Ca was not lost This information is in accordance with the higher levels of Si found in BCS (Table 1). At higher pyrolysis temperature (350 °C) (Figure 1a and 1c) the predominant form of Mg is periclase (MgO) and is associated with a loss of elements when enhancing pyrolysis temperatures, forming, in some cases, even graphite (higher peaks in Figures 1b and 1d).

By increasing the C content and reducing the O content during the pyrolysis process and with a further increase in the applied temperature, the O/C ratio will be affected. This ratio is related to the dehydration reactions that take place during pyrolysis and the biochar's affinity to water, thus these materials become more hydrophobic with pyrolysis. Moreover, this ratio is related to the recalcitrance of the material and the development of more stable structures, indicating that

pyrolysis at increasingly higher temperature lead to the development of aromatic structures in the biochars. With a lower O/C ratio it can be inferred that the biochar will mineralize at a faster rate when applied to the soil (Yao et al., 2011). This fact was confirmed by Novais et al. (2017) when applying poultry manure biochar to the soil and measuring the emission of greenhouse gases (GHG) and the microbial biomass of the soil. These authors observed higher GHG mitigation when applying biochar in comparison to the raw material. Contrastingly, BCS presented a higher GHG mitigation potential, presenting lower microbial biomass, despite having a smaller emission difference when compared to its raw material. This fact was attributed to the recalcitrant nature of sugarcane straw when compared to poultry manure.

Contrary to other findings in literature (Yao et al., 2011; Cantrell et al., 2012; Wang et al., 2013) this study reported a reduction in macro and micronutrients for poultry litter biochar with increasing pyrolysis temperature. The variability in poultry manure composition and the very high initial concentrations of such elements could be the explanation for this observation.

The best fit of the Lagmuir isotherm data, compared to those of Freundlich (Table 1), is in agreement with the main use of these isotherms. The Langmuir isotherm is considered a mono-layer process, in which the MPAC shows the affinity between adsorbent and adsorbate (Desta, 2013). This isotherm is recommended for data that have a "plateau", as is the case of elements like P, adsorbed by covalence and with a well-defined MPAC. The Freundlich isotherm is considered a multi-layered process, in which the amount of the adsorbed product increases gradually as the concentratio of the adsorbent increases (Desta, 2013). This isotherm is commonly used in processes of adsorption of contaminants, such as xenophobic ones (Niandou et al., 2016).

The inability of the biochars to adsorb P is developed by the doping process, which proves that such materials, without a treatment, are incapable of adsorbing anions. The higher MPAC of BPM is justified by the characteristics of the raw material, with its reactivity being superior to that of the sugarcane straw. As found in other studies (Lehman and Joseph, 2015; Fang et al., 2015; Jung et al., 2016b) the initial properties of the raw material greatly affect biochars properties, consequently inlfuencing the MPAC. The negative effect of pyrolysis at high temperatures with respect to P adsorption, is also related to the initial reactivity of the raw material, which is reduced by increasing the pyrolysis temperature. Jung et al. (2016b) observed increased ash content, pH, electrical conductivity and C content by raising the pyrolysis temperature from 200 to 400 and 600 to 800 °C. By gradually raising the pyrolysis temperature, these authors also observed a reduction of the H, N and O contents, and consequently the H/C and O/C ratios, as well as surface area and pore volume, which typically reduce the characteristics of the reactivity sites. These authors encountered a higher MPAC in the biochar pyrolyzed at 400 °C (18.1 mg g^{-1}), with an increasing

reduction of this value as the pyrolysis temperature was enhanced, with the lowest value (12.97 mg g^{-1}) reported for the biochar pyrolyzed at 800 °C. Dai et al. (2017) also observed an increasing reduction in MPAC in a biochar from crab shells when enhancing the pyrolysis temperature from 300 to 400 and 500 to 600 °C.

Takaya et al. (2016), while studying different biochars, pyrolyzed at various temperatures, clearly observed an effect, not only of the raw material, but also the pyrolysis temperature, in further distancing the biochar from the characteristics of the source material. The biochar from the filter cake of an anaerobic digester, with higher reactivity (lower levels of C, H, N and O and higher ash content), presented MPAC of 37 mg g^{-1} when pyrolyzed at 250 °C, which was reduced to 7.8 mg g^{-1} by raising the pyrolysis temperature to 400-450°C. As a more recalcitrant material, oak wood biochar presented a reduction in P adsorption from 26.6 to 5.5 mg g^{-1} after raising the pyrolysis temperature from 250 to 450 °C, respectively. The biochar from greenhouse residue, with a higher CEC compared to the previous materials, did not adsorb P after pyrolysis at 250 ºC, but presented an MPAC of 18.7 mg g^{-1} when pyrolyzed at 400-450°C and 9.1 mg g^{-1} at 600-650 °C. The material produced after pyrolysis at 250 ºC is not considered a biochar, but a hydrochar by these and other authors (Schimmelpgenning et al., 2017; Fornes et al., 2017).

The greater need for successive extractions to remove the adsorbed P in materials produced at higher pyrolysis temperatures (Table 2) are in agreement with the higher values of the K_L and K_F isotherm constants (Table 1) and demonstrate an advantage of pyrolysis at high temperatures. On one hand, the treatment reduces the MPAC, but on the other hand it increases the P binding energy, forcing the adsorbed P to be released at a slower rate, making the supply of this element more sustainable, an ideal condition in weathered tropical soils where the soil competes with the plant for this nutrient.

If a hypothetical recommendation of 90 kg ha^{-1} of P_2O_5 is considered for a highly weathered tropical soil, with P deficiency, and knowing that Single Superphosphate (SS) contains 18 % P_2O_5 and Triple Superphosphate (TS) contains 43 % of soluble P_2O_5, to achieve this recommendation, 500 kg ha^{-1} or 209.30 kg ha^{-1} of SS or TS would be required, respectively. BPM pyrolyzed at 350 °C has an MPAC of 250.76 mg g^{-1} (Table 2) and a desorption of 89.2 % (223.70 mg g^{-1} of P), when using the acidic extractor (Table 3). Based on this desorption value, 174.92 kg ha^{-1} of this biochar (BPM-Mg 350 °C) would be required to meet the recommendation of 90 kg ha^{-1} of P_2O_5. Furthermore, the rest of the adsorbed P (27.06 mg g^{-1} of P) that was not recovered by the extractor, may be available to the plants in the medium to long-term.

With these calculations, it can be noted that the use of biochars to recover eutrophic/wastewater, possible only after doping, is not their only benefit. The application of

biochars to agricultural soils has great potential, in this case the dose required is 2.8 times lower than that of SS and 1.2 time lower than TS. Additionally, biochar has proven to be an approach to enhance soil properties, especially in low fertility conditions (Lehman and Joseph, 2015; Agegnehu et al., 2016; Sánchez-García et al., 2016). For example, the application of hydrogel in planting pits, to preserve moisture retention, especially in forest plantations, is not a recent practice (Navroski et al., 2015). Biochar application, which also has this benefit, could be an interesting alternative from an ecological point of view, since it is an organic product, contrary to some hydrogels that can contain synthetic substances that are not biodegradable in the short-term (Senna and Botaro, 2017). Morevoer, biochars have a high pH with an action similar to liming (Butnan et al., 2015). This attribute is particularly interesting in tropical soils with elevated P adsorption capacity, due to the low pH and consequent high Al^{3+} levels, which limits P fertilization effectiveness. Finally, biochars have the potential to improve the effectiveness of P fertilization in higly weathered tropical soils by steadly releasing P for plant uptake (Novais & Smith, 1999).

4.5. CONCLUSIONS

The raw materials, poultry manure and sugarcane straw, after passing through the process of pyrolysis, had their recalcitrance increased, making these residues ideal for the production of biochars. All the biochars, independently of the pyrolysis temperature, did not possess the capacity to adsorb P. However, after the doping process, such ability is installed. Due to the initial high stability of the raw material, the pyrolysed sugarcane straw had a lower MPAC than that of poultry manure biochar, even after a successful doping with Mg. The pyrolysis temperature significantly affect the MPAC of the poultry manure biochar and the binding energy of the adsorbed P increased with an increase in the pyrolysis temperature for both biochars. Thus, only the acid extractor (H_2SO_4 0.5 mol L^{-1}) removed considerly the P retained in both biochars produced at 650 °C. Findings from this study suggest that doped biochar has a high potential to be used as slow-release fertilizer, being an extremly important soil fertility strategy in highly weathered tropical soils. Although further research is needed, we believe this approach can be combined to eutrophic/wastewater treatment to develop a sustainable phosphate fertilizer.

REFERENCES

Agegnehu, G., Bass, A.M., Nelson, P.N., Bird, M.I. (2016). Benefits of biochar, compost and biochar–compost for soil quality, maize yield and greenhouse gas emissions in a tropical agricultural soil. Science of the Total Environment, 543, 295-306. doi:10.1016/j.scitotenv.2015.11.054

Butnan, S., Deenik, J.L., Toomsan, B., Antal, M.J., Vityakon, P. (2015). Biochar characteristics and application rates affecting corn growth and properties of soils contrasting in texture and mineralogy. Geoderma, 237, 105-116. doi:10.1016/j.geoderma.2014.08.010

Cantrell, K.B., Hunt, P.G., Uchimiya, M., Novak, J.M., Ro, K.S. (2012). Impact of pyrolysis temperature and manure source on physicochemical characteristics of biochar. Bioresource Technology, Oxford, 107, 419–428. doi:10.1016/j.biortech.2011.11.084

CONAMA (2005). Resolution. 357, March 17, 2005. Provides for the classification of water bodies and environmental guidelines for their classification, as well as establishing the conditions and standards for effluent releases. Brasília.

Conz, R.F., Abbruzzini, T.F., Andrade, C.A., Milori, D.M. B. P., Cerri C.E.P. (2017). Effect of Pyrolysis Temperature and Feedstock Type on Agricultural Properties and Stability of Biochars. Agricultural Sciences. In press.

Cui, X., Dai, X., Khan, K. Y., Li, T., Yang, X., He, Z. (2016). Removal of phosphate from aqueous solution using magnesium-alginate/chitosan modified biochar microspheres derived from Thalia dealbata. Bioresource Technology, 218, 1123-1132. doi:10.1016/j.biortech.2016.07.072

Dai, L., Tan, F., Li, H., Zhu, N., He, M., Zhu, Q., Zhao, J. (2017). Calcium-rich biochar from the pyrolysis of crab shell for phosphorus removal. Journal of Environmental Management, 198, 70-74. doi:10.1016/j.jenvman.2017.04.057

Desta, M.B. (2013). Batch sorption experiments: Langmuir and Freundlich isotherm studies for the adsorption of textile metal ions onto teff straw (Eragrostis tef) agricultural waste. Journal of thermodynamics. doi:10.1155/2013/375830

Drenkova-Tuhtan, A., Meyer, C., Schneider, M., Mandel, K., Gellermann, C., Franzreb, M., Steinmetz, H. (2016). Application of magnetic microsorbents for seperation, concentration and recovery of phosphate from wastewater streams. In The 13th IWA Leading Edge Conference on Water and wastewater Technologies.

Fang, C., Zhang, T., Li, P., Jiang, R.F., Wang, Y.C. (2014). Application of magnesium modified corn biochar for phosphorus removal and recovery from swine wastewater. International journal of environmental research and public health, 11(9), 9217-9237. doi:10.3390/ijerph110909217

Fang, C., Zhang, T., Li, P., Jiang, R., Wu, S., Nie, H., Wang, Y. (2015). Phosphorus recovery from biogas fermentation liquid by Ca–Mg loaded biochar. Journal of Environmental Sciences, 29, 106-114. doi:10.1016/j.jes.2014.08.019

Fink, J.R., Inda, A.V., Bavaresco, J., Barrón, V., Torrent, J., Bayer, C. (2016). Adsorption and desorption of phosphorus in subtropical soils as affected by management system and mineralogy. Soil and Tillage Research, 155, 62-68. doi:10.1016/j.still.2015.07.017

Fornes, F., Belda, R.M., Fernández de Córdova, P., Cebolla-Cornejo, J. (2017). Assessment of biochar and hydrochar as minor to major constituents of growing media for containerized tomato production. Journal of the Science of Food and Agriculture. doi: 10.1002/jsfa.8227

IBI (2015) Standardized Product Definition and Product Testing Guidelines for Bi- ochar that Is Used in Soil, International Biochar Initiative. http://www.biochar-international.org/characterizationstandard

Jing, R., Li, N., Li, L., An, J., K., Zhao, L., Ren, N. Q. (2015). Granulation and ferric oxides loading enable biochar derived from cotton stalk to remove phosphate from water. Bioresource technology, 178, 119-125. doi:10.1016/j.biortech.2014.09.071

Jung, K.W., Ahn, K.H. (2016a). Fabrication of porosity-enhanced MgO/biochar for removal of phosphate from aqueous solution: application of a novel combined electrochemical modification method. Bioresource technology, 200, 1029-1032. doi:10.1016/j.biortech.2015.10.008

Jung, K.W., Hwang, M. J., Ahn, K.H., Ok, Y.S. (2015). Kinetic study on phosphate removal from aqueous solution by biochar derived from peanut shell as renewable adsorptive media. International Journal of Environmental Science and Technology, 12(10), 3363-3372. doi:10.1007/s13762-015-0766-5

Jung, K.W., Kim, K., Jeong, T.U., Ahn, K.H. (2016b). Influence of pyrolysis temperature on characteristics and phosphate adsorption capability of biochar derived from waste-marine macroalgae (Undaria pinnatifida roots). Bioresource technology, 200, 1024-1028. doi:10.1016/j.biortech.2015.10.016

Klein, C., Agne, S.A.A. (2013). Phosphorus: from nutrient to pollutant! *Revista Eletrônica em Gestão, Educação e Tecnologia Ambiental*, *8*(8), 1713-1721.

Lehmann, J., Joseph, S. (2015). Biochar for environmental management: science, technology and implementation, Routledge.

Moazzam, A., Jamil, N., Nadeem, F., Qadir, A., Ahsan, N., Zameer, M. (2017). Reactive Dye Removal by a Novel Biochar/MgO Nanocomposite. Journal of the Chemical Society of Pakistan, 39(1).

Navroski, M.C., Araújo, M.M., Reininger, L.R.S., Muniz, M.F.B., Pereira, M.D.O. (2015). Doses of hydrogel influencing growth and nutritional content in seedlings *Eucalyptus dunnii*. Floresta, 45(2), 315-328. doi:10.5380/rf.v45i2.34411

Niandou, M.A.S., Luster-Teasley, S., Bansode, R.R., Novak, J.M., Rehrah, D., Ahmedna, M. (2016). Adsorption Isotherm Parameters of Atrazine and Metolachlor with Pecan Shell-based Activated Carbons. International Journal of Agricultural Science and Technology. doi:10.12783/ijast.2016.0402.01

Novais, R.F., Smyth, T.J. (1999). Phosphorus in soil and plant in tropical conditions. Viçosa, MG, Federal University of Viçosa, p. 399.

Novais, S.V., Zenero, M.D.O., Frade Junior, E.F., Lima, R.P., Cerri, C.E.P. (2017). Mitigation of greenhouse gas emissions from tropical soils amended with poultry manure and sugar cane straw biochars. Agricultural Sciences, 8(9). In Press.

Novotny, E.H., Maia, C.M.B.D.F., Carvalho, M.T.D.M., Madari, B.E. (2015). Biochar: pyrogenic carbon for agricultural use-a critical review. Revista Brasileira de Ciência do Solo, 39(2), 321-344. doi:10.1590/01000683rbcs20140818

Roy, E.D., Richards, P.D., Martinelli, L.A., Della Coletta, L., Lins, S.R.M., Vazquez, F.F., Porder, S. (2016). The phosphorus cost of agricultural intensification in the tropics. Nature plants, 2, 16043. doi:10.1038/NPLANTS.2016.43

Sánchez-García, M., Sánchez-Monedero, M.A., Roig, A., López-Cano, I., Moreno, B., Benitez, E., Cayuela, M.L. (2016). Compost vs biochar amendment: a two-year field study evaluating soil C build-up and N dynamics in an organically managed olive crop. Plant Soil 408, 1–14. doi:10.1007/s11104-016-2794-4

Schimmelpfennig, S., Kammann, C., Mumme, J., Marhan, S., Bamminger, C., Moser, G., Müller, C. (2017). Degradation of Miscanthus× giganteus biochar, hydrochar and feedstock under the influence of disturbance events. Applied Soil Ecology, 113, 135-150. doi:10.1016/j.apsoil.2017.01.006

Senna, A.M., Botaro, V.R. (2017). Biodegradable hydrogel derived from cellulose acetate and EDTA as a reduction substrate of leaching NPK compound fertilizer and water retention in soil. Journal of Controlled Release. doi:10.1016/j.jconrel.2017.06.009

Takaya, C.A., Fletcher, L.A., Singh, S., Anyikude, K.U., Ross, A.B. (2016). Phosphate and ammonium sorption capacity of biochar and hydrochar from different wastes. Chemosphere, 145, 518-527. doi:10.1016/j.chemosphere.2015.11.052

Wang, Y., Hu, Y., Zhao, X., Wang, S., Xing, G. (2013). Comparisons of biochar properties from wood material and crop residues at di ff erent temperatures and residence times. Energy & Fuels, Washington, 27, 5890–5899. doi:10.1021/ef400972z

Wang, Z., Shen, D., Shen, F., Li, T. (2016). Phosphate adsorption on lanthanum loaded biochar. Chemosphere, 150, 1-7. doi:10.1016/j.chemosphere.2016.02.004

Yao, Y., Gao, B., Zhang, M., Inyang, M., Zimmerman, A.R. (2012). Effect of biochar amendment on sorption and leaching of nitrate, ammonium, and phosphate in a sandy soil. Chemosphere, 89(11), 1467-1471. l rights reserved. doi:10.1016/j.chemosphere.2012.06.002

Yu, P., Xue, Y., Gao, F., Liu, Z., Cheng, X., Yang, K. (2016). Phosphorus Removal from Aqueous Solution by Pre-or Post-Modified Biochars Derived from Agricultural Residues. Water, Air & Soil Pollution, 227(10), 370. doi:10.1007/s11270-016-3066-x

Zhang, H., Chen, C., Gray, E.M., Boyd, S.E., Yang, H., Zhang, D. (2016). Roles of biochar in improving phosphorus availability in soils: A phosphate adsorbent and a source of available phosphorus. Geoderma, 276, 1-6. doi:10.1016/j.geoderma.2016.04.020

Zhang, M., Gao, B., Yao, Y., Xue, Y., Inyang, M. (2012). Synthesis of porous MgO-biochar nanocomposites for removal of phosphate and nitrate from aqueous solutions. Chemical Engineering Journal, 210, 26-32. doi:10.1016/j.cej.2012.08.052

5. PHOSPHORUS REMOVAL FROM EUTROPHIC WATER USING MODIFIED BIOCHAR

ABSTRACT

Increasing problems related to water eutrophication, commonly caused by the high concentration of phosphorus (P), are stimulating studies aimed at an environmentally safe solution. Moreover, some research has focused on the reuse of P due to concerns about the end of its natural reserves. Biochar appears to be a solution to both problems and may act as a recovery of eutrophic/residual water with the subsequent reuse of P in agriculture, the purpose of which is to test such an assertion. Samples of biochar from poultry manure (BPM) and sugarcane straw (BCS) had their maximum adsorption capacities of Al obtained by Langmuir isotherm. These values were used to conduct the so-called post-doping process, conferring P adsorption capacity to the pyrolysed materials. Langmuir and Freudelich isotherms were adjusted for the same biochar types (Al-doped) at increasing P concentrations, in order to obtain their maximum P adsorption capacities (MPAC) and their parameters. The desorption of the adsorbed P in its MPAC was tested by three extractors: H_2SO_4, $NaHCO_3$, and H_2O. Finally, these biochar types were used in competitive adsorption assays of phosphate, sulfate, chloride and nitrate anions and applied in a hypothetical eutrophic water. These materials underwent several characterization analyses that confirmed the success of the post-doping process with Al and the adsorption capacity of P. The high values of MPAC of the powder materials (701.6 and 758.9 mg g^{-1} of P for BPM and BCS, respectively) are reduced by almost half for the fragment materials (356.1 and 468.8 mg g^{-1} of P for BPM and BCS, respectively), these values being almost entirely extracted by acid and basic extractors. Its application in eutrophic/residual water, in addition to presenting a good MPAC, these materials adsorbed, in equal proportions, phosphates and sulfates, as well as to a lesser extent, nitrates and chlorides. Thus, biochar from poultry manure and sugarcane straw, after post-doping with Al, have high MPAC, being excellent materials for the recovery of eutrophic/residual water and a possible subsequent reuse in agriculture.

Keywords: Sugar cane straw; Poultry manure; Al doping; P desorption; Potencial reuse; Langmuir isotherm

5.1. INTRODUCTION

Increasing concerns regarding the exhaustion of P natural reserves, after estimates for its end by 2050 by [1], have caused researchers to seek the reuse or recycling of this element, reducing somewhat the apprehension generated, mainly around its use as fertilizer in tropical soils, which are so poor in P.

Adsorption techniques have been used for several years for the recovery of eutrophic water, which predispose the high growth of microorganisms and aquatic plants, causing a rapid consumption of oxygen, with the subsequent death of the aquatic fauna. Adsorbent materials such as Fe and Al oxyhydroxides are commonly used because of their low cost and easy handling in water quality recovery [2, 3].

Recently, several authors have focused on biochar as a source of study for this purpose in several experiments. The biochar generated after the pyrolysis of plant or animal residues is characterized by several soil benefits, such as increased physical qualities, increased microbial biomass, and soil organic carbon, as well as xenophobic removal, acting to recover contaminated environments [4]. In addition to these positive aspects, the modified biochar has been shown in a number of papers as a potent adsorbent of P, which can act in the recovery of eutrophic waters [5-8]. Thus, the P of eutrophic and residual water can be reused. The recovery of this P in solution/suspension and its subsequent application to the soil as a phosphate fertilizer is becoming an increasingly widespread idea, thus closing a cycle of P utilization, which addresses not only the problem but also ensures its reuse, thus increasing the time for the exhaustion of world reserves of phosphate rocks [9, 10].

Nevertheless, such a scenario is not as simple, and to close this reuse/recycling cycle as desired, some biochar modification techniques are needed. The biochar, due to the large amount of phenolic and carboxylic groups and a high proportion of fulvic and humic acids, is seen as a large anion [11] which, without previous treatment, would not be able to adsorb significant amounts of phosphate. A technique called "doping," which consists of saturating the biochar with a metal cation, making it an "anionic adsorbent," ensures its electropositivity, allowing the material to adsorb anions, no longer repelling them. A number of cations are used for doping, with Mg and Ca being more commonly used due to their low cost and easy handling [5, 12-14].

[13] found an adsorption of 3.7 and 8.3 mg g^{-1} of P in the source material (seaweed) and the biochar of this pyrolyzed material at 600 °C, respectively. The adsorption value rises to 16.1 mg g^{-1} of P in this material after doping with $MgCl_2$, increasing to 19.8 mg g^{-1} by subjecting the same doped biochar to an electric field. The electric field increases the surface area and amount of micropores, promoting more adsorption sites of P. [14], in another work, using biochar from seaweed pyrolyzed at 600 °C and doped with Ca found a P adsorption of 63.3, 94.5 and 127.5 mg g^{-1}, after maintaining the adsorption temperature at 10 °C, 20 °C and 30 °C, respectively. In the adsorption/desorption work, [5] find a maximum P adsorption capacity (MPAC) greater than 100 mg g^{-1} of P in the Mg-doped tomato leaf biochar and a desorption of 7.55 mg g^{-1} of P in the material extracted with Mehlich-3. The value recovered accounts for 18 % of the total amount adsorbed,

this value being higher than the concentration found in many phosphate fertilizers and sufficient to meet the demand of the plant. The authors confirmed this fact after finding a germination of 53-85 % higher in seeds that received the doped biochar as a source of P.

These procedures, characterized by saturating the material to be pyrolyzed with metal cations, following the pyrolysis process normally after immersion of the material in a solution of Mg or Ca in excess (pre-pyrolysis doping). Nevertheless, some authors propose that the doping process should be done after complete pyrolysis, i.e. following production of the biochar, using cations such as Al^{3+} or Fe^{3+} (post-pyrolysis doping). Such a procedure, according to [15], would lead not only to a reduction in the time of production of the modified biochar, but also to an increase in its physical and chemical qualities, such as an increase in surface area and production of AlOOH nanoparticles. These authors found a MPAC of 647 mg g^{-1} of P after 8 h of reaction with the Al-doped seaweed biochar, which is much higher than that found in other experiments using the pre-pyrolysis doping process. Contrarily, [12] found a MPAC of 1.35 and 17.41 mg g^{-1} of P and As, respectively, with $AlCl_3$-doped biochar, conducing the pre-pyrolysis process.

Nevertheless, such situations occur in an ideal environment where there is no competition between anions for the adsorption sites. MPAC values are usually reduced by including other anions in the solution. [16] found a small reduction (3.02 %) in the MPAC by adding 0.1 mol L^{-1} of Cl^-, NO_3^- and SO_4^{2-} with 100 mg L^{-1} of P, and SO_4^{2-} was the one that presented greater affinity in the exchange sites due to their greater valence and predominance of covalent bonds. [17] observed a reduction in P removal of 59.9 % and 72.5 % after addition of 0.15 and 0.50 mmol L^{-1}, respectively, of arsenate and a reduction of 26.2 % and 40.2 % on the P adsorption by adding HCO_3^- at the same concentrations. The addition of NO_3^- and SO_4^{2-} did not significantly reduce the P adsorption. The high adsorption of As by the Fe-doped biochar leads the authors consider their removal in conjunction with P in water decontamination.

These techniques are being increasingly studied, aiming at the day when the use of these materials can become routine, not only as a means to recover eutrophic/residual water, but also to mitigate another major problem: the exhaustion of the natural reserves of P. Thus, the purpose of this paper was the production of Al-modified biochars from sugarcane straw and poultry manure doped by the post-pyrolysis process. The determination of adsorption and desorption isotherms of P in a pure solution and with competitive anions was also the subject of this paper, closing a cycle of adsorption (recovery of eutrophic and residual water) and desorption (reuse of P adsorbed as phosphate fertilizer).

5.2. MATERIAL AND METHODS

5.2.1. Selection of raw materials for biochar production

Two raw materials were selected according to their contrasting characteristics and their large production, often being an environmental problem: poultry manure (PM), collected at a farm called Frango Feliz, located at ESALQ-USP, and sugarcane straw (CS) from a sugar/ethanol production site in Piracicaba, SP.

5.2.2. Biochar production

The pyrolysis process was performed by the SPPT company in a metallic reactor, in an atmosphere saturated with N_2, raising the temperature by 10 °C every minute in the first 30 min and then at 20 °C every minute until the desired temperature was reached.

Two pyrolysis temperatures – 350 °C and 650 °C – were used based on values mentioned in the literature and because they cover the main phases of transformation of the raw material, being responsible for its changes and for the characteristics of the biochar produced. Temperatures below 350 °C are considered as torrefaction rather than pyrolysis, while pyrolysis above 650 °C results in reduced biochar production [18].

5.2.3. Characterization of the material

5.2.3.1. Differential scanning calorimetry (DSC) and Thermogravimetric analysis (TGA)

The DSC and TGA analyses were obtained using a Netzsch TGA-DSC device, STA 409 PC Luxx model, coupled to a Netzsch mass spectrometer, QMS 403 C-Aeolos model, using an alumina crucible. The heating rate was 10 °C min^{-1} until the maximum temperature of 1000°C was reached in synthetic air (80 % N_2 and 20 % O_2).

5.2.3.2. X-ray diffraction (XRD)

Powder X-ray diffraction (PXRD) was conducted with the Shimadzu XRD-6000 device, using graphite crystal as a monochromator to select the radiation of Cu-$K\alpha_1$ with λ= 1.5406 Å, with a resolution of 0.02 s^{-1} in the angular domain 4- 70°.

5.2.3.3. Molecular absorption spectroscopy in the infrared region (FTIR)

Fourier-transform infrared (FTIR) spectra of biochars were collected by an FTIR appliance (Jasco ATR/FTIR 4100). The biochar was pressed into pellets for analysis, and the infrared spectra were collected in the range of 4000-400 cm^{-1} with 120 scans.

5.2.3.4. Scanning electron microscope (SEM) and energy-dispersive spectroscopy (EDS)

Scanning electron microscopic observations were carried out with a JSN 5600 LV (Jeol, Tokyo, Japan) instrument coupled to a NORAN energy dispersive spectrometer (ThermoFisher Scientific, Waltham, MA, USA). Coating with gold was used to coat non-conductive samples.

5.2.3.5. X-ray photoelectron spectroscopy (XPS)

Chemical surface evaluations of raw biochars, Al-doped biochars and Al-doped biochars after P adsorption, were carried out by X-ray photoelectron spectroscopy (XPS), using a K-Alpha X-ray photoelectron spectrometer (Thermo Fisher Scientific, U.K.) equipped with a monochromatic Al Kα (1486.6 eV) radiation source. High-resolution spectra for C, Al and P were acquired using pass energy of 50 eV. The binding energies were referenced to the C1s peak at 284.6 eV for calibration. The deconvolution of XPS peaks was conducted using the CasaXPS software with Gaussian-Lorentzian (30 %) and Tougaard background subtraction. The XPS results correspond to an average of three independent measurements collected in different regions of each sample.

5.2.4. Al adsorption isotherm (post-doping)

To determine the concentration of Al used in the doping process, an adsorption isotherm of this cation was adjusted, with increasing Al concentrations varying from 5 to 3000 mg L^{-1} (5.0; 10.0; 25.0; 50.0; 70.0; 80.0; 90.0; 100.0; 120.0; 150.0; 200.0; 300.0; 500.0; 800.0; 1000.0; 1500.0; 1800.0; 2000.0; and 3000.0 mg L^{-1}). These concentrations were shaken with 0.3 g of biochar and 300 mL of the $AlCl_3$ solutions, and this high biochar mass/solution volume ratio with Al (1/1000) allowed the pH to be maintained below 3.0, adjusted with HCl, enabling the permanence of the Al^{3+} form in solution (Greenland, 2015). Stirring occurred for 24 h, and the suspension was filtered on white Whatman filter paper. The extracts were read in Inductively Coupled Plasma (ICP), and the values were used in the Langmuir adsorption isotherm adjustments (Equation 1), with the aim of estimating the maximum aluminum adsorption capacity (MAlAC).

$$q_e = K_L C_e / (1 + K_L C_e) \qquad \text{(Equation 1)}$$

Where: K_L represents the adsorption energy of Al (L mg^{-1}), q_e is the maximum adsorption capacity of this element (mg g^{-1}) and Ce is the Al concentration in the equilibrium solution (mg L^{-1}).

After the stirring period of the suspensions, the material was filtered and washed successively with deionized water until the biochar buffer allowed the original pH value to be sought (6.0), ensuring complete hydrolysis of Al ions in the biochar structure and establishing the development of positive charges in the material by the cationic bridges formed. Finally, the doped biochar was oven-dried for 20 minutes at 100 °C and passed through a 2-mm sieve.

5.2.5. P adsorption isotherms

For the determination of the MPAC, isotherms using 0.15 g of Al-biochar, in powdered or fragmented form (pieces as out of the pyrolyzer, with approximately 1 cm in size) were used, stirring with 75 mL of solutions with increasing P concentrations. These concentrations ranged from 0 to 3000 mg L^{-1} of P (0.0; 10.0; 25.0; 50.0; 100.0; 250.0; 500.0; 750.0; and 3000.0 mg L^{-1}) were shaken with the Al-biochar for 24 h and subsequently filtered on white Whatman filter paper. The determination of the P concentration in the solution was obtained in the UV/Vis spectrophotometer [19] and subjected to the Langmuir (Equation 1) and Freudlich (Equation 2) isotherm adjustments, obtaining its parameters.

$$q_e = K_F Cne \quad \text{(Equation 2)}$$

Where: K_F represents the Freudlich affinity coefficient (L mg^{-1}), q_e is the equilibrium concentration (mg g^{-1}), n is the linearity constant of Freudlich and C_e is the concentration of the sorbate in the equilibrium solution (mg L^{-1}).

5.2.6. P desorption

After determination of the MPAC for each biochar, the desorption of P from these materials was determined. To do this, successive extractions were made with deionized H_2O, 0.5 mol L^{-1} $NaHCO_3$ at pH 8.5 (Olsen extractor), and 0.5 mol L^{-1} H_2SO_4, until all P adsorbed was no longer detected. These extractors were also used by [20] to desorb P from different biochars and were adopted in this work because they cover distinct situations (alkaline and acid medium), in addition to being used in the extraction of available P from the soil [21].

A sample of 1 g of each biochar, with P previously applied, at a dose corresponding to its MPAC, and 300 mL of each extractor (solid-solution ratio of 1:300) were stirred for 48 h on a horizontal shaker at 120 rpm, as proposed by [20]. The suspensions were filtered on white Whatman filter paper, and the extracts were analyzed in a UV/Vis Spectrophotometer [19] for the determination of the P concentration desorbed. The process was repeated successively, in four replicates, until the P desorbed was no longer detected. At each stage of separation (filtration), the amount of biochar was reduced (a small portion was lost in the filter paper), requiring a readjustment of the extractor amount, always maintaining the solid-liquid ratio of 1:300.

5.2.7. Effect of competitive anions on P adsorption

For the study of the anionic selectivity of the biochars regarding their affinity for the phosphate anion, a test was conducted to verify the competitiveness of other anions on P adsorption. Solutions were prepared with 0.1 mol L^{-1} or 0.2 mol L^{-1} of the anions in salts KCl, KNO_3, K_2SO_4 and KH_2PO_4, which were subjected to shaking with both biochars, separately, doped with Al in their MAlAC for 48 h, on a horizontal shaker at 120 rpm, as proposed by [16]. The first concentration (0.1 mol L^{-1}) was taken from the work of [16], this being the most concentrated solution. Due to the high adsorption potential of the biochars, we chose to double

this concentration, guaranteeing that, at the end of the contact time, there would be an excess of anions, not adsorbed, for analysis. The solid-liquid ratio was maintained at 1:500 (0.15 g of biochar in 75 mL solution) as in the assay for obtaining MPAC. All treatments were conducted in four replicates and the extracts were determined by a continuous flow analyzer (FIAstar 5000) through analysis of the remaining concentrations of Cl^-, NO^{3-} and $PO4^{3-}$ anions in solution. The concentration of the remaining SO_4^{2-} was made by Inductively Coupled Plasma (ICP).

5.2.8. Adsorption in eutrophic water

Both biochars (poultry manure and sugarcane straw) were applied in a hypothetical eutrophic water for simulation of their use in a practical situation. The production of this water took into account values of the anion concentrations found by [22] in the Pampulha lagoon, located in Belo Horizonte, MG, one of the most well-known and studied lagoons in Brazil. Only the anions contained in the analysis were considered, as only they will be adsorbed in the Al-biochars and will compete for the P adsorption sites.

A "eutrophic water" was prepared with 4.53 mg L^{-1} sulfate, in the form of K_2SO_4, 8.83 mg L^{-1} chloride, in the form of KCl, 4.16 mg L^{-1} nitrate, in the form of KNO_3, and 0.55 mg L^{-1} phosphate, in the form of KH_2PO_4. These values were established based on the mean concentrations found by [22], at the surface and in depth in several sampling points in the lake. For the adsorption of P under these conditions, 0.15 g of biochar was stirred with 75 mL of the solution ("eutrophic water") for 12 h, on a horizontal shaker at 120 rpm, and the suspension was filtered on white Whatman filter paper. To ensure exhaustion of the adsorption sites, the solution, representing the eutrophic water, was replaced after every hour of shaking. The extract was analyzed by a continuous flow analyzer (FIAstar 5000), obtaining the concentrations of the remaining anions of NO^{3-}, Cl^- and $PO4^{3-}$ and by Inductively Coupled Plasma (ICP), obtaining the concentration of the remaining $SO4^{2-}$.

5.3. RESULTS AND DISCUSSION

5.3.1. Characterization of materials

5.3.1.1. Thermogravimetric Analysis (TGA)

Two distinct processes of mass loss occurs in the TGA of the poultry manure (Fig 1a), the first being an endothermic process, characterizing the initial water loss (m/z = 18), composed of adsorbed water, and the second being an exothermic process in which the mass loss line (TGA) did not stabilize at the maximum temperature of 1000 °C. The maintenance of the inflection, also indicating a mass loss, shows that the process has not yet finished, as the end of such procedure would be the graphitization of the material, which is not the purpose of this paper.

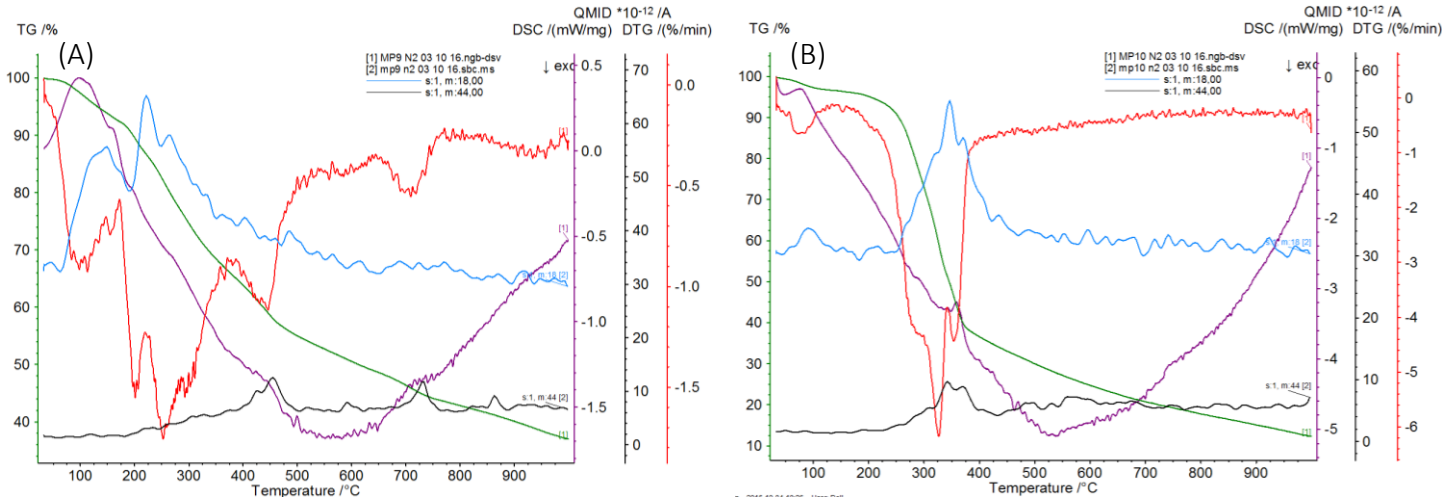

Fig 1. Differential scanning calorimetry (DSC) and Thermogravimetric analysis (TGA).
(A) Poultry manure as raw material and (B) sugar cane straw as raw material.

The second stage of water loss, characterized by the structural water, occurs around the temperature of 250 °C, and in the pyrolysis temperature used in this experiment (350 °C), almost all endothermic, water loss, adsorbed water or structural processes have already occurred. Concomitantly, exothermic processes occur, characterized by loss of CO_2 (m/z = 44). Such loss is small and occurs in three phases: 450 °C, 720 °C, and 860 °C. Mass reduction by the loss of CO_2, commonly reduced in non-oxidizing atmospheres, such as the N_2 used in this analysis, is of interest for materials such as biochar and the use intended herein.

In summary, on the processes that occur for this source material (poultry manure), we can say that the mass reduction is caused essentially by the loss of water (m/z = 18), being very little influenced by the CO_2 loss (m/z = 44), culminating in a total mass loss of 70 % at the pyrolysis temperature used in this experiment (350°C).

In contrast, sugarcane straw as the source material (Fig 1b) has a small loss of adsorbed water (m/z = 18) in the region of 100 °C, which is common for dry materials such as straws, characterizing the first difference between this material and poultry manure. In the 350 °C region, the inflection of the mass loss curve occurs, in this case with a total mass loss of 50 % of the

original material. Also at this temperature, the loss of structural water occurs, being the main agent responsible for the large mass loss. Equally, at 350 °C, the largest exothermic loss (CO_2) is also reduced due to the N_2 atmosphere used in this analysis, as discussed above.

5.3.1.2. X-ray diffraction (XRD)

In the X-ray diffractograms (Fig 2), the range of 10–23° 2θ showed typical low-crystallinity materials, likely from cellulose structures [23] also presented in the biochar [24]. After the doping process, a low-crystallinity phase of the newly-prepared aluminum oxide hydroxide, such as pseudoboehmite, may also contribute to a diffraction pattern in this region [25]. The presence of quartz (SiO_2) was identified by a well-defined peak at 3.333 Å, this being a common impurity in the biochar from poultry manure [24]. The presence of periclase (MgO) was identified by peaks at 2.046 Å and 1.445 Å.

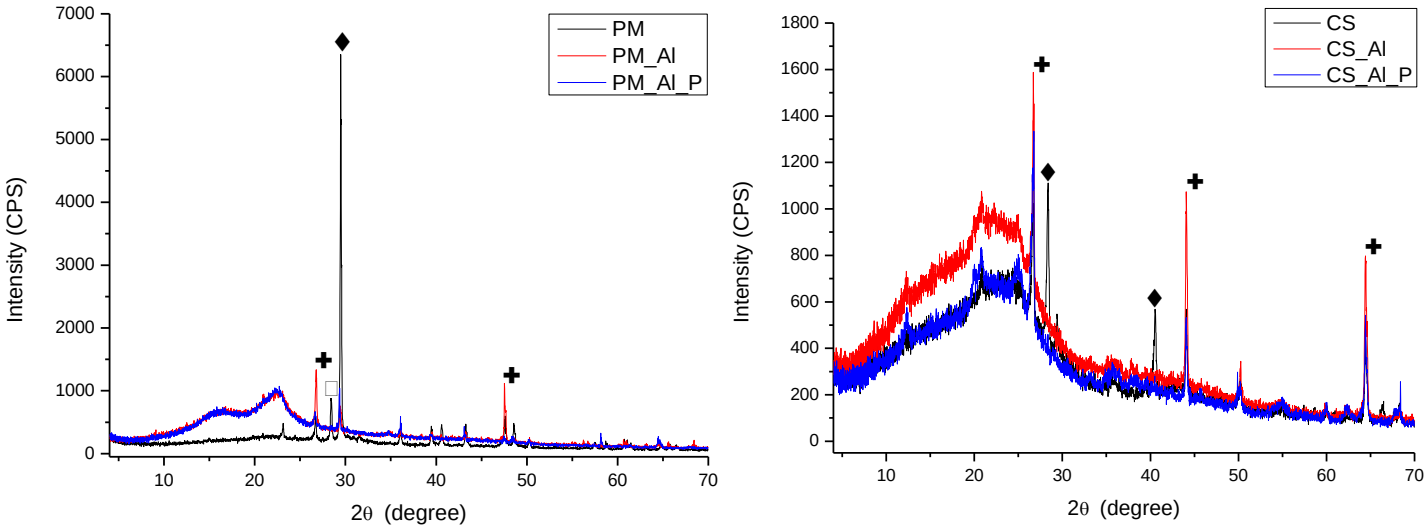

Fig 2. X-ray diffraction (XRD).
Biochar of poultry manure (PM), poultry manure doped with Al (PM_Al), poultry manure doped with Al and in its MPAC (PM_Al_P) and of biochars of sugar cane straw (CS), sugar cane straw doped with Al (CS_Al) and sugar cane straw doped with Al and in it MPAC (CS_Al_P). The simbols are for: ♦MgSiO (Pyroxene); ◀MgO (Periclase); ✚AlSiO (Kyanite).

5.3.1.3. Infrared Spectrophotometer (FTIR)

The appearance of bands related to the carboxylic acids (1500 cm^{-1} region) for the BPM (Fig 3a) and bands related to the aromatic C-H (840 cm^{-1} region) and their disappearances after

application of Al (BPM_Al and BPM_Al_P) corroborate with the inference that this element is being linked in these groups. This fact also occurs for BCS (Fig 3b), although with less intensity. In the 1100 cm^{-1} region, characterized by phosphates, we can observe the highest intensity for the biochar doped in its MPAC, both for BPM (Fig 3a) and BCS (Fig 3b). Finally, by this analysis we can also confirm the success of the doping process, with the highest intensity in the region of 400 cm^{-1}, responsible for the binding of metals with oxygen, for both biochars after the addition of Al. The region of 2927 and 2853 are responsible for CH_2/CH_3 vibrations and 2300 for the CO_2 of the environment.

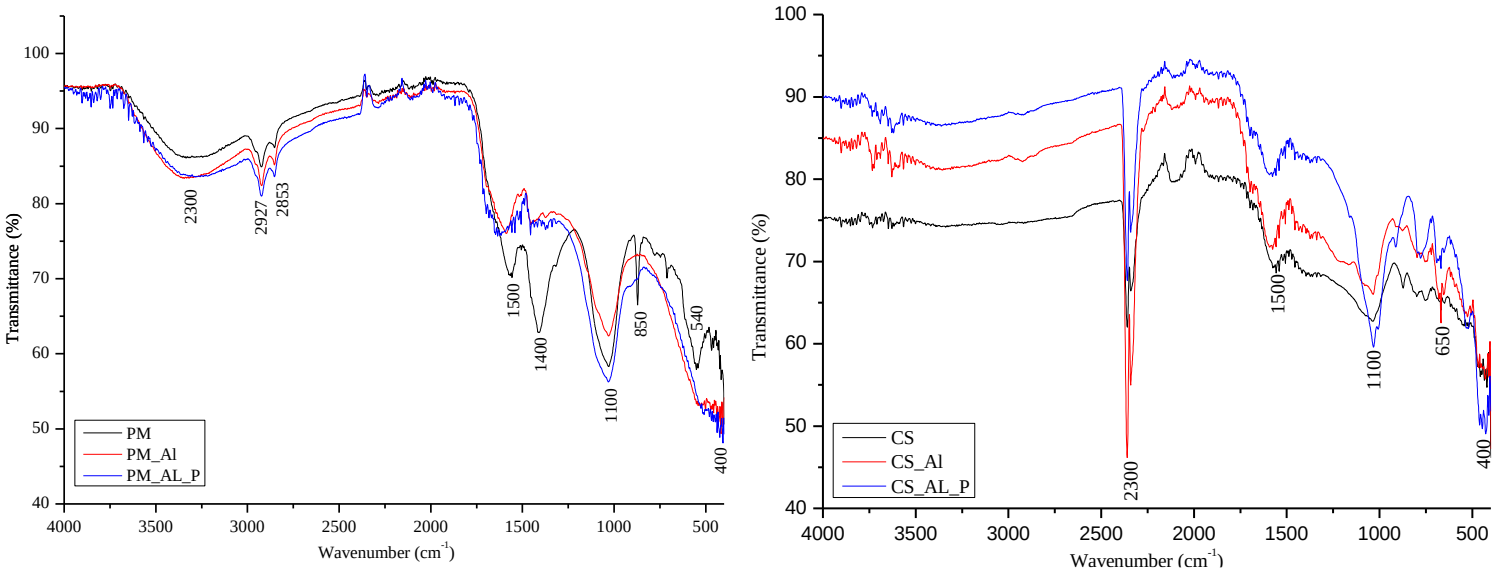

Fig 3. Molecular absorption spectroscopy in the infrared region (FT-IR).
Biochars of poultry manure (PM), poultry manure doped with Al (PM_Al), poultry manure doped with Al and in its MPAC (PM_Al_P) and of biochars of sugar cane straw (CS), sugar cane straw doped with Al (CS_Al) and sugar cane straw doped with Al and in it MPAC (CS_Al_P).

5.3.1.4. Scanning electron microscopy and energy dispersive spectroscopy (SEM and EDS)

The images obtained by SEM for BPM, before (Fig 4a) or after doping in their MPAC (Figura 4b), do not demonstrate morphological alteration of the material after addition of Al or P. Some pores are observed in the images, possibly coming from materials not well digested by poultrys, such as corn (Fig 4c). In these pores, the EDS did not detect Al (or detected with little intensity) when it was added to the sample, as opposed to the intense Al peaks found on the surface

(Fig 4b), allowing us to infer that the attraction of this element to the material is so high that adsorption occurs rapidly upon entering in contact with the surface, not migrating to the pores.

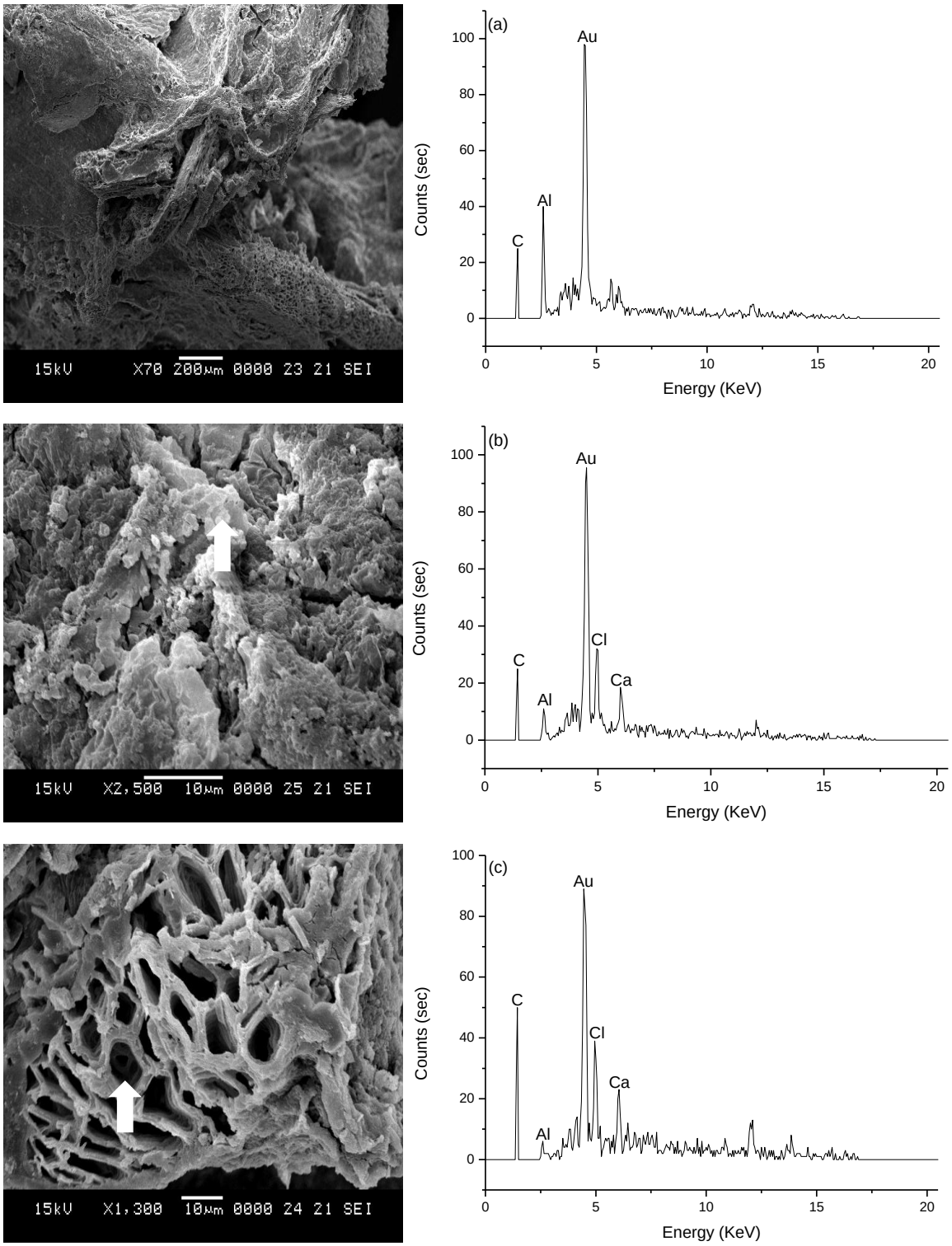

Fig 4. Images of scanning electron microscope (SEM) and energy-dispersive X-ray (EDS).

(a) Biochar of poultry manure (BPM) before Al doping; (b) after Al doping and in its MPAC and (c) approximate image of pores found in the material after Al doping and in its MPAC.
The arrows in the pictures represent where the EDS was performed. The peak at 2.12keV (Au) is due to the sample coating with gold. In image "a" the EDS wasa performed in total area.

In contrast, the BCS images showed cubic Al crystals throughout their extent as a consequence of their addition (Figs 5a and 5b). In this sample, EDS also finds Cl in the stomata in low intensities, probably from the aluminum source used ($AlCl_3$) (Fig 5b). Phosphate structures in cylindrical and longitudinal format were observed in this material after addition of Al and P (Fig 5c). Such structures appear to be phosphate spicules and are commonly reported in urine with alkaline pH [26], as is the case with the high pH of our biochar.

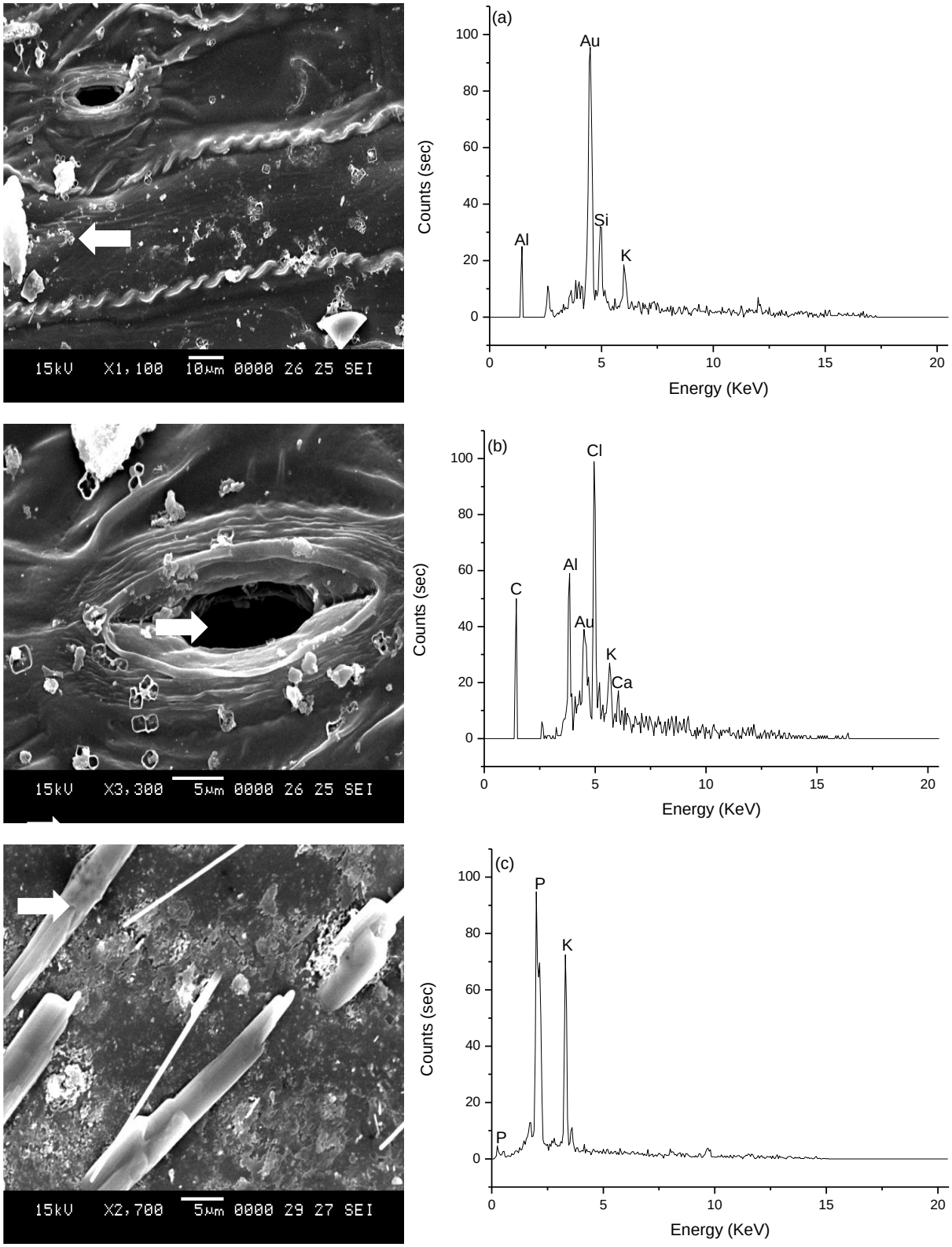

Fig 5. Images of scanning electron microscope (SEM) and energy-dispersive X-ray (EDS). (a)Biochar of sugar cane straw (BCS) before Al doping; (b) after Al doping and (c) after Al doping and in its MPAC.

The arrows in the pictures represent where the EDS was performed. The peak at 2.12keV (Au) is due to the sample coating with gold.

5.3.1.5. X-ray photoelectron spectroscopy (XPS)

The chemical species distribution in the biochar surfaces from XPS has good overlapping with the results of the abovementioned techniques. After Al doping and P adsorption, the amount of high-reactivity carbon sites decreased (Table 1), in particular the carbonyl groups (C=O). This group is responsible for adding elements and promoting chemical attack due to the resonance between C and O, which creates polarity in the molecule. As the Al-doping process was carried out in low pH (3.0) [27], which ensured high amounts of Al^{3+} (≈ 100 %) in the solution, this cation is likely to have joined the carbonyl structure.

Table 1. C1s bonding state and its relative atomic percentage on biochar surfaces as determined by 3.5 X-ray photoelectron spectroscopy (XPS).

Samples	C1s [a]			
	284.6 eV	285.8 eV	287.2 eV	288.8 eV
	aliphatic/aromatic carbon groups (CHx, C–C/C═C)	hydroxyl and ether groups (-C-OR)	carbonyl groups (>C ═O)	carboxylic groups, esters and lactones
BPM	50	39	11	-
BPM-Al	67	23	-	10
BPM-Al-P	63	32	-	5
BCS	63	24	8	5
BCS-Al	60	31	2	7
BCS-Al-P	53	38	-	9
	Al2p [b]			
	74.8 eV $Al(OH)_3$	75.2 eV AlO(OH)		
BPM	-	-		
BPM-Al	-	100		
BPM-Al-P	-	100		
BCS	100	-		
BCS-Al	100			
BCS-Al-P	100			
	P2p [b]			
	133.4 eV $CaHPO_4$ and $Ca_3(PO_4)_2$	134.4 eV Al-P ($Al_{0.54}P_{0.45}O_2$ and/or $AlPO_4.2H_2O$)		
BPM	100	-		
BPM-Al	-	100		
BPM-Al-P	-	100		
BCS	100	-		
BCS-Al	-	-		
BCS-Al-P	-	100		

Compound definitions followed: (a) Yao et al., 2010; Srinivasan et al., 2015; Yang et al., 2016 and (b) NIST (https://srdata.nist.gov/xps)

The pH increase after the doping process promotes the polymerization of newly-added Al in the low crystallinity minerals, which could be viewed in the SEM analysis (Figs 4 and 5), as well as in the XPS, whereas the Al peak was about 74.8 and 75.2 eV (Table 1), which is typical of Al hydroxides [28], such as $Al(OH)_3$ and AlO(OH). These new compounds are notable for having high capacity for adsorbing phosphate in soils [29] and are presented in [30-32], which ensured high P absorption by the doped biochar.

The P compounds identified in the raw material and doped biochar were those already existing. Ca-P minerals are probes for formation after pyrolysis [33, 34] (Table 1). The BPM after Al doping already presented Al-P complexation in accordance with the high P availability in this material. The P signal from BCS after Al doping cannot be identified. Most likely, the Al structures recovered, as seen in the SEM images (Fig 5), avoided the XPS signal from P. The same Al-P species were identified after P landing in both biochars.

5.3.2. Al adsorption

The high adsorption capacity of Al by both biochars (Table 2) allows the doping process by the technique used to be so advantageous. High values arise from the formation of many P adsorption sites (Al bridges), which is confirmed later by the high MPAC of these biochars after doping (Table 3).

Table 2. K_L, q_e, K_F, n and R^2 values for Langmuir and Freudelich isotherms after Al doping.

	Langmuir		
	K_L	q_e	R^2
	L mg^{-1}	mg g^{-1}	
BPM	0.000037	1072.8	0.90
BCS	0.000028	1183.5	0.94

BPM, biochars of poultry manure in powder; BCS, sugar cane straw in powder

Table 3. K_L, q_e, K_F, n and R^2 values for Langmuir and Freudelich isotherms, after Al doping and P addition.

	Langmuir		
	K_L	q_e	R^2
	L mg^{-1}	mg g^{-1}	
BPM	0.00351	701.6	0.95
BPMF	0.00896	356.0	0.93
BCS	0.00295	758.9	0.98
BCSF	0.00689	468.8	0.95
	Freudelich		
	K_F	n	R^2
	L mg^{-1}		
BPM	26.52	2.32	0.85
BPMF	1.70	1.44	0.89
BCS	22.80	2.17	0.91
BCSF	2.53	1.58	0.89

BPM, biochars of poultry manure in powder; BCS, sugar cane straw in powder; BPMF, biochars of poultry manure in fragment; BCSF, biochar of sugar cane straw in fragment.

Nevertheless, the low value of the binding energy (K_L) suggests that the interaction between the biochars and Al is not high (Table 2), contrary to that of P, which has high binding energy (Table 3). This fact, along with Al adsorption values greater than 100 % (1072.85 and 1183.54 mg g^{-1} Al for BPM and BCS, respectively), allows us to infer that, besides adsorption, a capping process occurs, thus causing high MPAC.

5.3.3. P adsorption isotherms

As expected, the best fit and, subsequently, the higher R^2 of the Langmuir isotherm, compared to that of Freudelich (Table 3), confirms the fact that this model describes the adsorption process in a more convenient manner, in addition to being more appropriate for the estimation of maximum point, as observed in this and in several other papers [5, 12, 13, 35].

The high MPAC of both biochars (Table 3), regardless of the biochar texture, corroborates with the theory that these materials, if doped, have a high potential for P recovery in waters with a high concentration of this element. In addition, the post-doping process with Al

generated a biochar with a higher MPAC than many values reported in the literature. For example, [36] reported a MPAC of 46.37 mg g^{-1} in a Lanthanum-doped oak bark biochar; [37] found a MPAC of 50 mg g^{-1} using magnesium-doped cane straw biochar; and [38] obtained a MPAC of 125.40 mg g^{-1} for a bismuth-doped wheat straw biochar. Nevertheless, in studies where doping is performed after pyrolysis, i.e., after the biochar is produced, MPAC values tend to be higher, such as that of [39], who found a maximum adsorption of 318 mg g^{-1} when using Fe-doped corn straw biochar in the post-pyrolysis process, or that of [40], who reported a MPAC of 250 mg g^{-1} with Mg- and Al-doped sugarcane straw biochar, also in the post-pyrolysis process.

The effect of the biochar texture, i.e., macerating the material, as expected, is of paramount importance in the final adsorption value (Table 3). When repeating the isotherm for the fragmented materials the initial MPAC value (701.65 and 758.96 mg g^{-1} of P for BPM and BCS, respectively) is reduced by almost half (356.04 and 468.84 mg g^{-1} of P for BPM and BCS, respectively), inferring that an important point for this technique is the specific surface. It is also believed that, besides the contribution of the post-doping process in the high MPAC for biochars, there is the effective involvement of the high affinity of Al, used as a cation for the generation of electropositivity, by P, the retention of this nutrient being a major problem in tropical soils, which act as a strong P drain [21].

5.3.4. P desorption

The need for larger successive extractions to desorb the P adsorbed to the BPM, regardless of the extractor used (Table 4), and the lowest desorbed percentage, compared to BCS, is in agreement with the higher K_F and K_L of this material (Table 3). These rates are related to the P adsorption strength, and the higher the binding energy, the more extractions are required for total desorption [41].

Table 4. Concentrations of P desorbed after successive extractions with H_2SO_4, $NaHCO_3$ and H_2O.

	Successive extractions							
Extractor	1	2	3	4	5	6	Total	Total
	mg L^{-1}							%
	BPM(1)							
H_2SO_4	417.23	12.67	7.63	0.71	0.43	0.23	438.90	62.5526
$NaHCO_3$	211.27	339.48	91.68	8.16	-	-	650.59	92.7229
H_2O	133.71	-	-	-	-	-	133.71	19.0565
	BCS(2)							
H_2SO_4	642.16	3.08	1.71	-	-	-	646.95	85.2416
$NaHCO_3$	602.34	77.95	39.66	8.19	-	-	728.14	95.9392
H_2O	187.56	-	-	-	-	-	187.56	24.7128

(1)biochar of poultry manure; (2)biochar of sugar cane straw

Sulfuric acid for both biochars extracted a lower amount of adsorbed P (total percentage), despite desorbing the largest amount already in the first extraction. Sodium bicarbonate extracted significant amounts in all successive extractions, obtaining a 92 % and 95 % extraction of the adsorbed P for BPM and BCS, respectively (Table 4). These observations are in agreement with the mode of extraction of both extractors: while extraction by sulfuric acid corresponds to the exchange of binders between adsorbed phosphate and the extractor sulfate, extraction by sodium bicarbonate corresponds to the exchange of binders between the phosphate adsorbed and hydroxyl groups from the extractor [42]. Water, as might be expected, was not an effective extractor in the process.

5.3.5. Effect of competing anions

The affinity of the anions with the Al-doped biochar (Fig 6) seems to follow the order proposed by Hofmeister, which states that the affinity increases with the increasing charge and reduction of the hydrated ionic radius [43]. This fact is in agreement with the one found by [16], who verified a reduction of 3.02 %, 4.80 % and 6.95 % in the phosphate adsorption of a rice husk biochar by adding chloride, nitrate and sulfate to the solution, respectively. [12] noted a reduction in P adsorption by corn biochar of 11.7 % and 41.4 %, respectively, after competition with NO^{3-} and CO_3^{2-}.

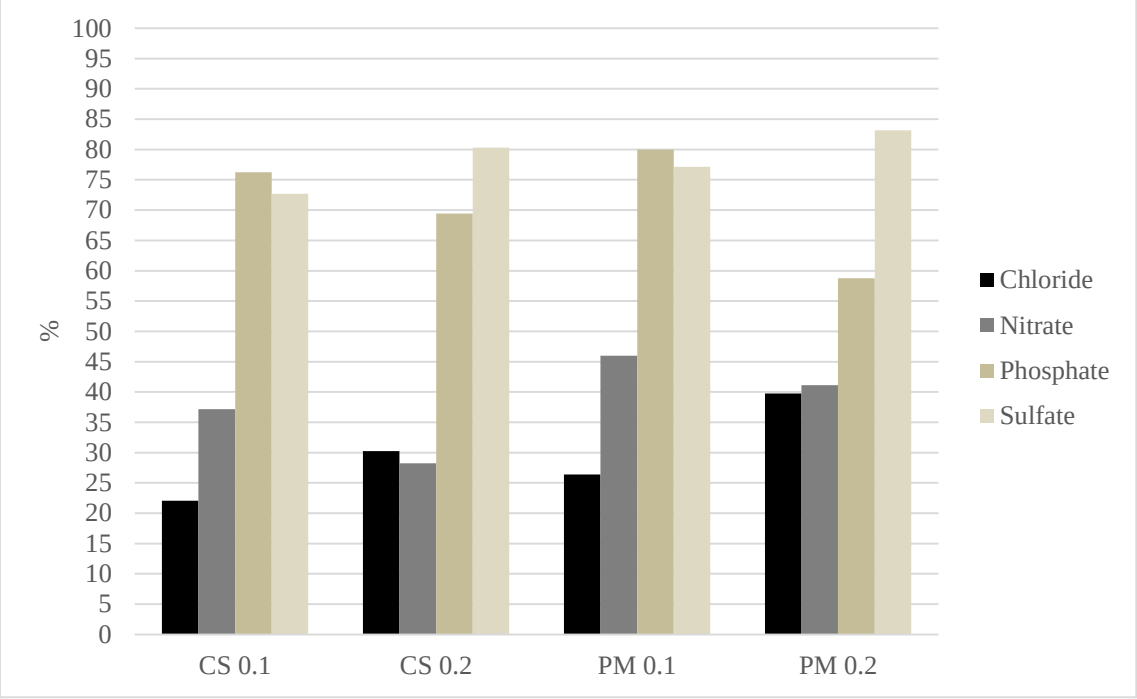

Fig 6. Percentage of adsorption of chloride, nitrate, phosphate and sulphate anions, in a competition test for the adsorption sites.
Equilibrium in the concentrations of 0.1 and 0.2 mol L^{-1} with the Al doped biochars of sugar cane straw (CS) and poultry manure (PM).

The predominant form of phosphate is variable according to the pH of the solution [44], and in pH values equal to 6, as is the case in this experiment, the predominant form is $H_2PO_4^-$, which is the reason why SO_4^{2-} was adsorbed with greater priority after adding the highest concentration solution (0.2 mol L^{-1}) and with the same priority after adding the solution with the lowest concentration (0.1 mol L^{-1}). [45] compared the competition between phosphate, chloride, nitrate and sulfate in the rice bark biochar adsorption sites at different pH values and found that, in a solution of pH 9.0, PO_4^{3-} which is the predominant form, with the possibility of forming complexes with the Ca/Mg used in the doping process, makes the presence of anions such as Cl^-, NO_3^- and SO_4^{2-} not cause great effects.

Such a variation between the solutions and the non-occurrence of a two-fold adsorption, for most anions, by doubling the added concentration, can be justified by ionic strength. The increase in ionic strength when increasing the concentration, with a subsequent decrease in anion activity, as reported by [45], allows the competition in the sites to be amplified and prevents the response from being greater, as one might expect.

5.3.6. Sorption in eutrophic water

With the successive changes of the solution in equilibrium, in order to guarantee the saturation of the adsorption sites, the biochar buffer was ruptured and, after doping, had its pH set at 6.0 and, with the addition of water, had its pH increased to 9.0 (the original pH value of the biochar before the doping process). This fact caused the predominant form of P in solution to be bivalent and trivalent rather than monovalent, as in the competition with anions at the same concentration (pH set at 6.0), ensuring that the phosphate had preferential adsorption (Fig 7), as opposed to the previous test (Fig 6).

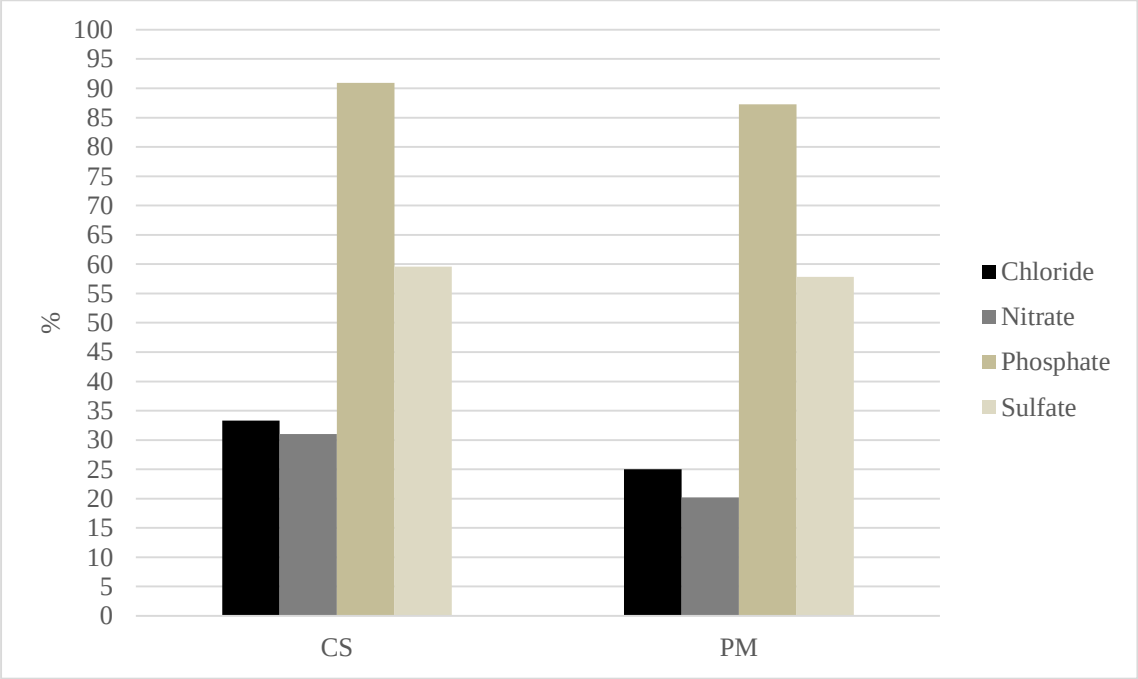

Fig 7. Percentage of adsorption of chloride, nitrate, phosphate and sulphate anions, in a competition test for the adsorption sites.
After equilibrium with a hypothetical eutrophic water, with the Al doped biochars of sugar cane straw (CS) and poultry manure (PM).

[46] found a preferential adsorption of fluoride (F^-), when the phosphate form in the solution is monovalent ($H_2PO_4^-$). The situation is reversed when the predominant form is bivalent or trivalent (HPO_4^{2-} and/or PO_4^{3-}), as the preferred exchange sequence is for higher-valence anions (Hofmeister series). The presence of the dissociated or hydrolyzed form is defined by the pH values, so the acidity of the medium changes the exchange preference, as illustrated by [47].

The chloride and nitrate anions follow the expected pattern, with lower adsorption compared to the others (Fig 7).

5.4. CONCLUSION

The high adsorption of Al by both biochars (poultry manure and sugarcane straw), with the capping of these materials with this cation and its hydrolysis products, ensures the efficiency of the post-doping process, allowing a high P adsorption capacity by the materials, its texture (specific surface) being of great importance in the magnitude of this capacity. P desorption is carried out in few successive extractions by the acid or base extractors, ensuring the removal of almost the entirety retained P, thus allowing its reuse as a slow-release phosphate fertilizer. Its use in eutrophic and residual water is plausible, despite the lower adsorption of P as a consequence of the competition of anions such as sulfates, chlorides, and nitrates.

REFERENCES

1. Gilbert N. Environment: The disappearing nutrient. Nature. 2009; 461(7265):716. doi:10.1038/461716a

2. Jan J, Borovec J, Kopáček J, Hejzlar J. Assessment of phosphorus associated with Fe and Al (hydr) oxides in sediments and soils. J Soils Sediments. 2105; 15(7): 1620-1629. doi:10.1007/s11368-015-1119-1

3. Jones C, Nomosatryo S, Crowe SA, Bjerrum CJ, Canfield DE. Iron oxides, divalent cations, silica, and the early earth phosphorus crisis. Geology. 2015; 43(2):135-138. doi:10.1130/G36044.1

4. Lehmann J, Joseph. Biochar for environmental management: science, technology and implementation. Routledge; 2015

5. Yao Y, Gao B, Chen J, Yang L. Engineered biochar reclaiming phosphate from aqueous solutions: mechanisms and potential application as a slow release fertilizer. Environ Sci Technol. 2013; 47:8700-8708. doi:10.1021/es4012977

6. Jung KW, Hwang MJ, Ahn KH, Ok YS. Kinetic study on phosphate removal from aqueous solution by biochar derived from peanut shell as renewable adsorptive media. Int J Environ Sci Technol. 2015; 12(10)-3363-3372. doi:10.1007/s13762-015-0766-5

7. Cui X, Dai X, Khan KY, Li T, Yang X, He Z. Removal of phosphate from aqueous solution using magnesium-alginate/chitosan modified biochar microspheres derived from Thalia dealbata. Bioresour Technol. 2016; 218:1123-1132. doi:10.1016/j.biortech.2016.07.072

8. Takaya CA, Fletcher LA, Singh S, Anyikude KU, Ross AB. Phosphate and ammonium sorption capacity of biochar and hydrochar from different wastes. Chemosphere. 2016; 145:518-527. doi:10.1016/j.chemosphere.2015.11.052

9. Trazzi PA, Leahy JJ, Hayes MHB, Kwapinski W. Adsorption and desorption of phosphate on biochars. Can J Chem Eng. 2016; 4(1):37-46. doi:10.1016/j.jece.2015.11.005

10. Roy ED, Richards PD, Martinelli LA, Coletta DL, Lins SRM, Vazquez FF, et al. The phosphorus cost of agricultural intensification in the tropics. Nature Plants. 2016; 2: 1-6. doi:10.1038/nplants.2016.43

11. Jing R, Li N, Li L, An JK, Zhao L, Ren NQ. Granulation and ferric oxides loading enable biochar derived from cotton stalk to remove phosphate from water. Bioresour Technol. 2015; 178:119-125. doi:10.1016/j.biortech.2014.09.071

12. Zhang M, Gao B. Removal of arsenic, methylene blue, and phosphate by biochar/AlOOH nanocomposite. Chem Eng Process. 2013; 226:286-292. doi:10.1016/j.cej.2013.04.077

13. Jung KW, Ahn KH. Fabrication of porosity-enhanced MgO/biochar for removal of phosphate from aqueous solution: application of a novel combined electrochemical modification method. Bioresour Technol. 2016; 200:1029-1032. doi:10.1016/j.biortech.2015.10.008

14. Jung KW, Jeong TU, Kang H J, Ahn KH. Characteristics of biochar derived from marine macroalgae and fabrication of granular biochar by entrapment in calcium-alginate beads for phosphate removal from aqueous solution. Bioresour Technol. 2016; 211:108-116. doi:10.1016/j.biortech.2016.03.066

15. Jung KW, Jeong TU, Hwang MJ, Kim K, Ahn KH. Phosphate adsorption ability of biochar/Mg–Al assembled nanocomposites prepared by aluminum-electrode based electro-assisted modification method with MgCl2 as electrolyte. Bioresour Technol. 2015; 198:603-610. doi:10.1016/j.biortech.2015.09.068

16. Dai L, Wu B, Tan F, He M, Wang W, Qin H, et al. Engineered hydrochar composites for phosphorus removal/recovery: Lanthanum doped hydrochar prepared by hydrothermal carbonization of lanthanum pretreated rice straw. Bioresour Technol. 2014; 161:327-332 doi:10.1016/j.biortech.2014.03.086

17. Cai R, Wang X, Ji X, Peng B, Tan C, et al. Phosphate reclaim from simulated and real eutrophic water by magnetic biochar derived from water hyacinth. J Environ Manage. 2017; 187:212-219. doi:10.1016/j.jenvman.2016.11.047

18. Crombie K, Masek O, Cross A, Sohi S. Biochar -Synergies and trade-offs between soil enhancing properties and C sequestration potential. GCB Bioenergy 7. 2015; 1161–1175. doi:10.1111/gcbb.12213/

19. Murphy J, Riley JP. A modified single solution method for the determination of phosphate in natural waters. Anal Chim Acta. 1962; 27:31-36.

20. Zhang H, Chen C, Gray EM, Boyd SE, Yang H, Zhang D. Roles of biochar in improving phosphorus availability in soils: A phosphate adsorbent and a source of available phosphorus. Geoderma. 2016; 276:1-6. doi:10.1016/j.geoderma.2016.04.020

21. Novais RF, Smyth TJ. Phosphorus in soil and plant in tropical conditions. Viçosa: Universidade Federal de Viçosa; 1999.

22. Beato D, Medeiros MJ, Drews M, Dutra GM. Urban Impacts in Groundwater - Pampulha Lagoon Basin, Belo Horizonte-MG. XII Brazilian Congress of Underground Waters; 2002. Available on: https://aguassubterraneas.abas.org/asubterraneas/article/viewFile/22690/14892

23. Park S, Baker JO, Himmel ME, Parilla PA, Johnson DK. Cellulose crystallinity index: measurement techniques and their impact on interpreting cellulase performance. Biotechnol Biofuels. 2010; 3(1):10. doi:10.1186/1754-6834-3-10

24. Domingues RR, Trugilho PF, Silva CA, Melo ICN, Melo LC, Magriotis ZM, et al. Properties of biochar derived from wood and high-nutrient biomasses with the aim of agronomic and environmental benefits. PloS One. 2017; 12(5): e0176884. doi:10.1371/journal.pone.0176884

25. Tanada S, Kabayama M, Kawasaki N, Sakiyama T, Nakamura T, Araki M, et al. Removal of phosphate by aluminum oxide hydroxide. J. Colloid Interface Sci. 2003; 257(1):135-140. doi:10.1016/S0021-9797(02)00008-5

26. Biasoli DWM. Atlas do sedimento urinário. 1980. Control Lab, Fortaleza, Brazil.

27. Kinraide TB. Identity of the rhizotoxic aluminium species. Plant and Soil. 1991; 134(1):167-178.

28. Naumkin AV, Kraut-Vass A, Gaarenstroom WS, Powell CJ. NIST X-ray Photoelectron Spectroscopy Database. NIST Standard Reference Database 20, Version 4.1. https://srdata.nist.gov/xps/

29. Gérard F. Clay minerals, iron/aluminum oxides, and their contribution to phosphate sorption in soils—A myth revisited. Geoderma. 2016; 262:213-226. doi:10.1016/j.geoderma.2015.08.036

30. Makris KC, O'Connor GA. Beneficial utilization of drinking-water treatment residuals as contaminant-mitigating agents. Develop Environ Science. 2007; 5:609-635. doi:10.1016/S1474-8177(07)05028-0

31. Razali M, Zhao YQ, Bruen M. Effectiveness of a drinking-water treatment sludge in removing different phosphorus species from aqueous solution. Sep Purif Technol. 2007; 55(3):300-306. doi:10.1016/j.seppur.2006.12.004

32. Babatunde, AO, Zhao YQ, Burke AM, Morris MA, Hanrahan JP. Characterization of aluminium-based water treatment residual for potential phosphorus removal in engineered wetlands. Environ Pollut. 2009; 157(10):2830-2836. doi:10.1016/j.envpol.2009.04.016

33. Uchimiya M, Hiradate S. Pyrolysis temperature-dependent changes in dissolved phosphorus speciation of plant and manure biochars. J Agric Food Chem. 2014; 62(8):1802-1809. doi:10.1021/jf4053385

34. Bruun S, Harmer SL, Bekiaris G, Christel W, Zuin L, Hu Y, et al. The effect of different pyrolysis temperatures on the speciation and availability in soil of P in biochar produced from the solid fraction of manure. Chemosphere. 2017; 169:377-386. doi:10.1016/j.chemosphere.2016.11.058

35. Li R, Wang JJ, Zhou B, Zhang Z, Liu S, Lei S, et al. Simultaneous capture removal of phosphate, ammonium and organic substances by MgO impregnated biochar and its potential use in swine wastewater treatment. J Clean Prod. 2017; 147:96-107. doi:10.1016/j.jclepro.2017.01.069

36. Wang Z, Shen D, Shen F, Li T. Phosphate adsorption on lanthanum loaded biochar. Chemosphere. 2016; 150:1-7. doi:10.1016/j.chemosphere.2016.02.004

37. Gong YP, Ni ZY, Xiong ZZ, Cheng LH, Xu XH. Phosphate and ammonium adsorption of the modified biochar based on Phragmites australis after phytoremediation. Environ Sci Pollut R. 2017; 24:8326–8335. doi:10.1007/s11356-017-8499-2

38. Zhu N, Yan T, Qiao J, Cao H. Adsorption of arsenic, phosphorus and chromium by bismuth impregnated biochar: Adsorption mechanism and depleted adsorbent utilization. Chemosphere. 2016; 164:32-40. doi:10.1016/j.chemosphere.2016.08.036

39. He X, Zhang T, Ren H, Li G, Ding L, Pawlowski L. Phosphorus recovery from biogas slurry by ultrasound/H 2 O 2 digestion coupled with HFO/biochar adsorption process. Waste Manag. 2017; 60:219-229. doi:10.1016/j.wasman.2016.08.032

40. Li R, Wang JJ, Zhou B, Awasthi MK, Ali A, Zhang Z, et al. Enhancing phosphate adsorption by Mg/Al layered double hydroxide functionalized biochar with different Mg/Al ratios. Sci Total Environ. 2016; 559:121-129. doi:10.1016/j.scitotenv.2016.03.151

41. Fang C, Zhang T, Li P, Jiang R, Wu S, Nie H, et al. Phosphorus recovery from biogas fermentation liquid by Ca–Mg loaded biochar. J Environ Sci. 2015; 29:106-114. doi:10.1016/j.jes.2014.08.019

42. Novais SV, Mattiello EM, Vergutz L, Melo LCA, Freitas ÍFD., Novais RF. Loss of Extraction capacity of MehLich-1 and Monocalcium phosphateas a variable of remaining p and its relationship to critical levels of soil phosphorus and sulfur. Rev Bras Ci Solo. 2015; 39(4):1079-1087. doi:10.1590/01000683rbcs20140551

43. Collins KD, Washabaugh MW. The Hofmeister effect and the behaviour of water at interfaces. Q Rev Biophys. 1985; 18(04):323-422.

44. Greenland DJ. The chemistry of soil processes. New India Publishing Agency; 2015.

45. Qian T, Zhang X, Hu J, Jiang H. Effects of environmental conditions on the release of phosphorus from biochar. Chemosphere. 2013; 93(9):2069-2075. doi:10.1016/j.chemosphere.2013.07.041

46. Cai P, Zheng H, Wang C, Ma H, Hu J, Pu Y, et al. Competitive adsorption characteristics of fluoride and phosphate on calcined Mg–Al–CO 3 layered double hydroxides. J Hazard Mater. 2012; 213:100-108. doi:10.1016/j.jhazmat.2012.01.069

6. FINAL REMARKS

The deposition of agricultural residues and animal wastes in the soil causes controversy around the emission of greenhouse gases (GHG), as well as the leaching of chemical elements and the consequent contamination of groundwater and watercourses. Enteric fermentation, animal waste and agricultural soils are responsible for about 70 % of GHG emissions in agriculture, forest and land use regions in general (IPCC, 2015), and the application of manure to soil causes a constant debate between pros and cons (Owens & Silver, 2014; Millardi & Angers, 2014).

The controversial final destination of some waste along with criticism of its maintenance in the soil, such as in the no-tillage system, makes environmentally safe forms of waste disposal to be sought. For example, sugarcane, widely cultivated in Brazil, with a planted area of 8.8 million hectares, generating around 250 million tons of straw (CONAB, 2013), has laws prohibiting its burning. In this same scenario, intense animal husbandry leads to intense manure production and its incorrect deposition to the soil, increasing GHG production (Kelly et al., 2016).

Biochar appears in these scenarios as a potential solution not only for GHG emissions, but also for recidivism pest and disease control, as a sustainable management of such materials, bringing a return to the physical, chemical and biological quality of the soil.

Chapter I we conclude that the pyrolysis of poultry manure and sugarcane straw leads to the mitigation of GHG in sandy soil and that the increase in pyrolysis temperature reduces emissions. The results allow inferring that the application of these biochars in the soil is an environmentally safe deposition of their source materials, at least in regard of GHG emission.

In Chapter II we conclude that pyrolysis of poultry manure and sugar cane straw leads to GHG mitigation and that regardless soil texture. Although such a benefit occurs despite the beneficial effects of biochar as a GHG mitigator, this advantage is best seen in sandy soil compared to clayey ones. The absence of variation between pyrolysis temperature for the biochar of sugarcane straw was attributed to the recalcitrance of this source material, not being influenced by changes of the medium. In this chapter, we also conclude (d) that the reduction of the originally alkaline pH of the biochars leads to a reduction in the GHG emission similar to the elevation of the pyrolysis temperature, which is an important consideration, since this would be an option to raise the pyrolysis temperature to achieve the same GHG mitigation potential

In chapter III we observe that although poultry manure and sugar cane straw biochars do not have the capacity to adsorb phosphorus (P), this ability is developed after a pre-doping process with Mg^{2+}. In addition, the high P desorption allows to infer that this product has potential to be used as slow release fertilizer, competing in quantity and quality with soluble commercial mineral

sources, since doses 2.8 and 1.2 times smaller are needed to apply the same amount of P, compared to simple superphosphate (SS) and concentrated superphosphate (CS), respectively.

In Chapter IV we find that the ability to adsorb anions can also be developed for these biochars by the post-doping process with Al^{3+}, conferring a higher maximum P adsorption capacity (MPAC) compared to the pre-doping process with Mg^{2+} in chapter III. We believe that an explanation for the higher MPAC can be that Al^{3+} is a trivalent cation, with high affinity for P. The high adsorption of Al corroborates this assertion.

In this chapter we also observe desorption of almost all of the adsorbed P by few successive extractions with chemical extractors, allowing to infer about their reuse as slow release fertilizer. Using the same logic in the previous chapter, we reached a dose of 8.9 and 3.7 times lower for the biochar of poultry manure and 9.7 and 4.1 times lower for the sugar cane straw biochar, compared to SS and CS, respectively. Finally, we can conclude from the results of this chapter that the use of these materials in the recovery of eutrophic or wastewater is plausible, despite the lower adsorption of P as a consequence of the competition of anions such as sulfates, chlorides and nitrates.

With these studies with biochars we observe the various benefits and potentials of pyrolyzing organic materials. The difference between products, being the poultry manure an extremely labile animal residue and the sugarcane straw a recalcitrant vegetal residue, allowe us to verify that the advantages are visible, independent of the raw material. We believe in the potential of biochar as a GHG mitigator, as a recover of eutrophic or wastewater and in the reuse or recycling of nutrients such as P, and as slow release fertilizer.

REFERENCES

Grabau, Z. J., Maung, Z. T. Z., Noyes, D. C., Baas, D. G., Werling, B. P., Brainard, D. C., & Melakeberhan, H. (2017). Effects of Cover Crops on Pratylenchus penetrans and the Nematode Community in Carrot Production. Journal of nematology, 49(1), 114.

Kelly, K. B. A., Ward, G.N. B., Hollier, & J. W. A. (2016). Greenhouse gas emissions from dung , urine and dairy pond sludge applied to pasture . 2 . Methane emissions.

Knight, I. A., Rains, G. C., Culbreath, A. K., & Toews, M. D. (2017). Thrips counts and disease incidence in response to reflective particle films and conservation tillage in cotton and peanut cropping systems. Entomologia Experimentalis et Applicata, 162(1), 19-29.

Maillard, É., & Angers, D. A. (2014). Animal manure application and soil organic carbon stocks: A meta-analysis. Global Change Biology, 20(2), 666-679.

Owens, J. J., Kebreab, E., & Silver, W. (2014). Greenhouse Gas Mitigation Opportunities in California Agriculture: Review of Emissions and Mitigation Potential of Animal Manure Management and Land Application of Manure. NI GGMOCA R, 6.

Reddy, P. P. (2017). Crop Residue Management and Organic Amendments. In Agro-ecological Approaches to Pest Management for Sustainable Agriculture (pp. 29-41). Springer, Singapore.

Regina, K., & Alakukku, L. (2010). Greenhouse gas fluxes in varying soils types under conventional and no-tillage practices. Soil and Tillage Research, 109(2), 144-152.

Rochette, P. (2008). No-till only increases N 2 O emissions in poorly-aerated soils. Soil and Tillage Research, 101(1), 97-100.